



Istituto Nazionale di Fisica Nucleare



The Science Case for a Southern Wide field of view detector

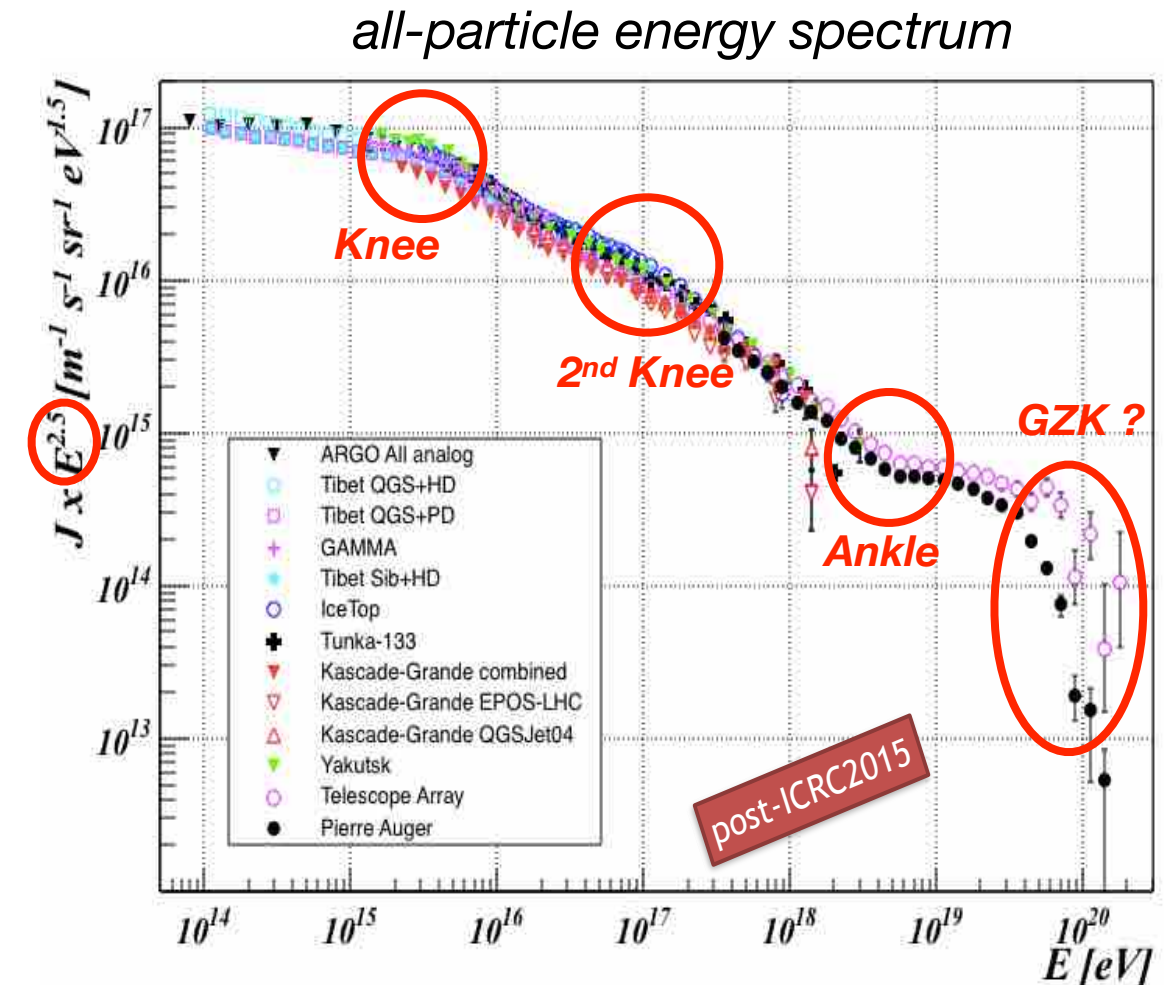
G. Di Sciascio

INFN - Roma Tor Vergata
disciascio@roma2.infn.it

*WASDHA 2018 - 9th Workshop on Air
Shower Detection at High Altitudes
Moscow, September 17-18, 2018*

The currently standard model

- CRs below 10^{17} eV are predominantly Galactic.
- **Standard paradigm:** Galactic CRs accelerated in SuperNova Remnants
→ *But smoking gun still missing !!!*
- Galactic CRs via *diffusive* shock acceleration ?
 $n_{CR} \propto E^{-\gamma}$ (at source), $\gamma \approx 2.1$
- Energy-dependent *diffusion* through Galaxy
 $n_{CR} \propto E^{-\gamma-\delta}$ (observed), $\delta \approx 0.6$



- Galactic CRs are scrambled by galactic magnetic field over very long time
→ arrival direction *mostly isotropic*
- Transition to extragalactic CRs occurs somewhere between 10^{17} and 10^{19} eV

The key questions

◆ **Origin of Cosmic Rays:** what are ***the sites*** that can accelerate particles up to $> 10^{20}$ eV ?
How many classes of sources at work ? Which cosmic accelerators dominate the CR flux in which energy range ?

- which ***acceleration*** mechanism? → injection spectrum
- total energy in CRs
- ***maximum energy of accelerated particles: the ‘proton knee’***

The description of how particles escape from a SNR shock has not been completely understood yet, the reason being the uncertainties related to ***how particles reach the maximum energies.***

◆ **Cosmic Ray propagation:** How do CRs propagate ?

- injected → observed spectrum
- Diffusion coefficients
- Why are CR confined in the Galaxy ? → magnetic field in the Galaxy
- spatial distribution of sources
- spatial distribution of CRs → anisotropy

◆ What is the ***elemental composition*** of the radiation as a function of the energy ?

Knee as end of Galactic population ?

Understanding *the origin of the "knee"* is *the key* for a comprehensive theory of the origin of CRs up to the highest observed energies.

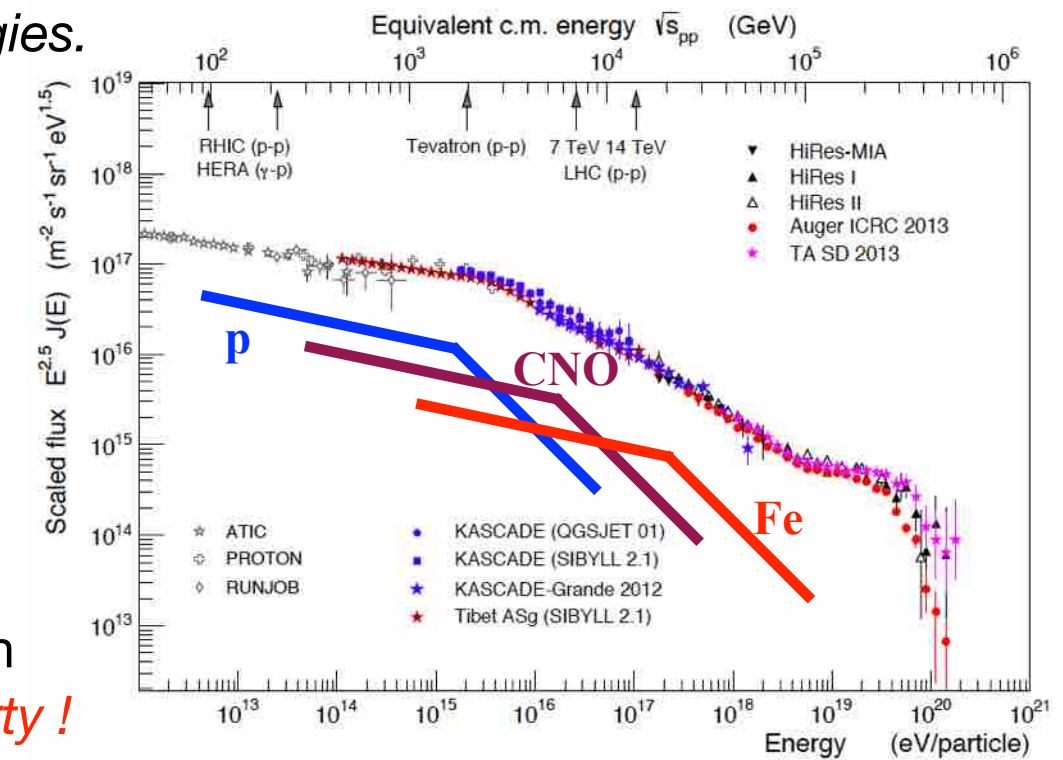
In fact, the knee is connected with the issue of the **end of the Galactic CR spectrum** and the transition from Galactic to extra-galactic CRs.

★ *Rigidity* models can be *rigidity-acceleration* models or *rigidity-confinement* models

- **Accelerator feature:** maximum energy of acceleration
→ implies that all accelerators are similar: *source property !*
- **Structure generated by propagation:** → we should observe a *knee that is potentially dependent on location*, because the propagation properties depend on position in the Galaxy
→ the (main) Galactic CR accelerators must be capable to accelerate to much higher energy
→ the Galaxy contains “*super-PeVatrons*” ! → *Gamma-Ray Astronomy above 100 TeV*

If the mass of the knee is *light* according to the standard model
→ Galactic CR spectrum is expected to end around 10^{17} eV

If the composition at the knee is *heavier* due to CNO / MgSi
→ we have a problem !



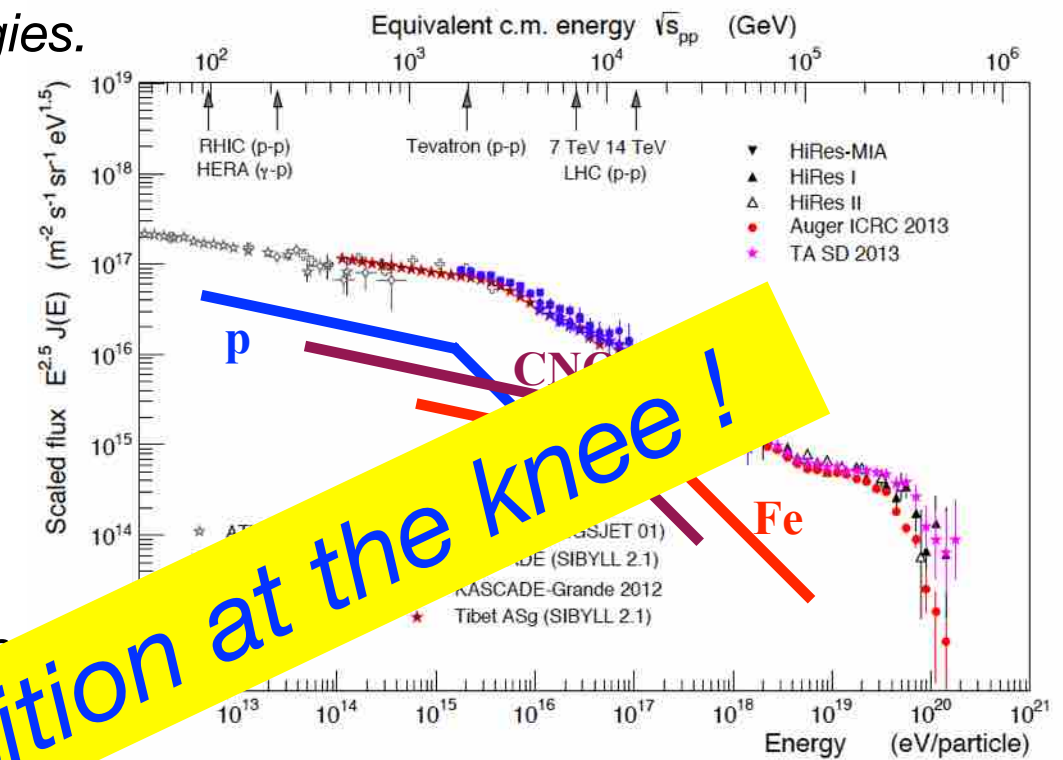
Knee as end of Galactic population ?

Understanding *the origin of the "knee"* is *the key* for a comprehensive theory of the origin of CRs up to the highest observed energies.

In fact, the knee is connected with the issue of the **end of the Galactic CR spectrum** and the transition from Galactic to extra-galactic CRs.

★ *Rigidity* models can be *rigidity-acceleration* models or *rigidity-confinement* models

- *Accelerator feature*: maximum energy of acceleration
→ implies that all accelerators are similar: *source rigidity* → *universal rigidity*
- *Structure generated by propagation*: we would observe a *knee that is potentially dependent on location*, because the propagation properties depend on position in the Galaxy
→ the (main) Galactic CR acceleration must be capable to accelerate to much higher energy
→ the Galaxy contains "accelerators" ! → *Gamma-Ray Astronomy above 100 TeV*



Strong Message: composition at the knee !
The knee is *light* according to the standard model
Galactic CR spectrum is expected to end around 10^{17} eV

If the composition at the knee is *heavier* due to CNO / MgSi
→ we have a problem !

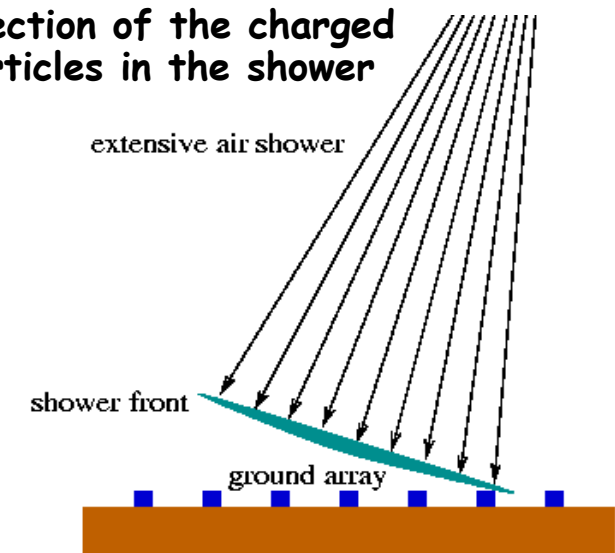
Ground-based gamma-ray detectors

Detecting Extensive Air Showers

Air Shower Arrays ($\approx 100 \text{ GeV} \rightarrow 1 \text{ PeV}$)

- High duty-cycle ($\approx 100\%$)
- Large field of view ($\approx 2 \text{ sr}$)
- Large energy range ($\approx \text{PeV}$)
- Higher energy threshold (ARGO $\approx 300 \text{ GeV}$),
Very strong zenith angle dependent ($\approx \cos \theta^{-(6-7)}$)
- Good bkg rejection ($> 80\%$)
- Good angular resolution (0.2-0.8 deg)
- Modest energy resolution ($\approx 50\%$)
- Good Sensitivity (5-10% Crab flux)
- Effective area shrinks with large zenith angle

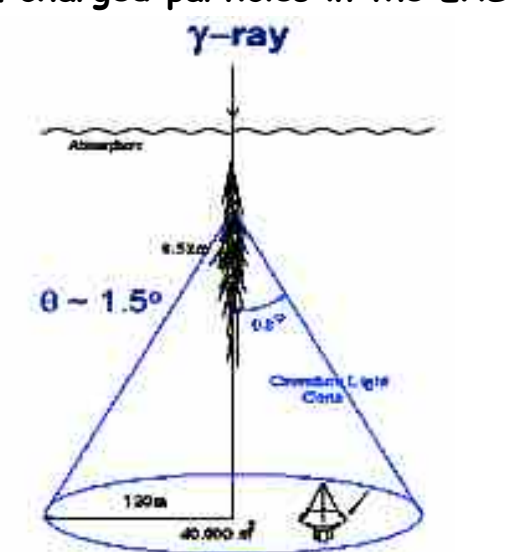
detection of the charged particles in the shower



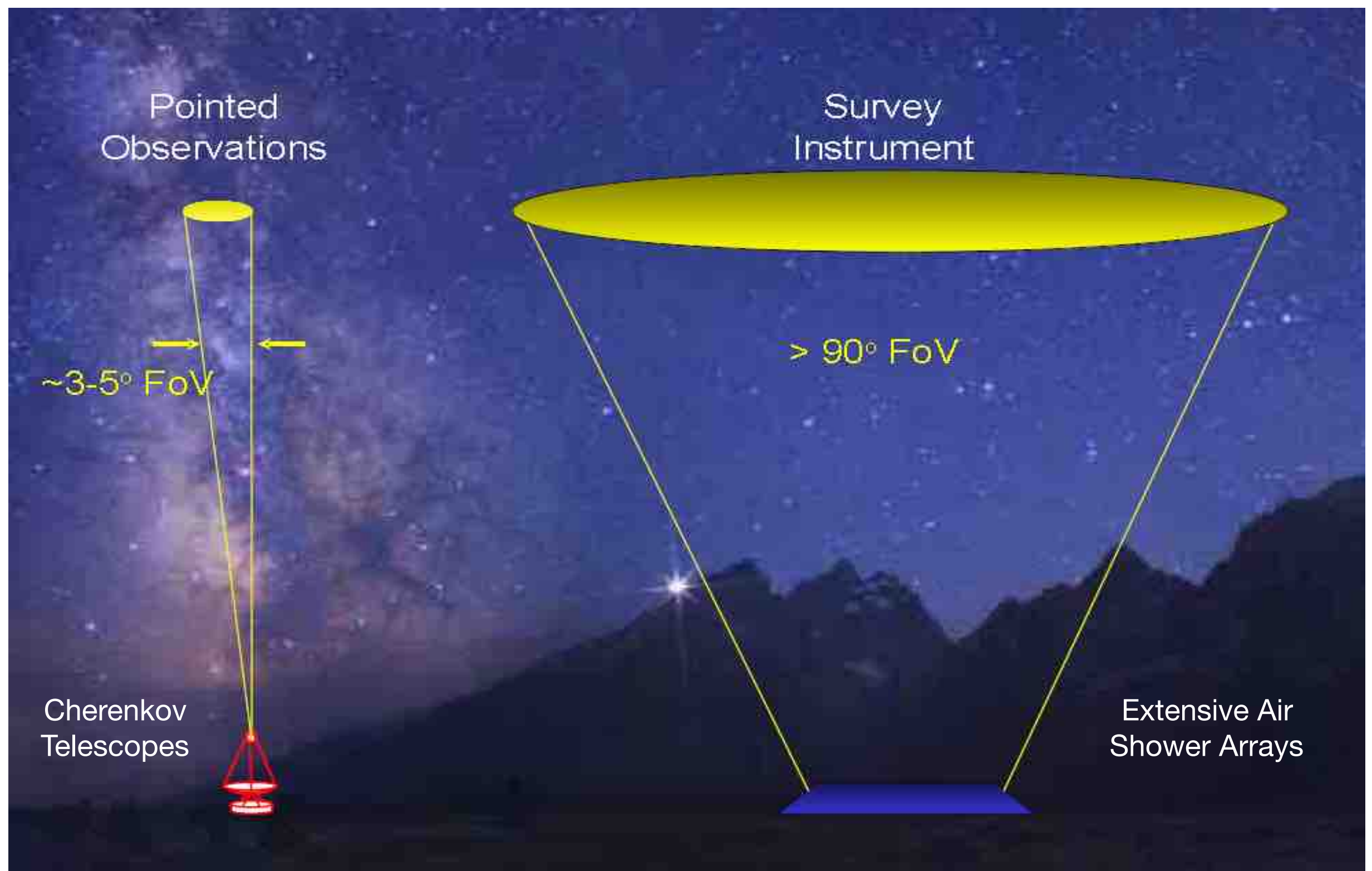
Cherenkov Telescopes ($\approx 10 \text{ GeV} \rightarrow 100 \text{ TeV}$)

- Very low energy threshold ($\approx 10 \text{ GeV}$)
- Excellent bkg rejection ($> 99\%$)
- Excellent angular resolution ($\approx 0.05 \text{ deg}$)
- Very good energy resolution ($\approx 15\%$)
- High Sensitivity (< % Crab flux)
- Effective area increase with zenith angle
- Small zenith angle dependent ($\approx \cos \theta^{-2.7}$)
- Low duty-cycle ($\approx 10-15\%$)
- Small field of view ($\approx 4-5 \text{ deg}$)
- Reduced maximum energy ($\approx 100 \text{ TeV}$)

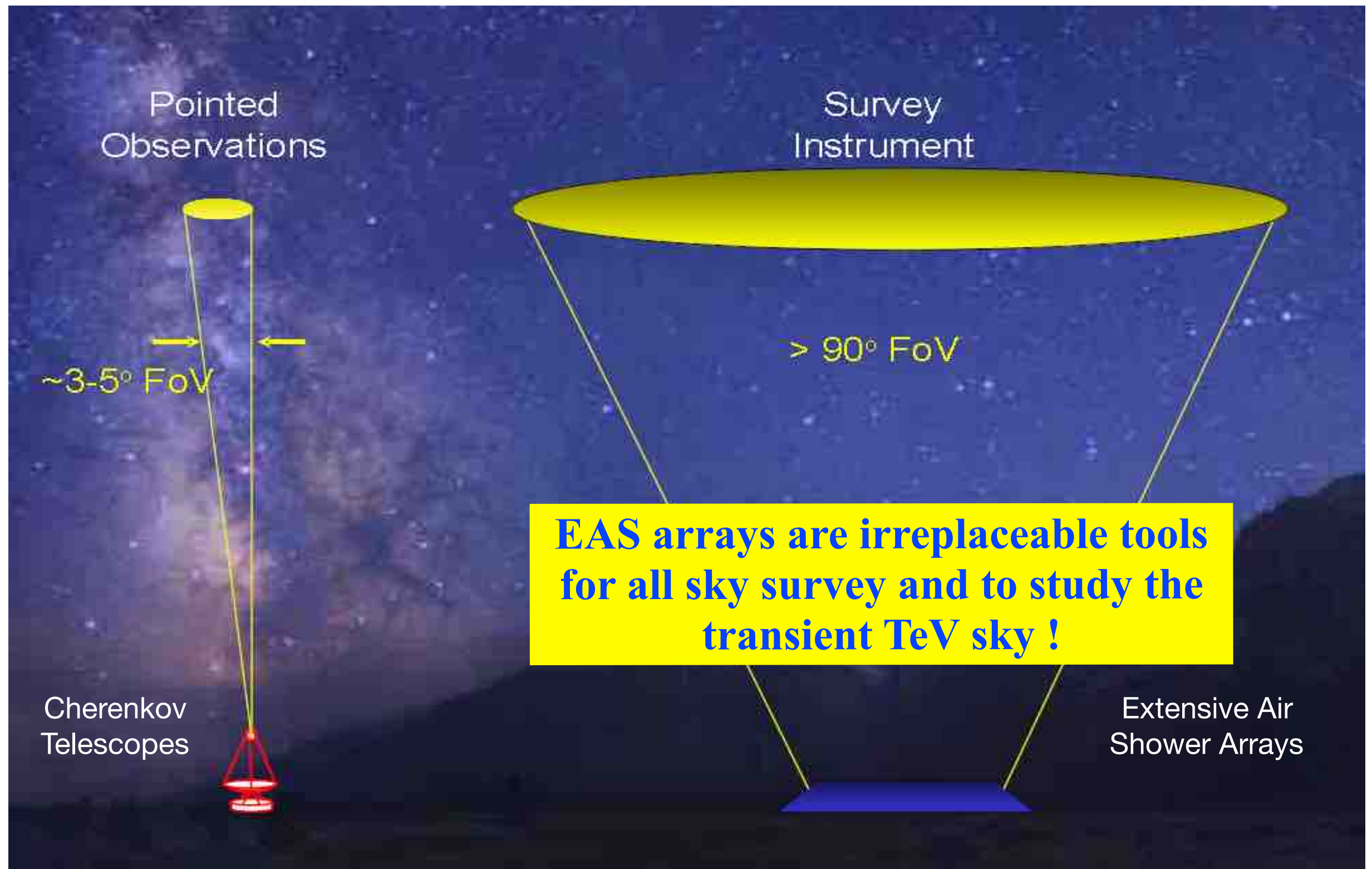
detection of the Cherenkov light from charged particles in the EAS



Wide field of view detectors



Wide field of view detectors



Why are Wide FoV instruments so cool ?

◆ **Origin of Cosmic Rays:** what are ***the sites*** that can accelerate particles up to $> 10^{20}$ eV ?
How many classes of sources at work ? Which cosmic accelerators dominate the CR flux in which energy range ?

- which ***acceleration*** mechanism? → injection spectrum
- total energy in CRs
- ***maximum energy of accelerated particles: the ‘proton knee’***

The description of how particles escape from a SNR shock has not been completely understood yet, the reason being the uncertainties related to ***how particles reach the maximum energies***.

◆ **Cosmic Ray propagation:** How do CRs propagate ?

- injected → observed spectrum
- Diffusion coefficients
- Why are CR confined in the Galaxy ? → magnetic field in the Galaxy
- spatial distribution of sources
- spatial distribution of CRs → anisotropy

◆ What is the ***elemental composition*** of the radiation ?

Why are Wide FoV instruments so cool ?

♦ **Origin of Cosmic Rays**: what are **the sites** that can accelerate particles up to $> 10^{20}$ eV ?
How many classes of sources at work ? Which cosmic accelerators dominate the CR flux in which energy range ?

- which *acceleration* mechanism? → injection spectrum
- total energy in CRs
- *maximum energy of accelerated particles*: *the 'proton knee'*

The description of how particles escape from a SNR shock has not been completely understood yet, the reason being the uncertainties related to *how particles reach the maximum energies*.

♦ **Cosmic Ray propagation**: How do CRs propagate ?

- injected → observed spectrum
- Diffusion coefficients
- Why are CR confined in the Galaxy ? → magnetic field in the Galaxy
- spatial distribution of sources
- spatial distribution of CRs → anisotropy

♦ What is the **elemental composition** of the radiation ?

Why are Wide FoV instruments so cool ?

- ◆ **Origin of Cosmic Rays**: what are **the sites** that can accelerate particles up to $> 10^{20}$ eV ?
How many classes of sources at work ? Which cosmic accelerators dominate the CR flux in which energy range ?

- which *acceleration* mechanism? → injection spectrum
- total energy in CRs
- *maximum energy of accelerated particles*: *the 'proton knee'*

The description of how particles escape from a SNR shell is not completely understood yet, the reason being the uncertainties related to *how* particles propagate ?

- ◆ **Cosmic Ray propagation**: How do particles propagate ?

- injected → observed spectrum
- Diffusion coefficient
- Why are CRs *anisotropic* in the Galaxy ? → magnetic field in the Galaxy

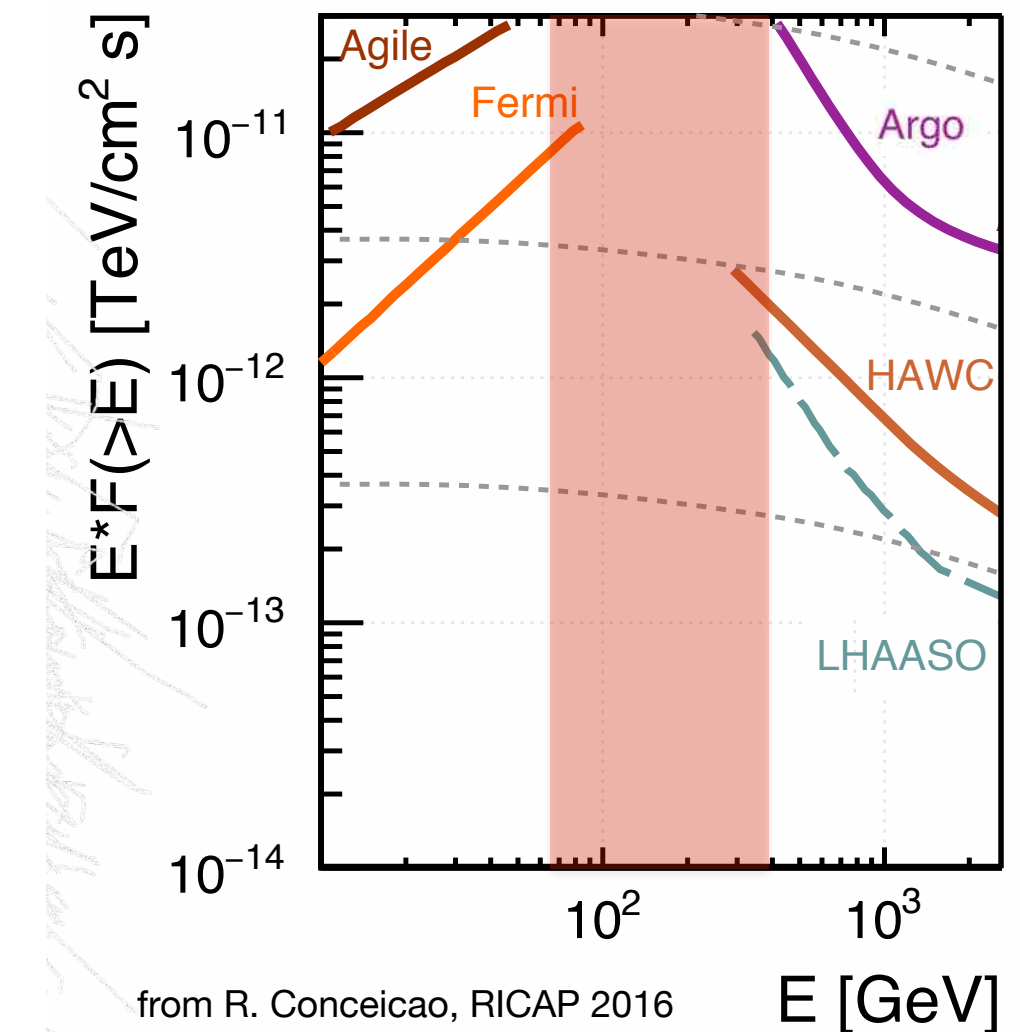
• spatial distribution of sources

• spatial distribution of CRs → anisotropy

- ◆ What is the **elemental composition** of the radiation ?

Why a new Wide FoV detector in the CTA era ?

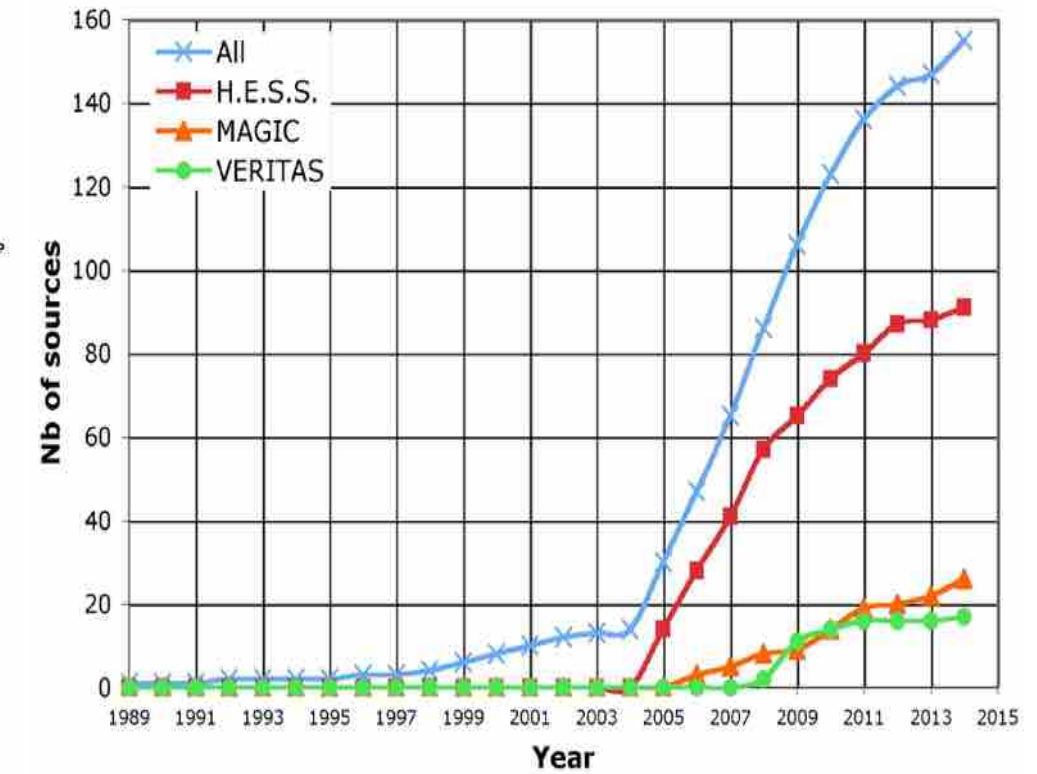
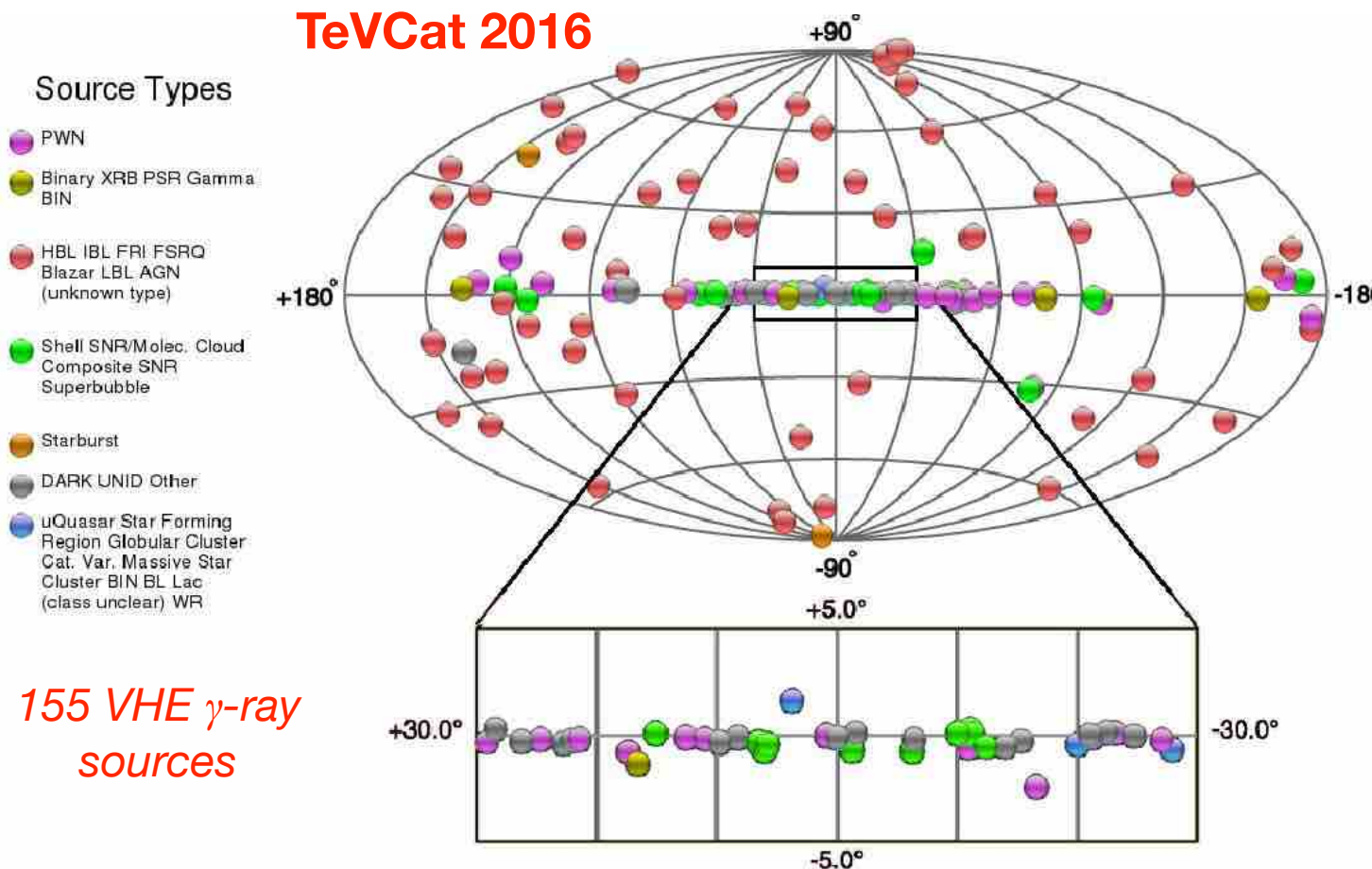
- ◆ Galactic/Extragalactic *unbiased survey*: detection of *unexpected sources*
- ◆ “Finder” telescope for CTA: provides *targets for in-depth observations*
- ◆ *Extended objects* (PWN, diffuse gamma-ray emission)
- ◆ High exposure for *flaring activity* (AGN, GRBs, solar flares): *transient factory*
- ◆ *Fundamental physics* (high mass dark matter > 10 TeV)
- ◆ “Classical” *Cosmic Ray Physics* (energy spectrum, elemental composition, anisotropy, hadronic interactions)
- ◆ *Multi-Messenger Instrument* (by definition)



No Wide FoV experiment to:

- *Explore the 100 GeV energy region*
- *Survey the Inner Galaxy and the Galactic Center*

The fascinating TeV γ -sky



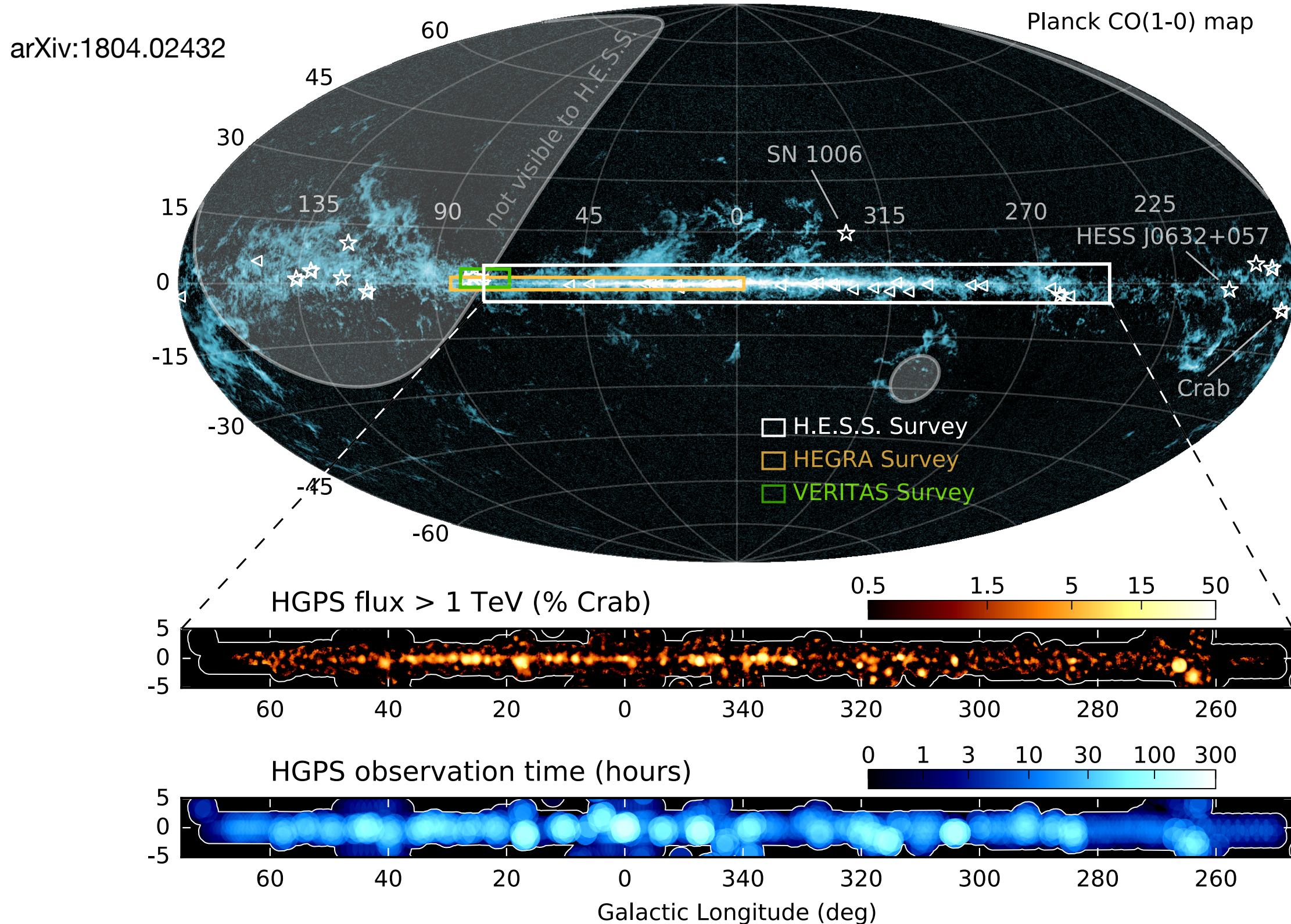
How complete is the Survey ?

If there is a (bright) PeVatron out there, would we have detected it already ?

- *Wide Field of View:* all-sky survey provides an *unbiased map of the sky*
- *Survey of the Southern sky*
- *High Energy Survey (100 TeV range)*



HESS Galactic Plane Survey



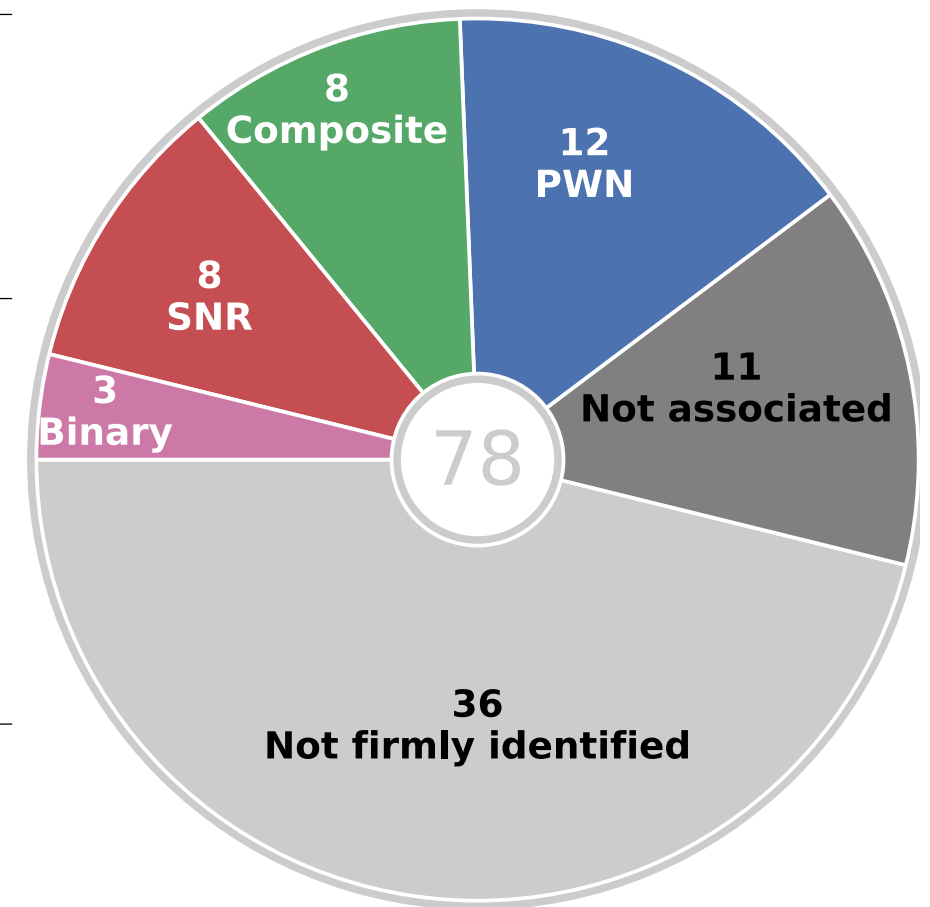
HESS Galactic Plane Survey

2700 hours observation from 2004 to 2013 at longitudes from $l=250^\circ$ to 65° and latitudes $|b| \leq 3^\circ$, angular resolution $\approx 0.08^\circ$ (≈ 5 arcmin), sensitivity $\leq 1.5\%$ Crab, energy range 0.2 TeV \rightarrow 100 TeV.

Table 3. Table of 31 firmly-identified objects among the HGPS sources. The object classes are γ -ray binary, shell-type supernova remnant (SNR), pulsar wind nebula (PWN), and composite SNR (in cases where it is not possible to distinguish between the shell and interior nebula). The evidence used to identify the VHE γ -ray emission include position, morphology, variability, and energy-dependent morphology (ED Morph.).

arXiv:1804.02432

Source name	Identified object	Class	Evidence	Reference
HESS J1018–589 A	1FGL J1018.6–5856	Binary	Variability	H.E.S.S. Collaboration et al. (2015e)
HESS J1302–638	PSR B1259–63	Binary	Variability	Aharonian et al. (2005c)
HESS J1826–148	LS 5039	Binary	Variability	Aharonian et al. (2006e)
HESS J0852–463	Vela Junior	SNR	Morphology	Aharonian et al. (2005e)
HESS J1442–624	RCW 86	SNR	Morphology	H.E.S.S. Collaboration et al. (2016e)
HESS J1534–571	G323.7–1.0	SNR	Morphology	H.E.S.S. Collaboration et al. (2017a)
HESS J1713–397	RX J1713.7–3946	SNR	Morphology	Aharonian et al. (2004b)
HESS J1718–374	G349.7+0.2	SNR	Position	H.E.S.S. Collaboration et al. (2015b)
HESS J1731–347	G353.6–0.7	SNR	Morphology	H.E.S.S. Collaboration et al. (2011a)
HESS J1801–233	W 28	SNR	Position	Aharonian et al. (2008d)
HESS J1911+090	W 49B	SNR	Position	H.E.S.S. Collaboration et al. (2016b)
HESS J0835–455	Vela X	PWN	Morphology	Aharonian et al. (2006c)
HESS J1303–631	G304.10–0.24	PWN	ED Morph.	H.E.S.S. Collaboration et al. (2012)
HESS J1356–645	G309.92–2.51	PWN	Position	H.E.S.S. Collaboration et al. (2011b)
HESS J1418–609	G313.32+0.13	PWN	Position	Aharonian et al. (2006f)
HESS J1420–607	G313.54+0.23	PWN	Position	Aharonian et al. (2006f)
HESS J1514–591	MSH 15–52	PWN	Morphology	Aharonian et al. (2005d)
HESS J1554–550	G327.15–1.04	PWN	Morphology	Section 5.6.5
HESS J1747–281	G0.87+0.08	PWN	Morphology	Aharonian et al. (2005a)
HESS J1818–154	G15.4+0.1	PWN	Morphology	H.E.S.S. Collaboration et al. (2014a)
HESS J1825–137	G18.00–0.69	PWN	ED Morph.	Aharonian et al. (2006g)
HESS J1837–069	G25.24–0.19	PWN	Morphology	Marandon et al. (2008)
HESS J1849–000	G32.64+0.53	PWN	Position	Section 5.6.15
HESS J1119–614	G292.2–0.5	Composite	Position	Section 5.6.1
HESS J1640–465	G338.3–0.0	Composite	Position	Abramowski et al. (2014b), Gotthelf et al. (2014)
HESS J1714–385	CTB 37A	Composite	Position	Aharonian et al. (2008c)
HESS J1813–178	G12.8–0.0	Composite	Position	Funk et al. (2007), Gotthelf & Halpern (2009)
HESS J1833–105	G21.5–0.9	Composite	Position	Section 5.6.10
HESS J1834–087	W 41	Composite	Morphology	H.E.S.S. Collaboration et al. (2015a)
HESS J1846–029	G29.7–0.3	Composite	Position	Section 5.6.13
HESS J1930+188	G54.1+0.3	Composite	Position	Acciari et al. (2010), Sect. 5.4



Important finding by HESS in the GC

A proton PeVatron:

a machine accelerating particles *up to 10^{15} eV* and beyond presently operates *in $R < 10$ pc* region of the Galactic Center with acceleration rate of protons above energy 10 TeV *at level 10^{37-38} erg/s*

This conclusion is based on *spectroscopic and morphological studies of diffuse VHE gamma-ray component* in so-called ~ 200 pc radius Central Molecular Zone (CMZ) of the GC

- ✓ for the first time, a gamma-ray spectrum is registered that continues without a cutoff or a break up to 20-30 TeV (most likely, 50 TeV)
- ✓ for the first time, the density profile of parent protons is derived based on analysis of spatial distributions of VHE gamma-rays and the gas in GC

VHE γ -ray spectra of the diffuse emission and the central source (HESS J1745-290)

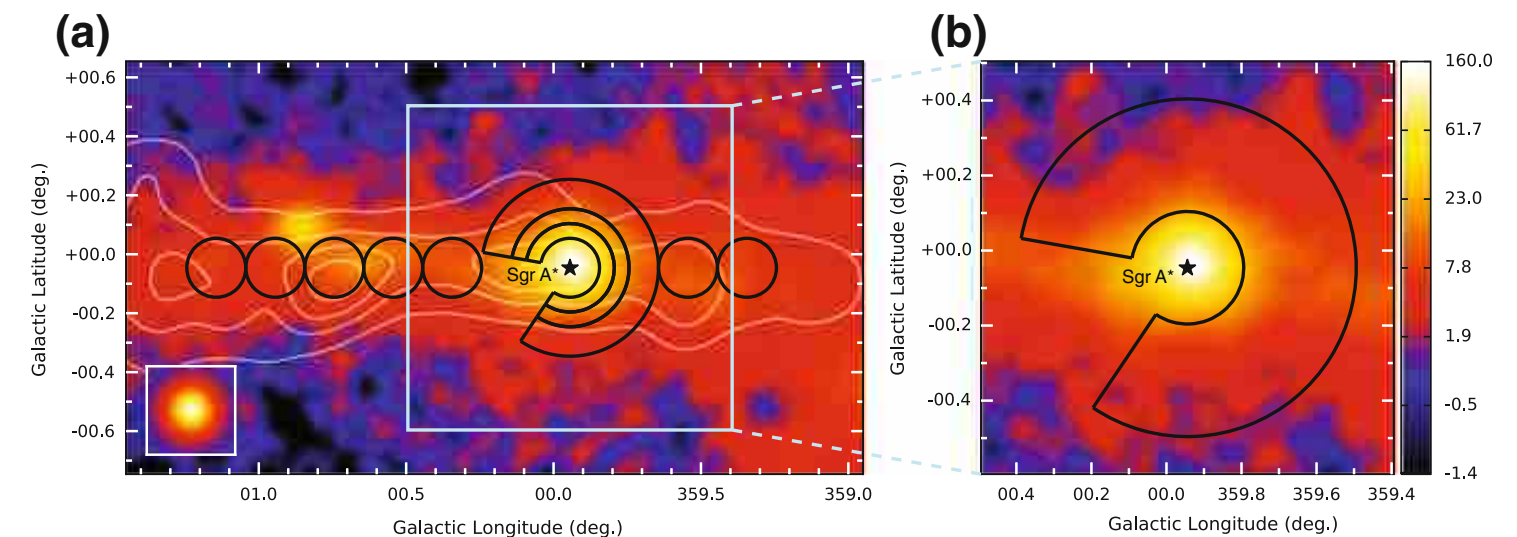
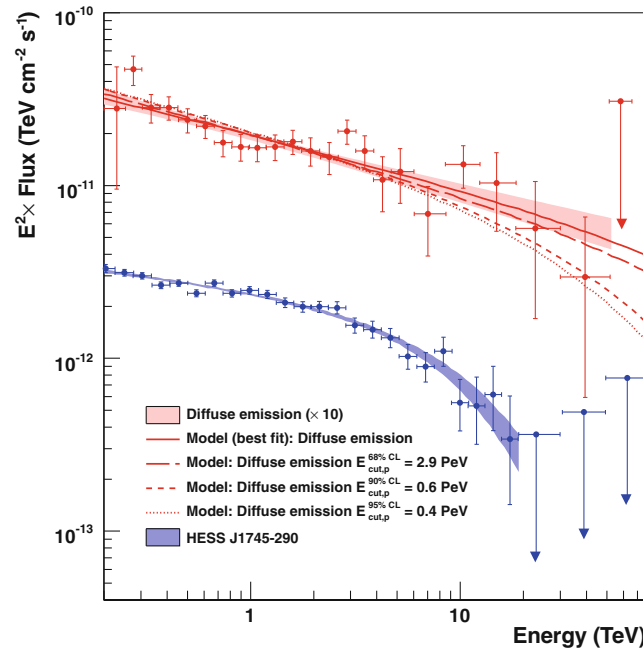
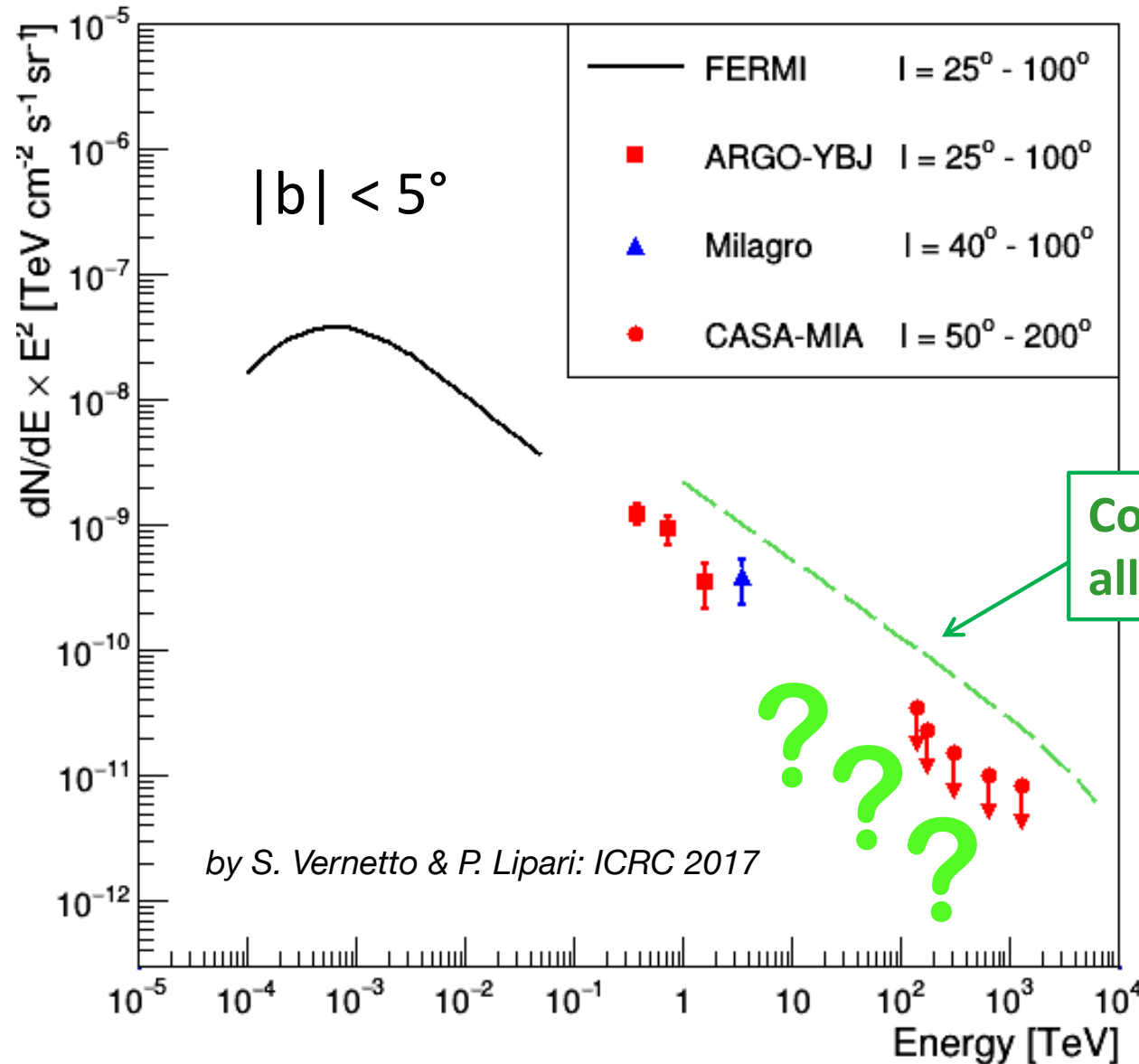


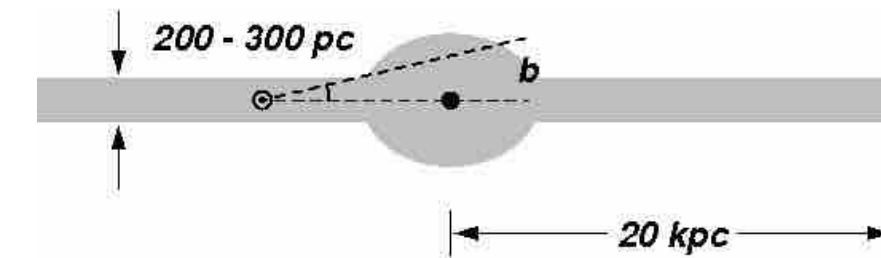
Fig. 17 VHE γ -ray image of the Galactic Centre region (from Ref. [55]). *Left panel* The black lines outline the regions used to extract the energy density of CRs. White contours indicate the density distribution of molecular gas. *Right panel* Zoomed view of the inner ~ 70 pc and the contour of the region used to extract the spectrum of the diffuse emission

Diffuse γ -rays from the Galactic Plane

Diffuse γ -rays are produced by relativistic electrons by bremsstrahlung or inverse Compton scattering on bkg radiation fields, or by protons and nuclei via the decay of π^0 produced in *hadronic interactions* with interstellar gas.

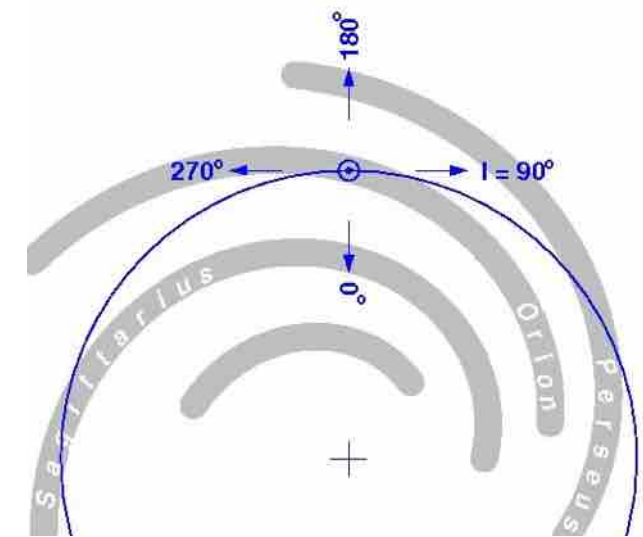


The space distribution of this emission can trace the location of the CR sources and the distribution of interstellar gas.



Cosmic rays
all particle flux $\times 10^{-4}$

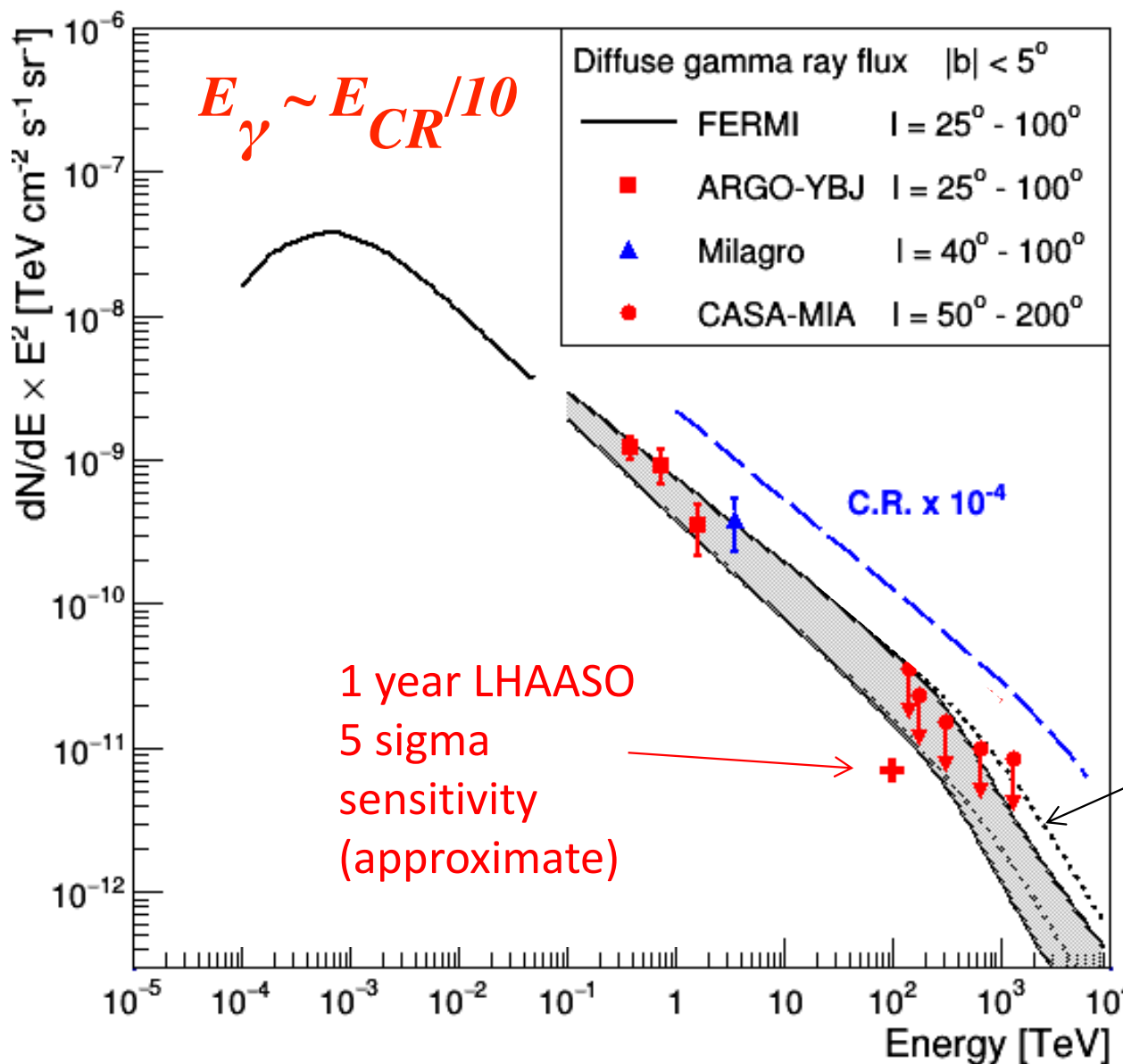
$$S_{ext} = S_{point} \cdot \frac{\theta_{PSF}}{\theta_{ext}}$$



Detectors with a 'poor' angular resolution are favoured in the extended source studies.

Expected Galactic diffuse γ -ray flux

Is **the knee a source property**, in which case we should see a corresponding spectral feature in the gamma-ray spectra of CR sources, or **the result of propagation**, so we should observe **a knee that is potentially dependent on location**, because the propagation properties depend on position in the Galaxy ?



Observing a location dependence of the knee energy (or of the spectral index !) would provide important clues on the nature of the knee.

by S. Vernetto & P. Lipari: ICRC 2017

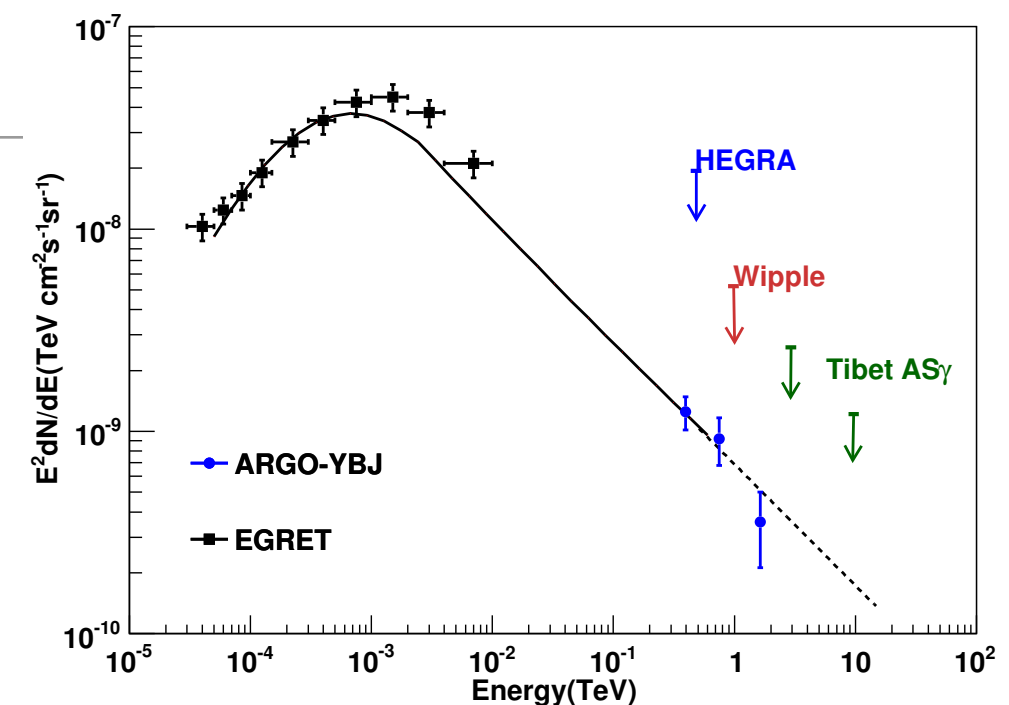
Diffuse Gamma Emission

Diffuse gamma-ray emission from the Galactic plane for $|b| < 5^\circ$

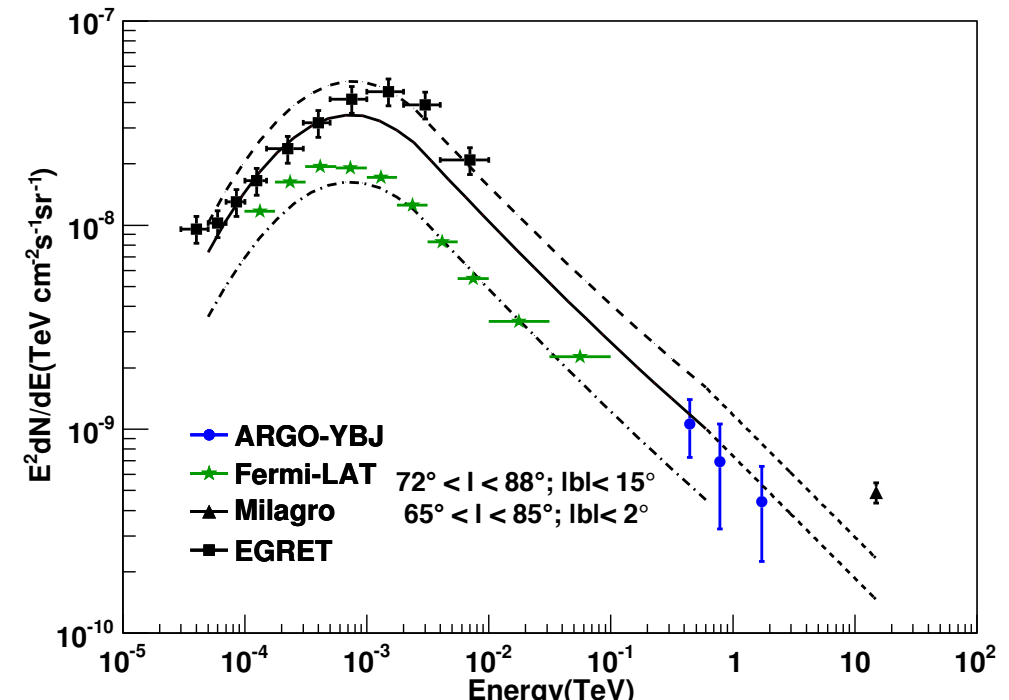
l Intervals	Significance	Spectral index	Energy(GeV)	Flux ^a
$25^\circ < l < 100^\circ$	6.9 s.d.	-2.80 ± 0.26	390	8.06 ± 1.49
			750	1.64 ± 0.43
			1640	0.13 ± 0.05
			1000 ^b	0.60 ± 0.13
$40^\circ < l < 100^\circ$	6.1 s.d.	-2.90 ± 0.31	350	10.94 ± 2.23
			680	2.00 ± 0.60
			1470	0.14 ± 0.08
			1000 ^b	0.52 ± 0.15
$65^\circ < l < 85^\circ$	4.1 s.d.	-2.65 ± 0.44	440	5.38 ± 1.70
			780	1.13 ± 0.60
			1730	0.15 ± 0.07
			1000 ^b	0.62 ± 0.18
$25^\circ < l < 65^\circ \& 85^\circ < l < 100^\circ$	5.6 s.d.	-2.89 ± 0.33	380	9.57 ± 2.18
			730	1.96 ± 0.59
			1600	0.12 ± 0.07
			1000 ^b	0.60 ± 0.17
$130^\circ < l < 200^\circ$	-0.5 s.d.	-	-	$< 5.7^c$

^aIn units of $10^{-9} \text{ TeV}^{-1} \text{ cm}^{-2} \text{ s}^{-1} \text{ sr}^{-1}$.

ApJ 806 (2015) 20



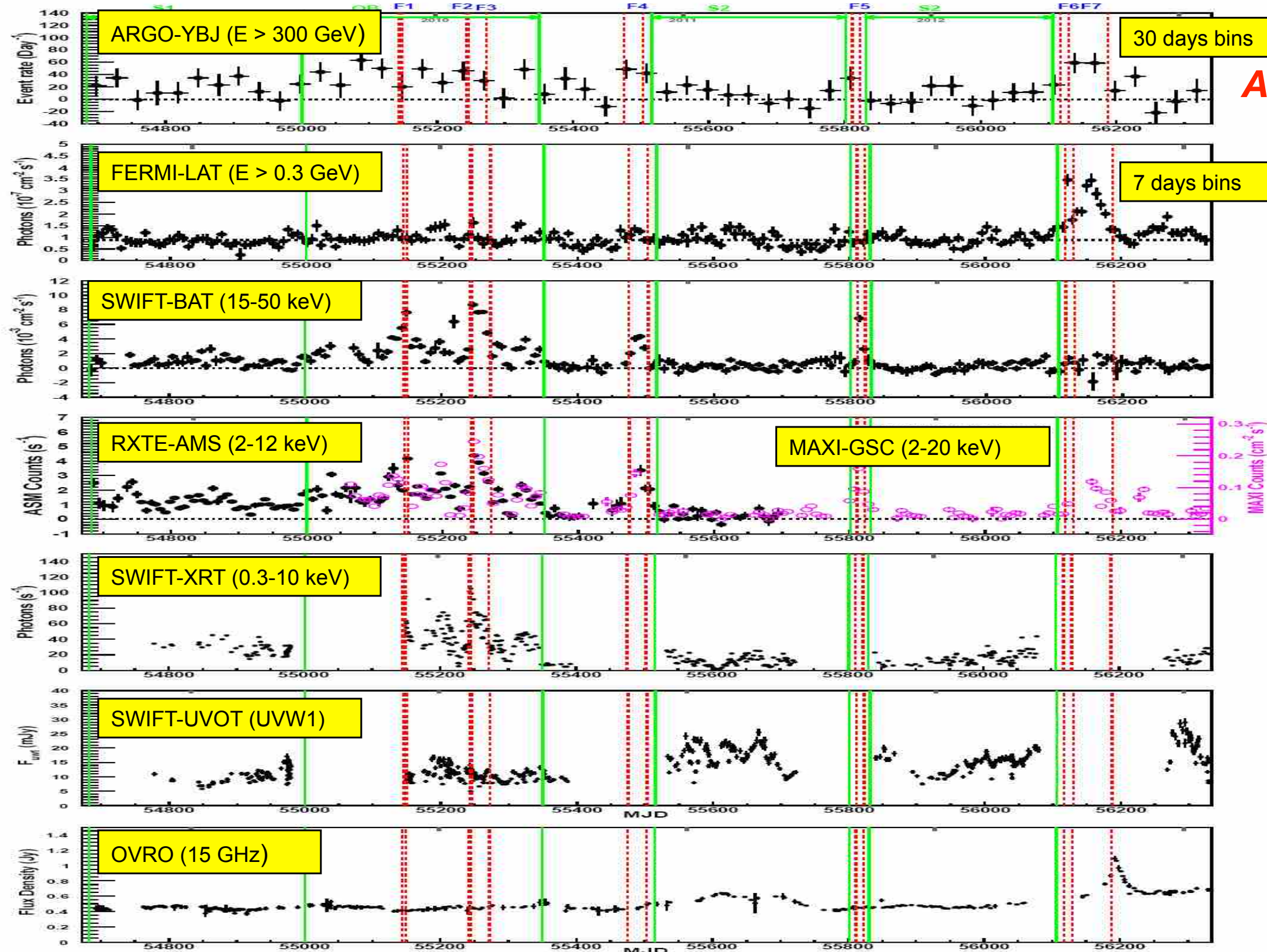
Cygnus region: $65^\circ < |l| < 85^\circ; |b| < 5^\circ$



Interestingly, *the energy spectrum of the light component ($p+He$) up to 700 TeV measured by ARGO-YBJ follows the same spectral shape as that found in the Cygnus region.*

A precise comparison of the spectrum of young CRs, as those supposed in the Cygnus region, with the spectrum of old CRs resident in other places of the Galactic plane, could help to determine the *distribution of the sources of CRs*.

The flaring γ -ray sky: Mrk421



One-zone Synchrotron Self-Compton model

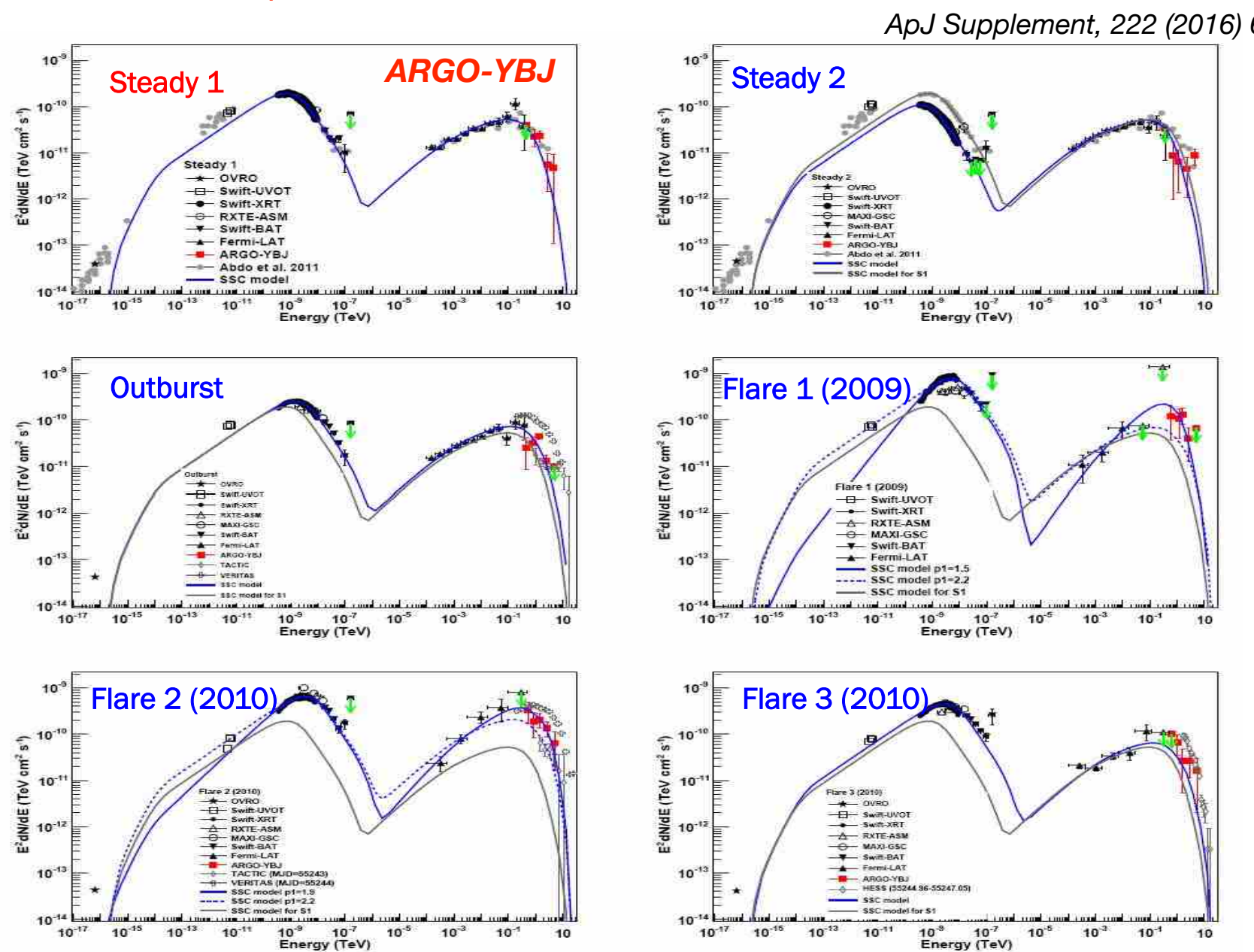
Consider a population of relativistic electrons in a magnetized region. They will produce *synchrotron radiation*, and therefore they will fill the region with photons. These synchrotron photons will have some probability to interact again with the electrons, by the *Inverse Compton* process.

Since the *electron “work twice”* (first making synchrotron radiation, then scattering it at higher energies) this particular kind of process is called *synchrotron self-Compton*, or *SSC* for short.

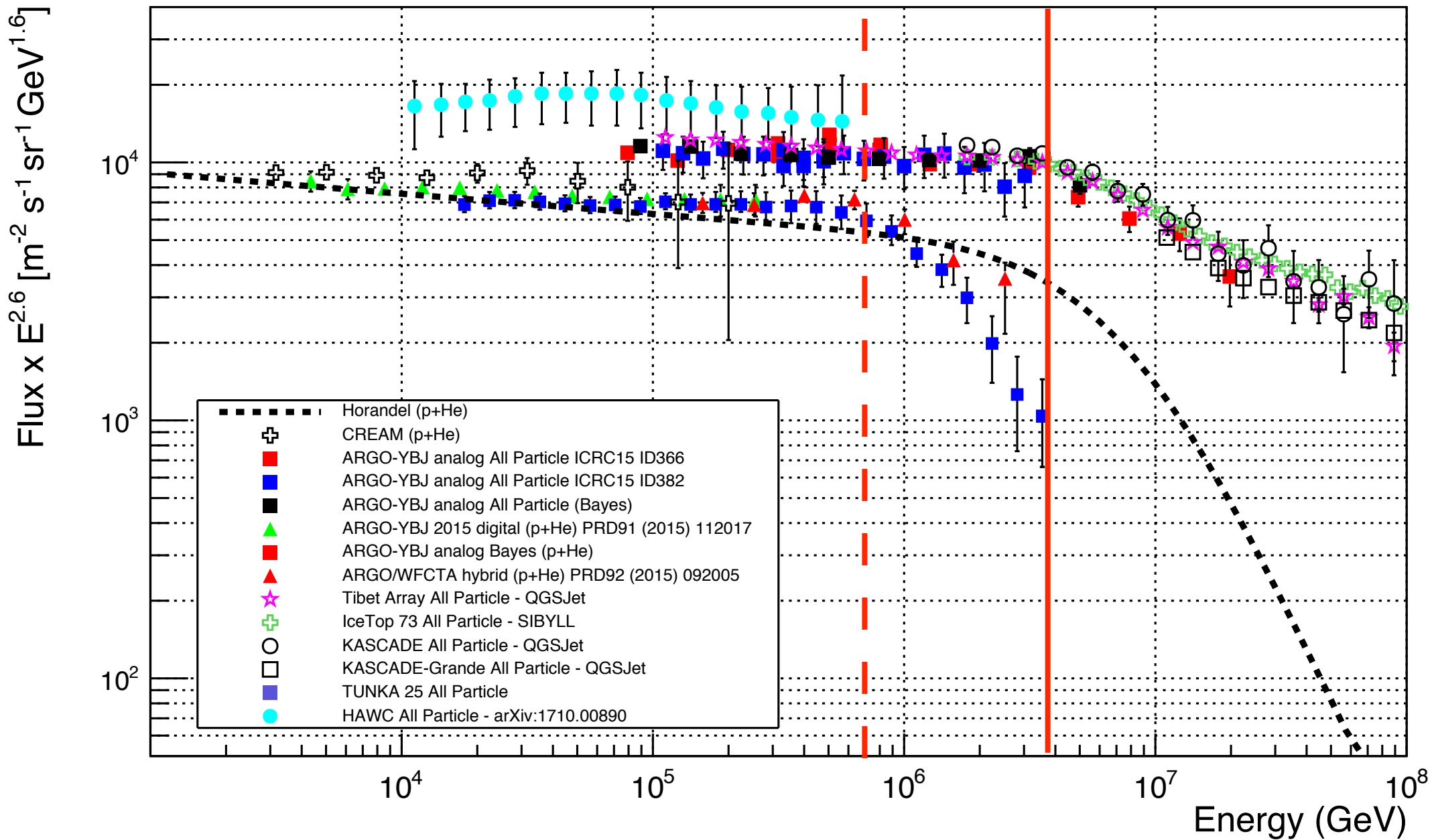
The *one-zone model* assumes that non-thermal radiations are produced in a single, homogeneous and spherical region in the jet.

The emission region moves relativistically toward us, and consequently the intrinsic radiation is strongly amplified due to the Doppler boosting.

Three parameters are needed to characterise the emission region: the comoving magnetic field, the Doppler factor and the comoving radius of the emission region.



CR energy spectrum: the overall picture



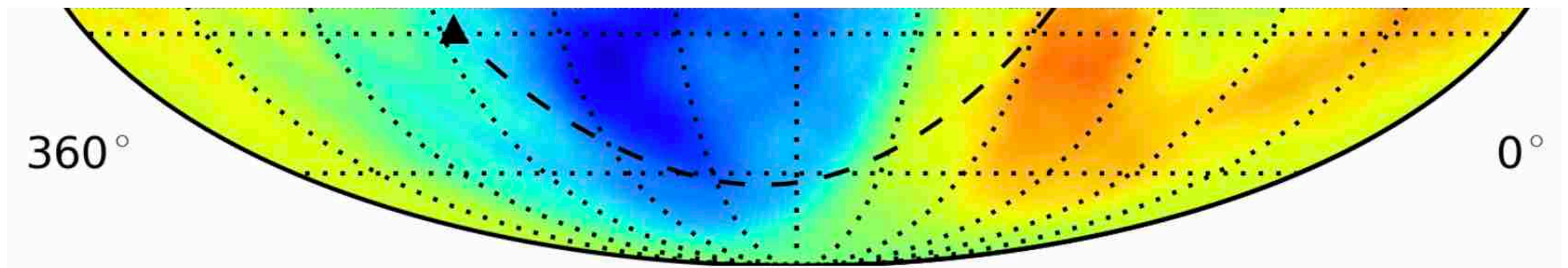
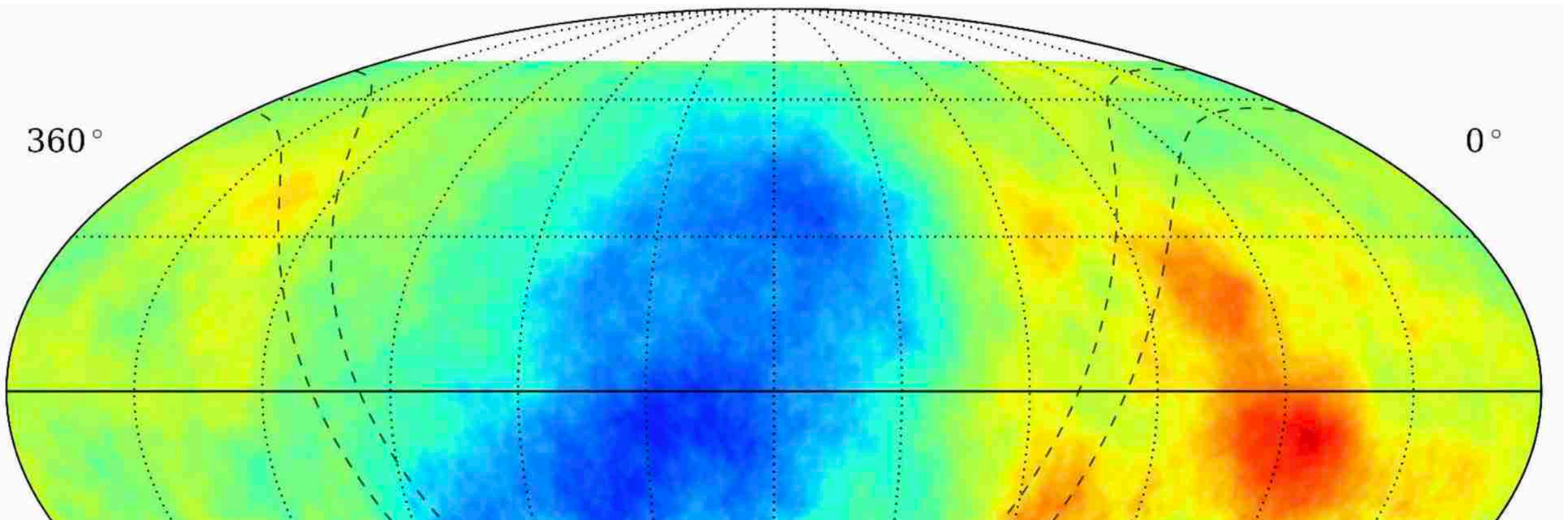
Experimental results in the knee region still conflicting:

ARGO-YBJ reports evidence for a *proton knee starting at about 700 TeV*

The proton knee is connected to the maximum energy of accelerated particles in CR sources !

Full-Sky Cosmic Ray Anisotropy

HAWC



Credit: P. Desiati & J.C. Diaz Velez

IceCube

Cosmic Ray mass dependency ?

Energy dependency (< knee)

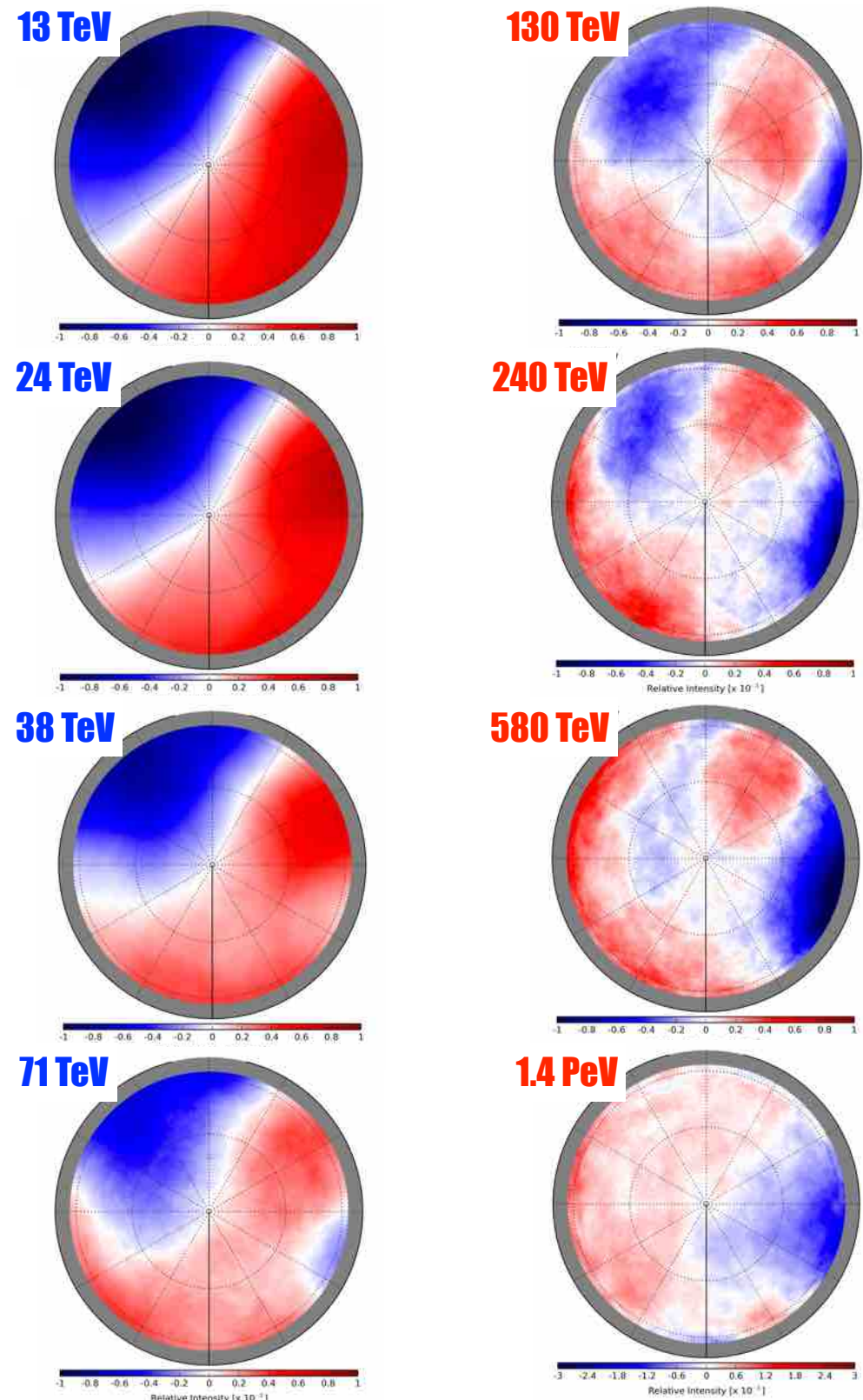
Anisotropy depends on primary energy

CR composition changes as well with energy

After IceCube/IceTop observations we know very well the anisotropy in the Southern Hemisphere at different angular scales but...

...we need anisotropy observations vs CR particle rigidity !

A *combined measurement* of CR energy spectrum, mass composition and anisotropy inevitably probes the properties and spatial distribution of their sources as well as of the long propagation journey through the magnetized medium.



Credit: P. Desiati

CTA and a new Wide FoV observatory

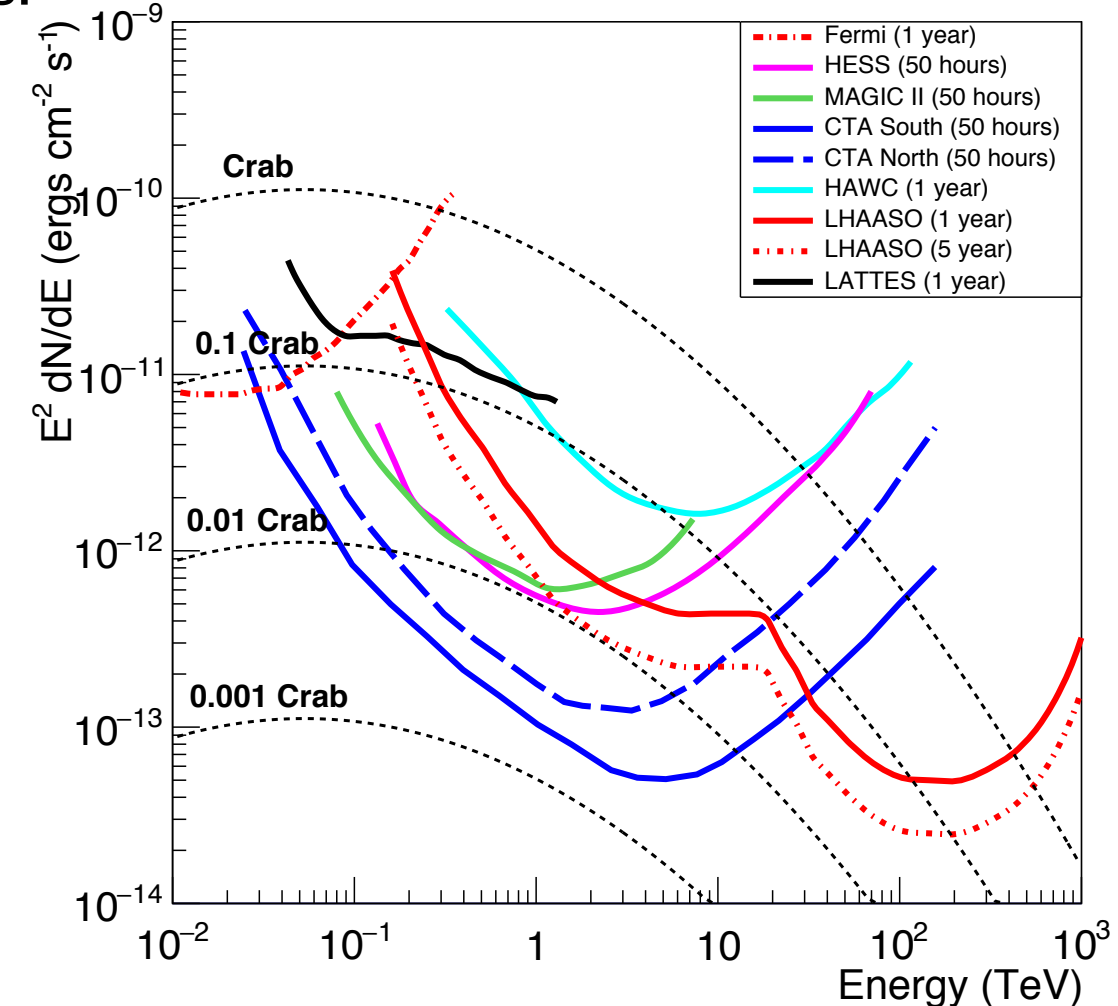
A future Wide FoV Observatory to be useful to CTA needs:

- <10% Crab sensitivity below TeV
- *Low energy threshold (≈ 100 GeV)*
- Ability to detect extragalactic transient (AGN, GRBs)
- *Southern hemisphere site*

★ Is this possible ?

Minimum Detectable Gamma-Ray Flux (1 year):

$$\Phi_{\gamma}^{MDF} \propto \sqrt{\Phi_B} \cdot \frac{1}{R \cdot \sqrt{A_{eff}^{\gamma}}} \cdot \psi_{70} \cdot \frac{1}{Q_f}$$



Φ_B = background flux

ψ_{70} = opening angle

$A_{eff}^{\gamma,p}(E)$ = effective area

$$R = \sqrt{\frac{A_{eff}^{\gamma}(E)}{A_{eff}^B(E)}}$$

$$Q_f = \frac{\text{fraction of surviving photons}}{\sqrt{\text{fraction of surviving hadrons}}}$$

The key parameters

$$S \propto \frac{\Phi_\gamma}{\sqrt{\Phi_{bkg}}} \cdot R \cdot \sqrt{A_{eff}^\gamma} \cdot \frac{1}{\sigma_\theta} \cdot Q$$

For the integral fluxes we can write $\Phi_\gamma \sim E_{thr}^{-\gamma}$ and $\Phi_{bkg} \sim E_{thr}^{-\gamma_{bkg}}$ and we obtain $\frac{\Phi_\gamma}{\sqrt{\Phi_{bkg}}} \sim E_{thr}^{-(\gamma - \gamma_{bkg}/2)} \sim E_{thr}^{-2/3}$ being $\gamma \sim 1.5$ and $\gamma_{bkg} \sim 1.7$.

The *key parameters* to improve the sensitivity are

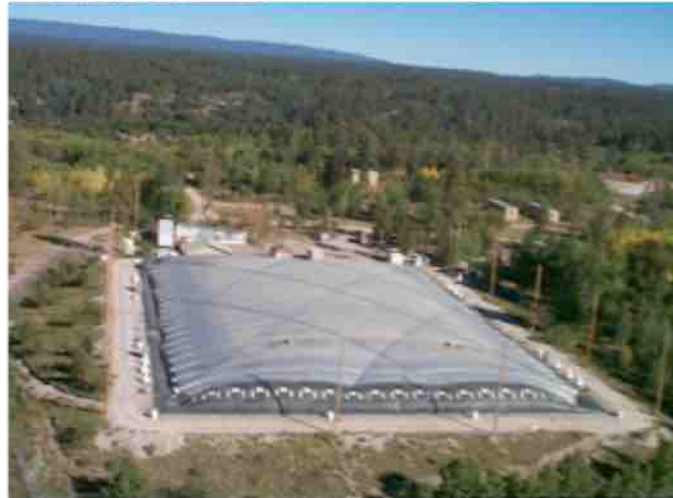
- The energy threshold
- R, the signal/background relative trigger efficiency
- The angular resolution
- Q-factor, the background rejection capability

Milagro vs ARGO-YBJ

2 different approaches in the last decade for ground-based survey instruments

Milagro

Water Cherenkov Technology



- operated from 2000 to 2008
- **2600 m** above sea level
- angular resolution $\approx 0.5^\circ$
- 1700 Hz trigger rate
- *Median Energy at the threshold:* $\approx 2 \text{ TeV}$
- *Energy range:* 2 - 40 TeV
- poor background rejection via muons (with outrigger)
- conversion of secondary photons in water

Widely used technology in cosmic ray physics

ARGO-YBJ

Resistive Plate Chamber Technology



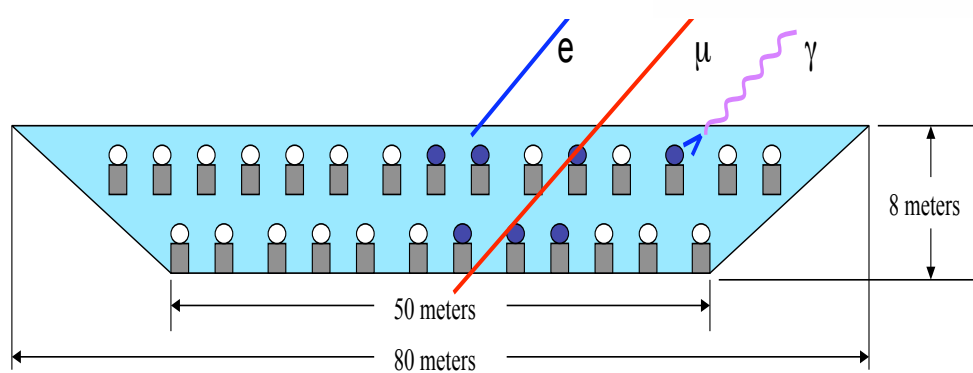
- operated from 2007 to 2012 (final configuration)
- **4300 m** above sea level
- angular resolution $\approx 0.5^\circ$
- 3500 Hz trigger rate
- high granularity of the readout
- *Median Energy at the threshold:* $\approx 360 \text{ GeV}$
- *Energy Range:* 360 GeV - 10 PeV
- NO background rejection (no muons identification)
- NO conversion of secondary photons (no lead)

Widely used technology in accelerator physics

Milagro vs ARGO-YBJ

Milagro

Water Cherenkov Technology



Central **80 m x 60 m x 8 m** water reservoir, containing two layers of PMTs

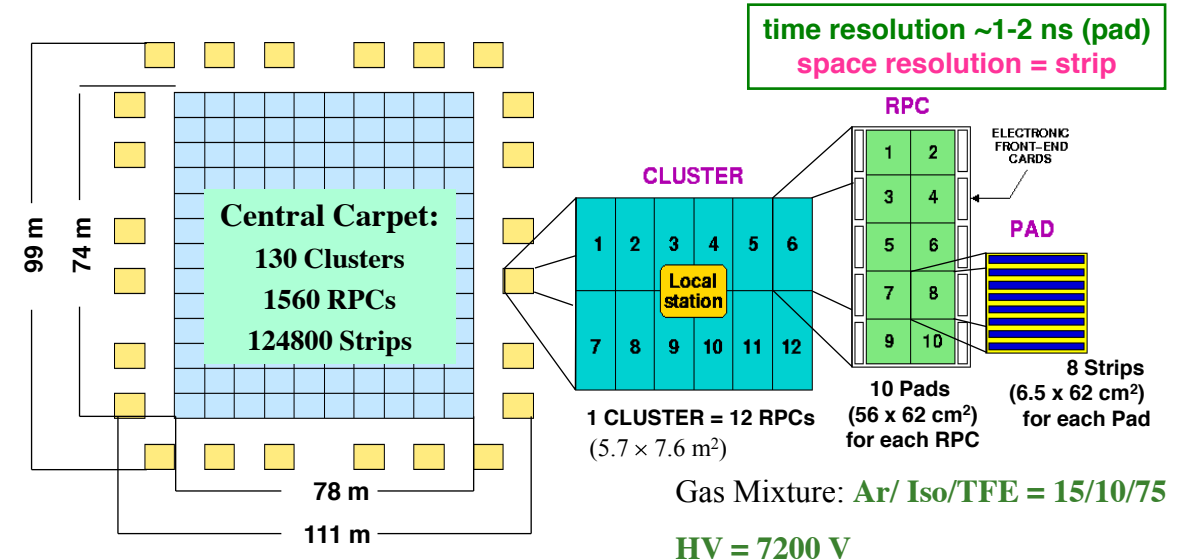
- 450 PMTs at 1.4 m below the surface (top layer)
- 273 PMTs at 6 m below the surface (bottom layer)

Outrigger Array, consisting of 175 tanks filled with water and containing one PMT, distributed on an area of **200 m x 200 m** around the central water reservoir.

→ **HAWC** and **LHAASO**

ARGO-YBJ

Resistive Plate Chamber Technology



Single layer of Resistive Plate Chambers (RPCs)
with a full coverage (92% active surface) of a large area (5600 m^2)
+ sampling guard ring (6700 m^2 in total)

Space pixels: **146,880 strips** ($7 \times 62\text{ cm}^2$)
Time pixels: **18,360 pads** ($56 \times 62\text{ cm}^2$)

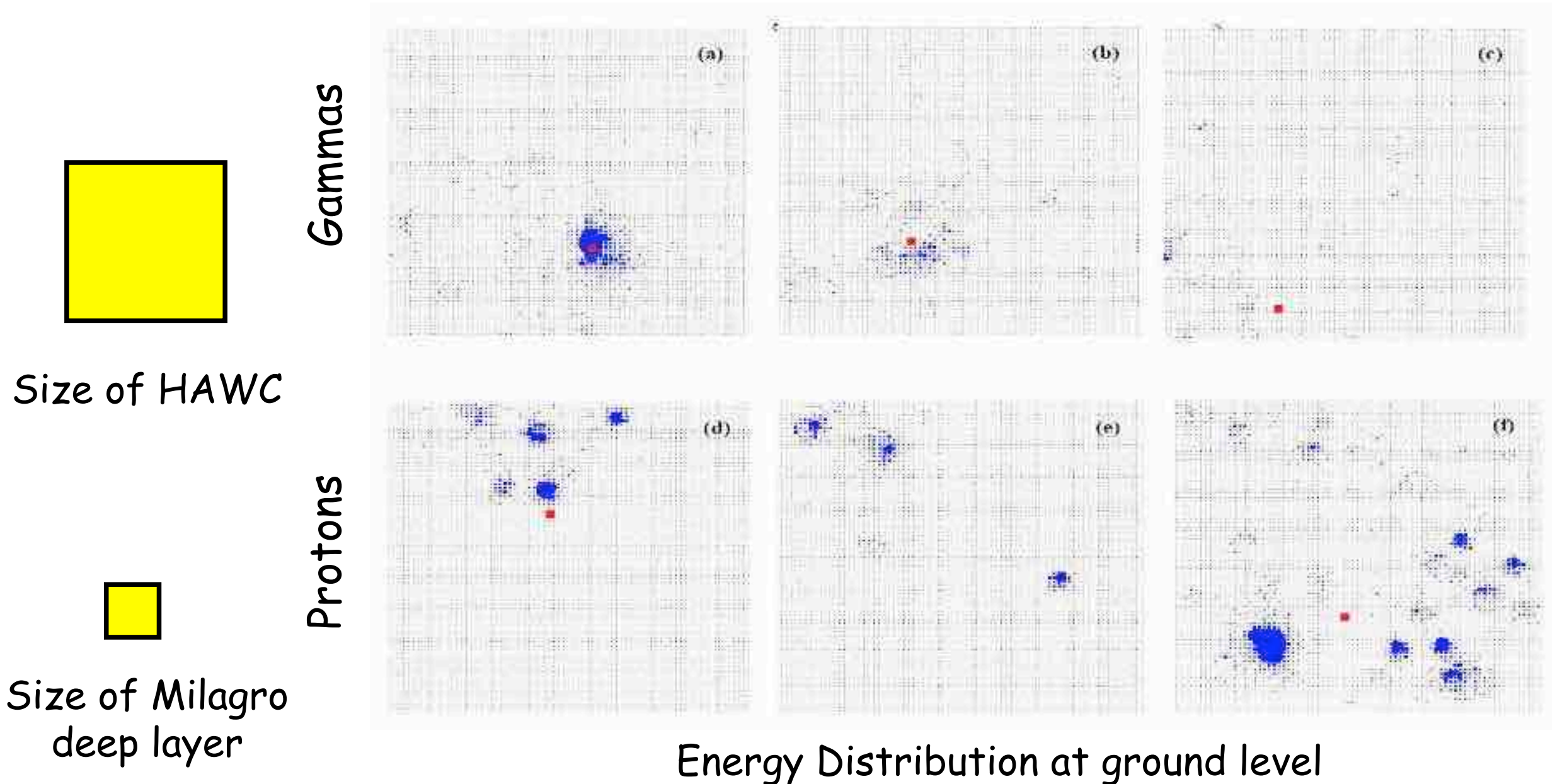
2 read-outs:

$$\rho_{max-strip} \approx 20 \text{ particles/m}^2$$

$$\rho_{max-analog} \approx 10^4 \text{ particles/m}^2$$

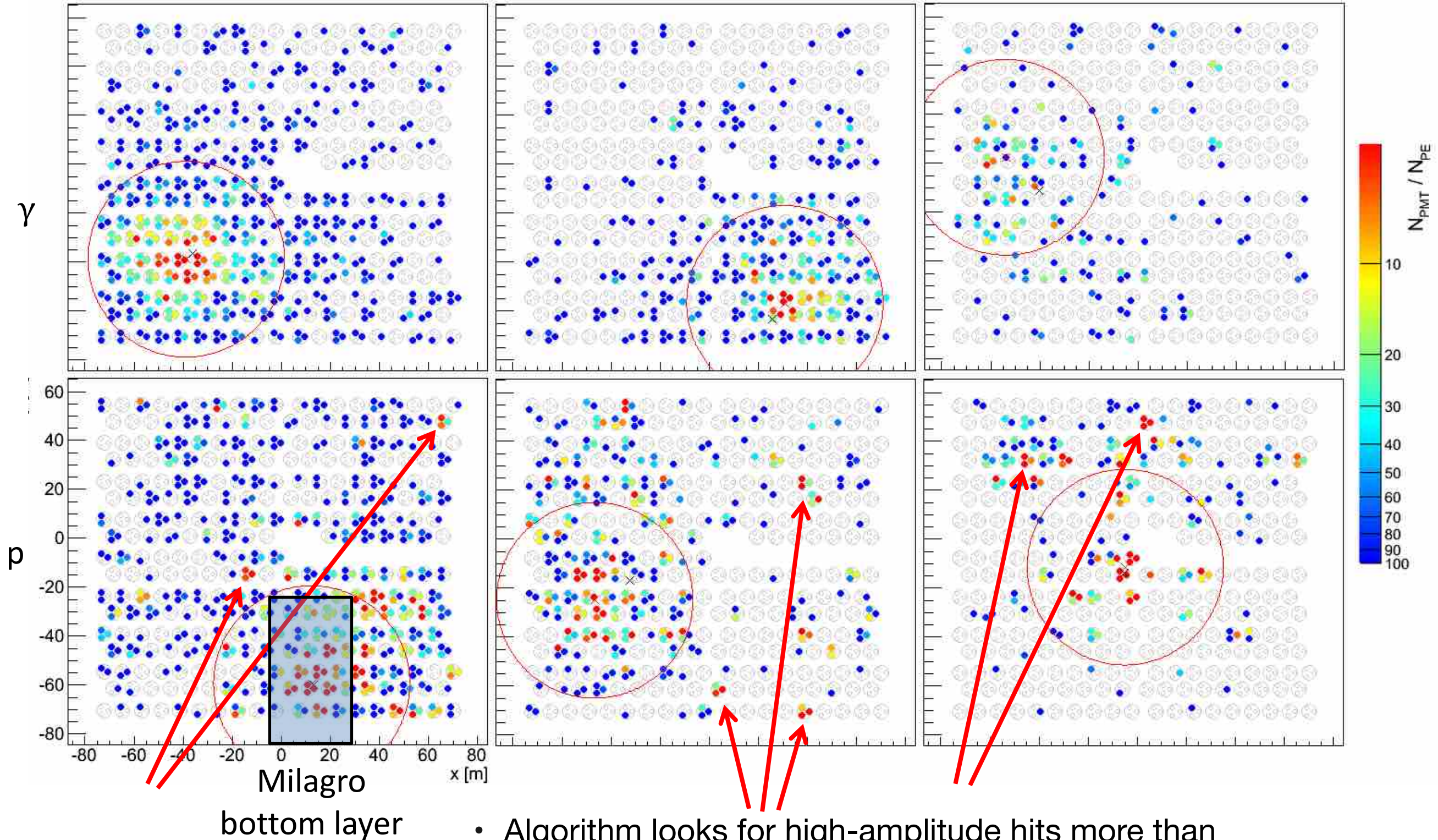
→ **MATHUSLA** proposal, CR and hadronic physics at CERN (RPC carpets above ATLAS)

Dimensions are important...



- Proton showers (with high P_T hadronic interactions) contain high-energy muons, hadrons and multiple EM clumps.
- Large energy depositions outside the core region indicate hadron-like showers.

Dimensions are important...



Scientific results

Milagro

Water Cherenkov Technology

- Gamma-ray Astronomy
- CR anisotropy
- *No results on selection of different primary masses and spectra of different elements*

HAWC

Water Cherenkov Technology

- Gamma-ray Astronomy
- CR anisotropy
- All-particle energy spectrum
- *Still no results on the selection of different primary masses*

ARGO-YBJ

Resistive Plate Chamber Technology

- Gamma-ray Astronomy
- CR anisotropy
- All-particle energy spectrum up to the knee range
- Study of the shower core region
- Selection of light component (p+He) and *observation of the proton knee*

With ARGO-YBJ we demonstrated that RPCs can be safely operated at extreme altitude for many years.

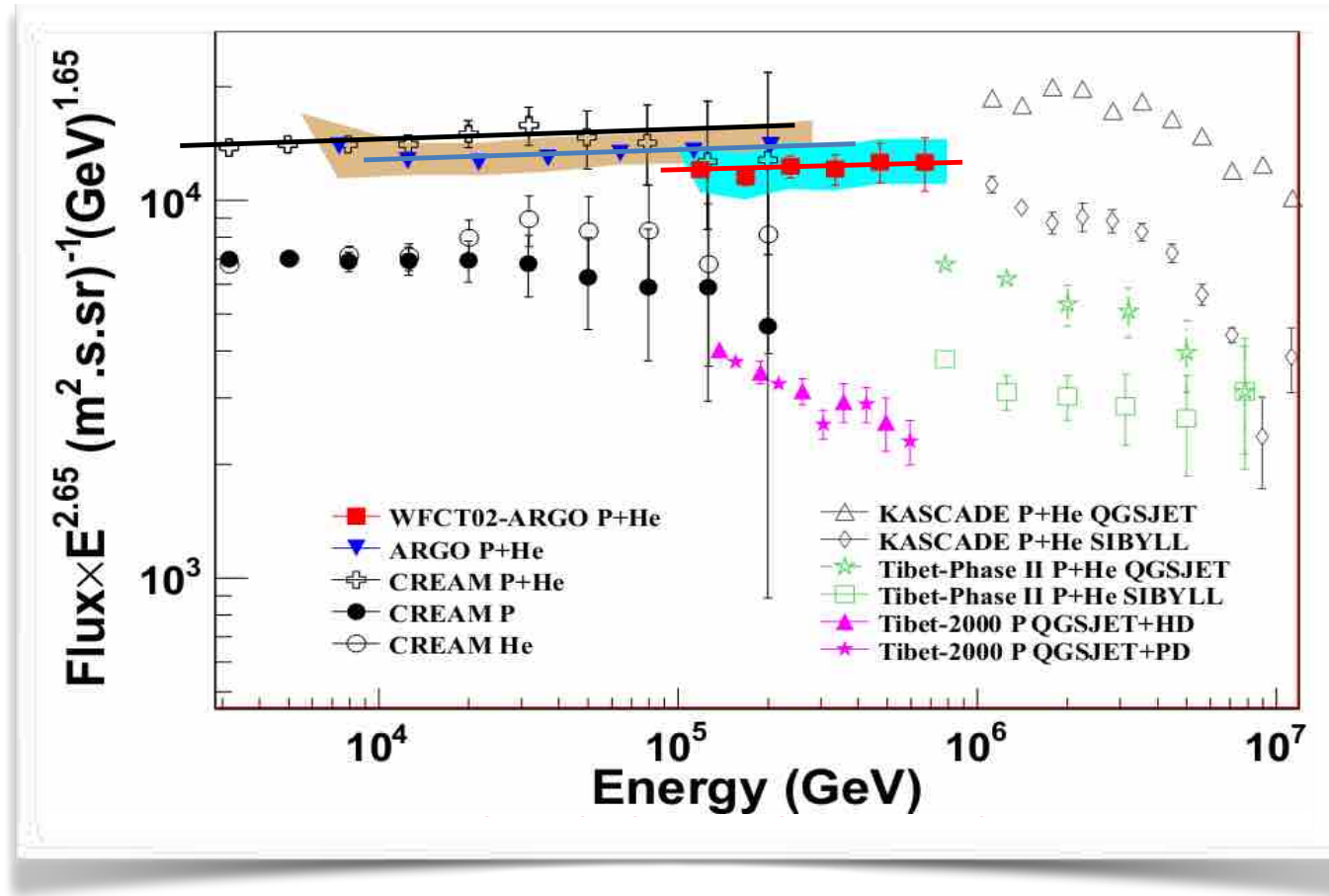
Benefits of RPCs in ARGO-YBJ:

- *dense sampling* → low energy threshold (≈ 300 GeV)
- *wide energy range*: ≈ 300 GeV → 10 PeV
- *high granularity of the read-out* → good angular resolution and unprecedented details in the core region



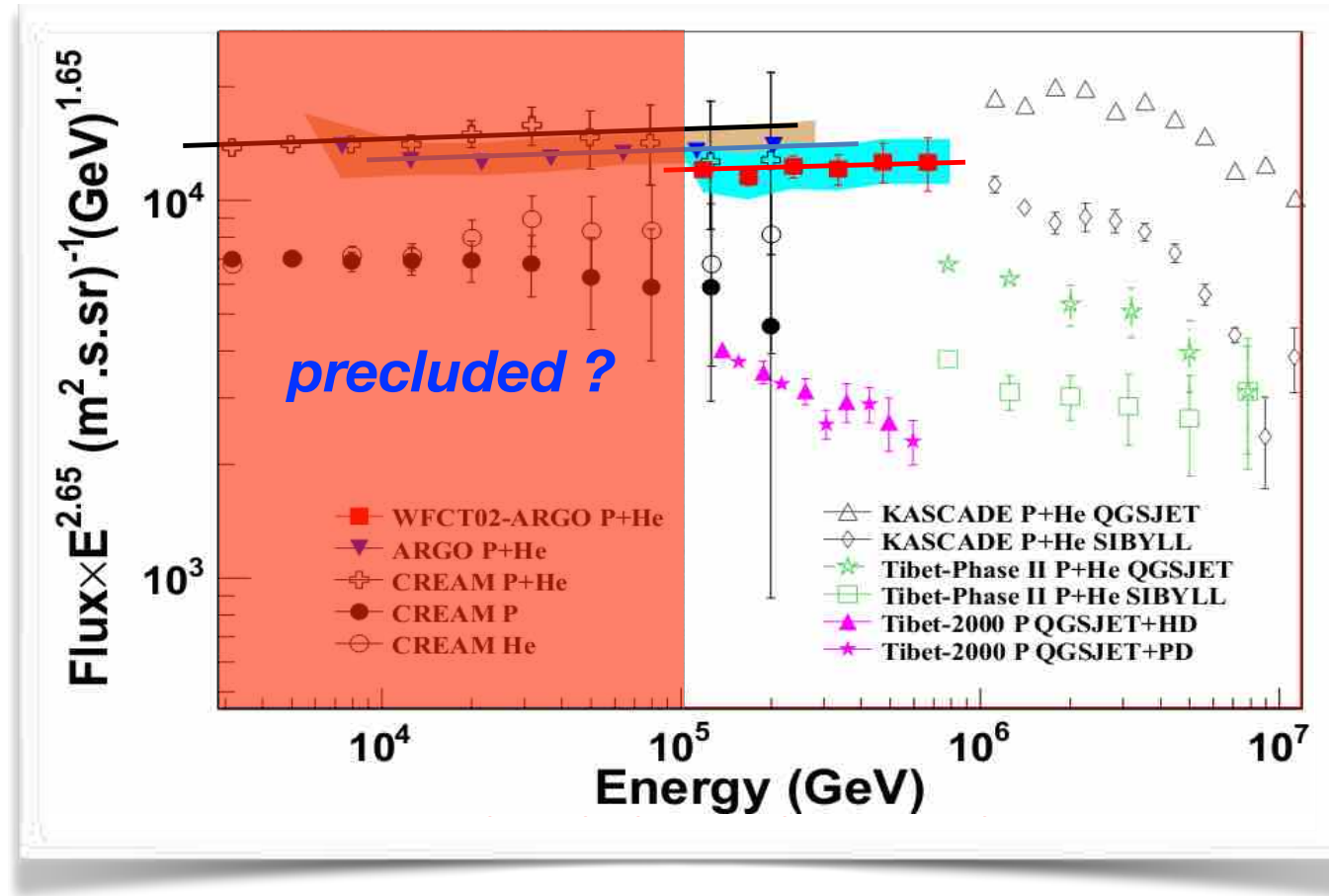
The capability of Water Cherenkov facilities in extending the energy range to PeV and in selecting primary masses must be investigated

Overposition with direct measurements

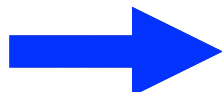


If Water Cherenkov facilities are not able to select primary masses, the measurements of light component is precluded to HAWC and will be possible to LHAASO only with WFCTA, but only starting above 100 TeV.

Overposition with direct measurements

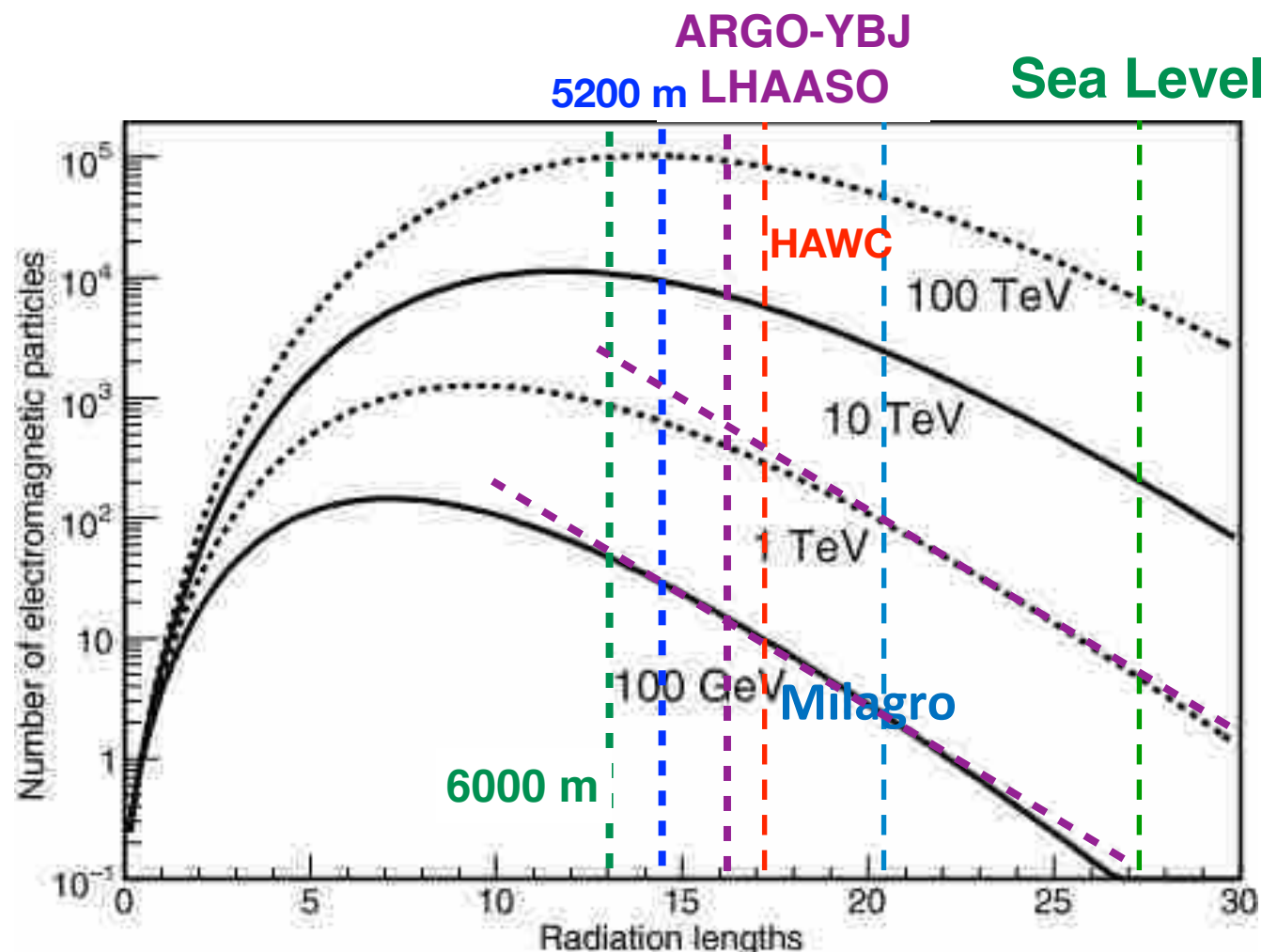


If Water Cherenkov facilities are not able to select primary masses, the measurements of light component is precluded to HAWC and will be possible to LHAASO only with WFCTA, but only starting above 100 TeV.



NO (or limited) overposition with direct measurement !
Limited calibration of the absolute energy scale !

Lowering the energy threshold: extreme altitude



This imply that the effective areas of EAS detectors increases at low energies.

Showers of all energies have the same slope after shower maximum: $\approx 1.65 \times$ decrease per r.l. .
So, for all energies, if a detector is located one radiation length higher in atmosphere, the result will be a $\approx 1.65 \times$ decrease in the energy observable.

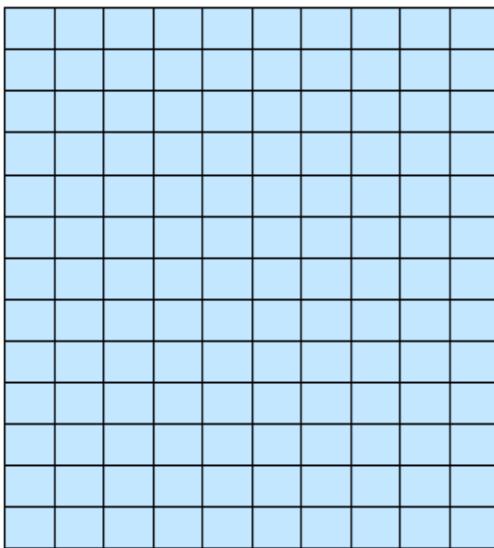
Lowering the energy threshold:

- *Extreme altitude ($\approx 5000 \text{ m asl}$)*
- *Detector and layout*
- *Coverage and granularity of the read-out*
- *Trigger logic*
- *Detection of secondary photons*

The full coverage approach

ARGO-YBJ is a high altitude **full coverage** EAS-array
optimized for the detection of small size air showers.

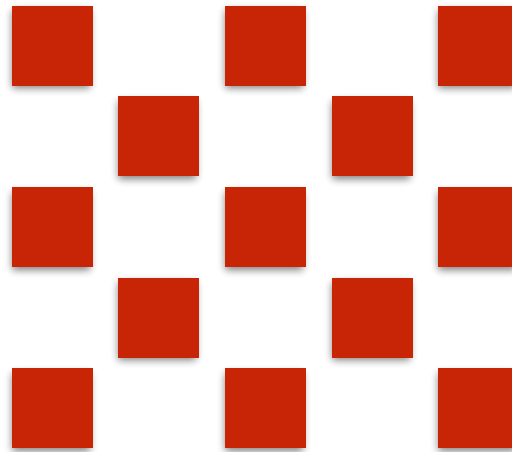
ARGO-YBJ central carpet



a continuous carpet of detectors

coverage factor ≈ 0.92

sparse array

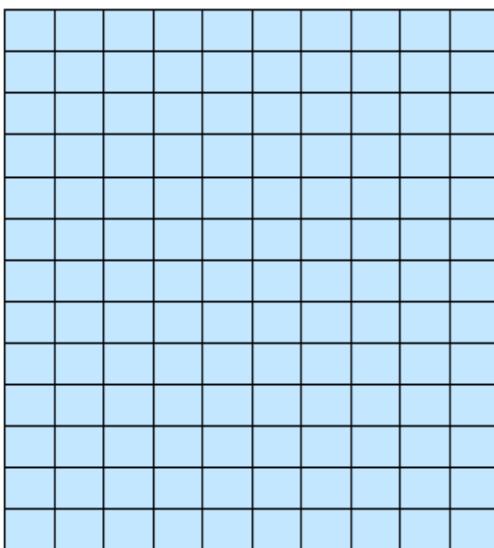


coverage factor $\approx 10^{-3} - 10^{-2}$

The full coverage approach

ARGO-YBJ is a high altitude **full coverage** EAS-array
optimized for the detection of small size air showers.

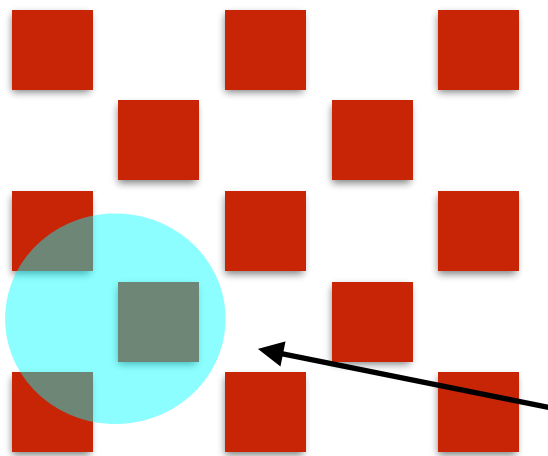
ARGO-YBJ central carpet



a continuous carpet of detectors

coverage factor ≈ 0.92

sparse array



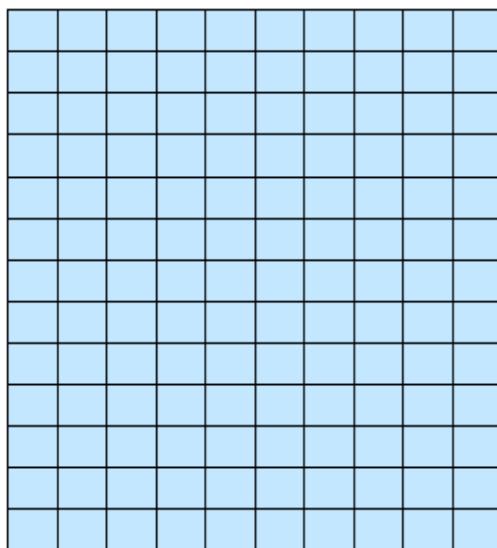
coverage factor $\approx 10^{-3} - 10^{-2}$

high energy shower = big shower
→ trigger

The full coverage approach

ARGO-YBJ is a high altitude **full coverage** EAS-array
optimized for the detection of small size air showers.

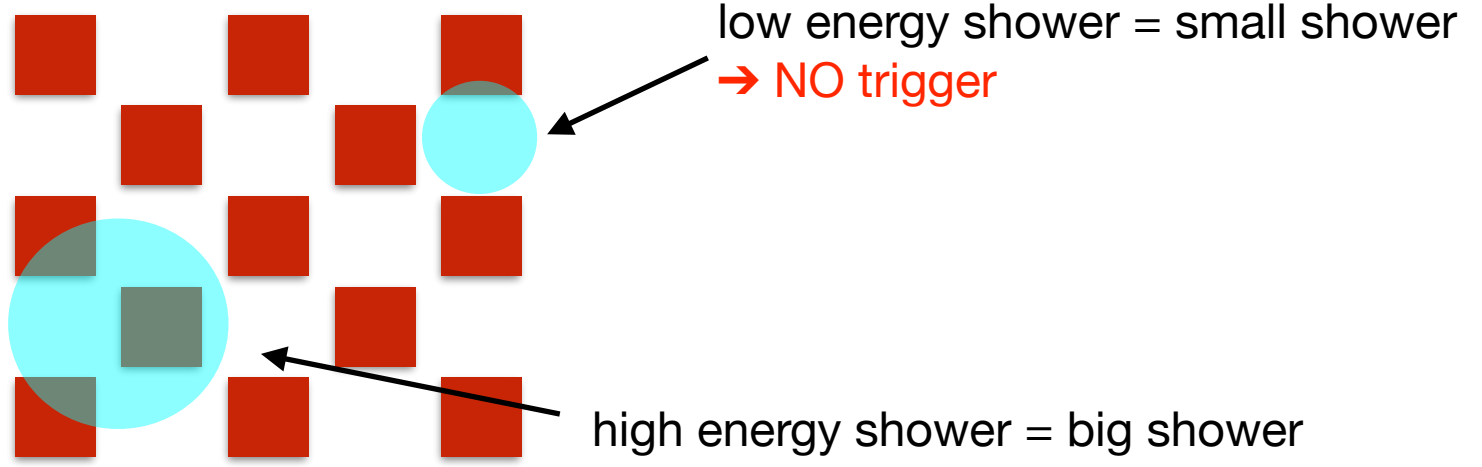
ARGO-YBJ central carpet



a continuous carpet of detectors

coverage factor ≈ 0.92

sparse array



high energy shower = big shower
→ trigger

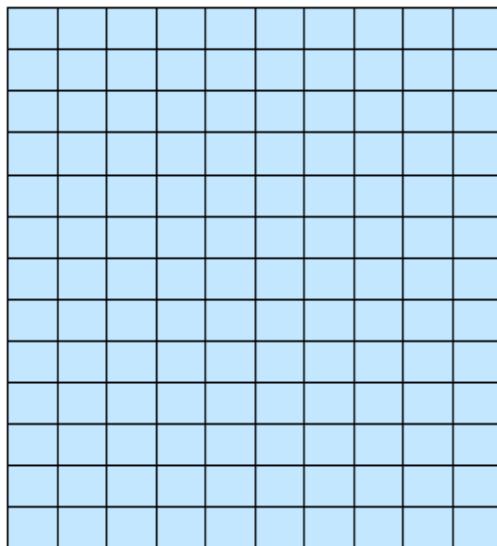
coverage factor $\approx 10^{-3} - 10^{-2}$

low energy shower = small shower
→ NO trigger

The full coverage approach

ARGO-YBJ is a high altitude **full coverage** EAS-array
optimized for the detection of small size air showers.

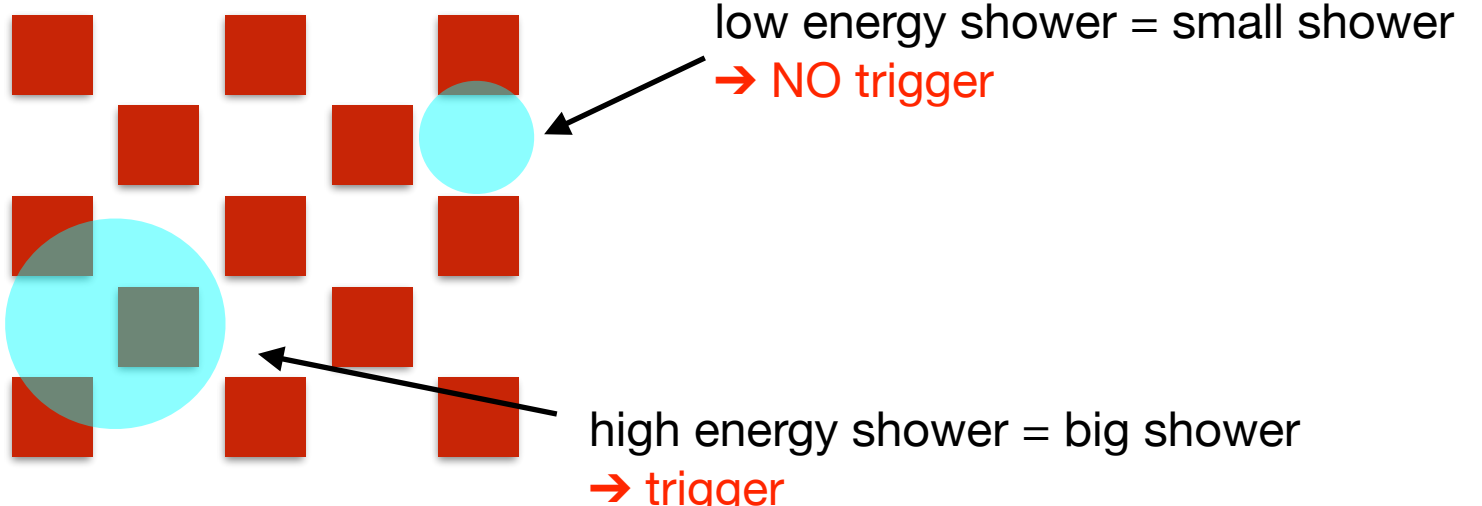
ARGO-YBJ central carpet



a continuous carpet of detectors

coverage factor ≈ 0.92

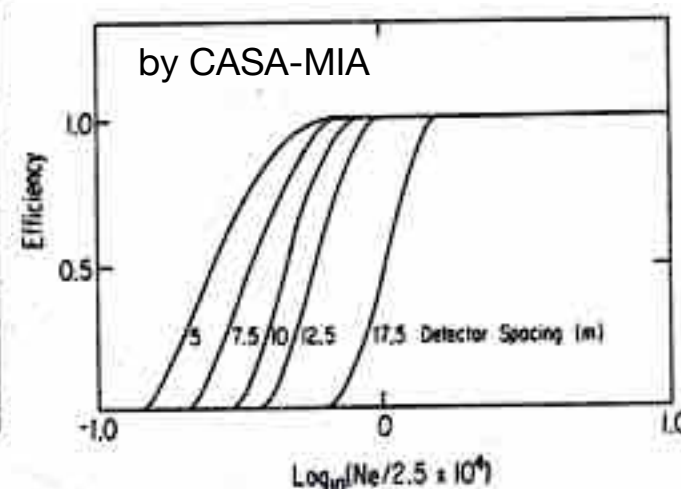
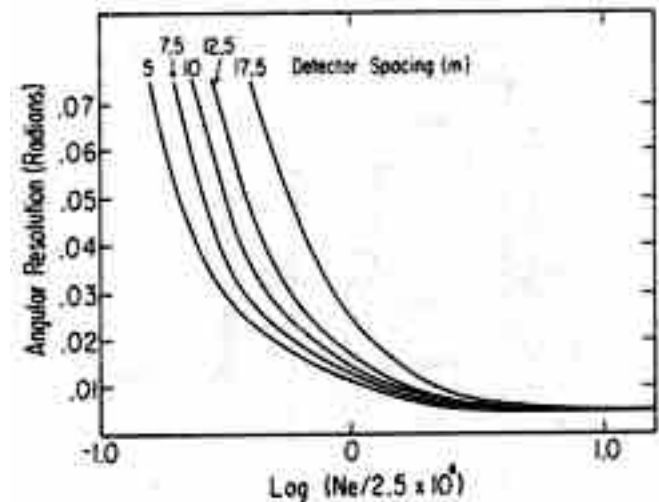
sparse array



low energy shower = small shower
→ NO trigger

high energy shower = big shower
→ trigger

coverage factor $\approx 10^{-3} - 10^{-2}$



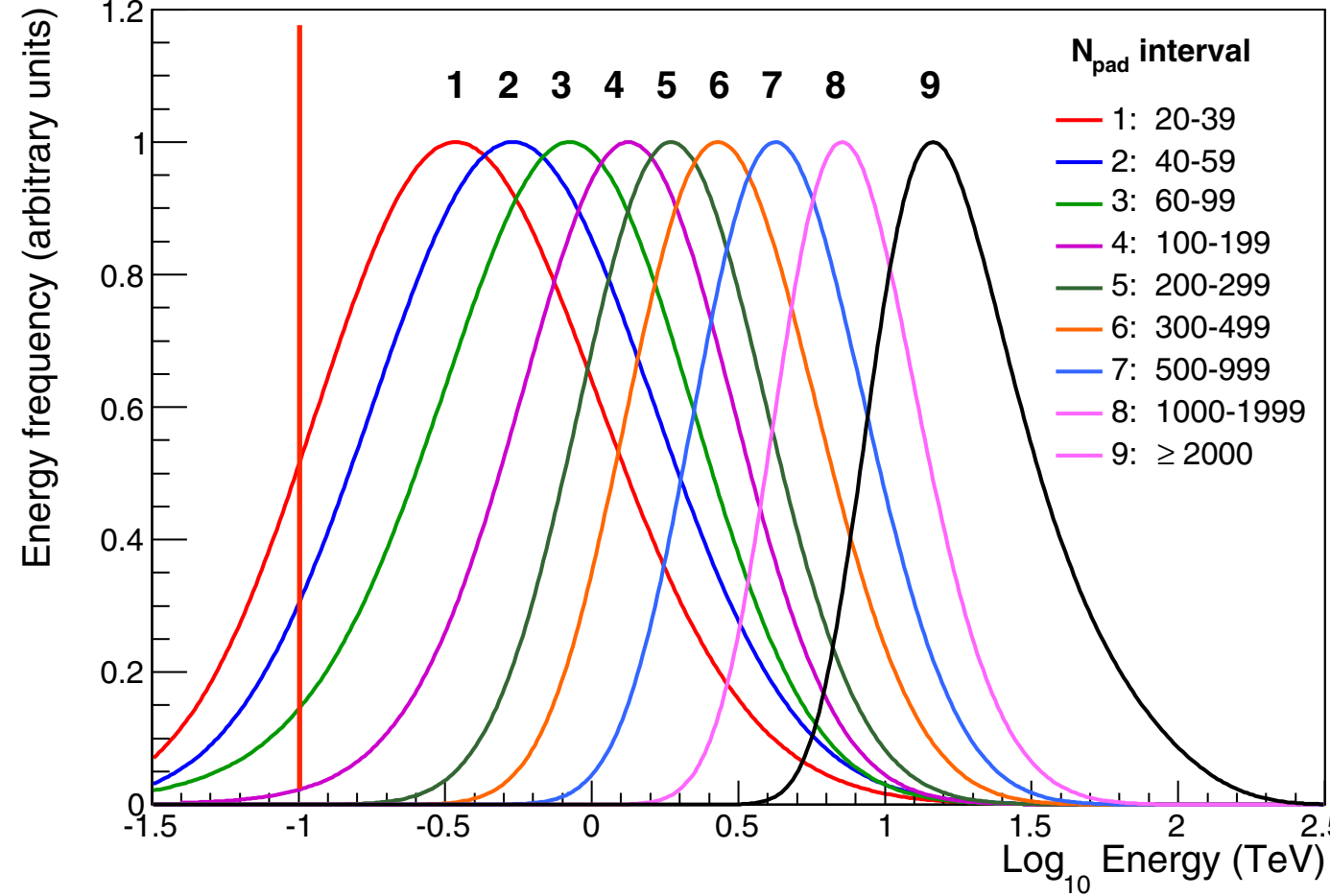
Increasing the sampling ($\sim 1\% \rightarrow 100\%$)

- Improves angular resolution
• Lowers energy threshold



Energy threshold

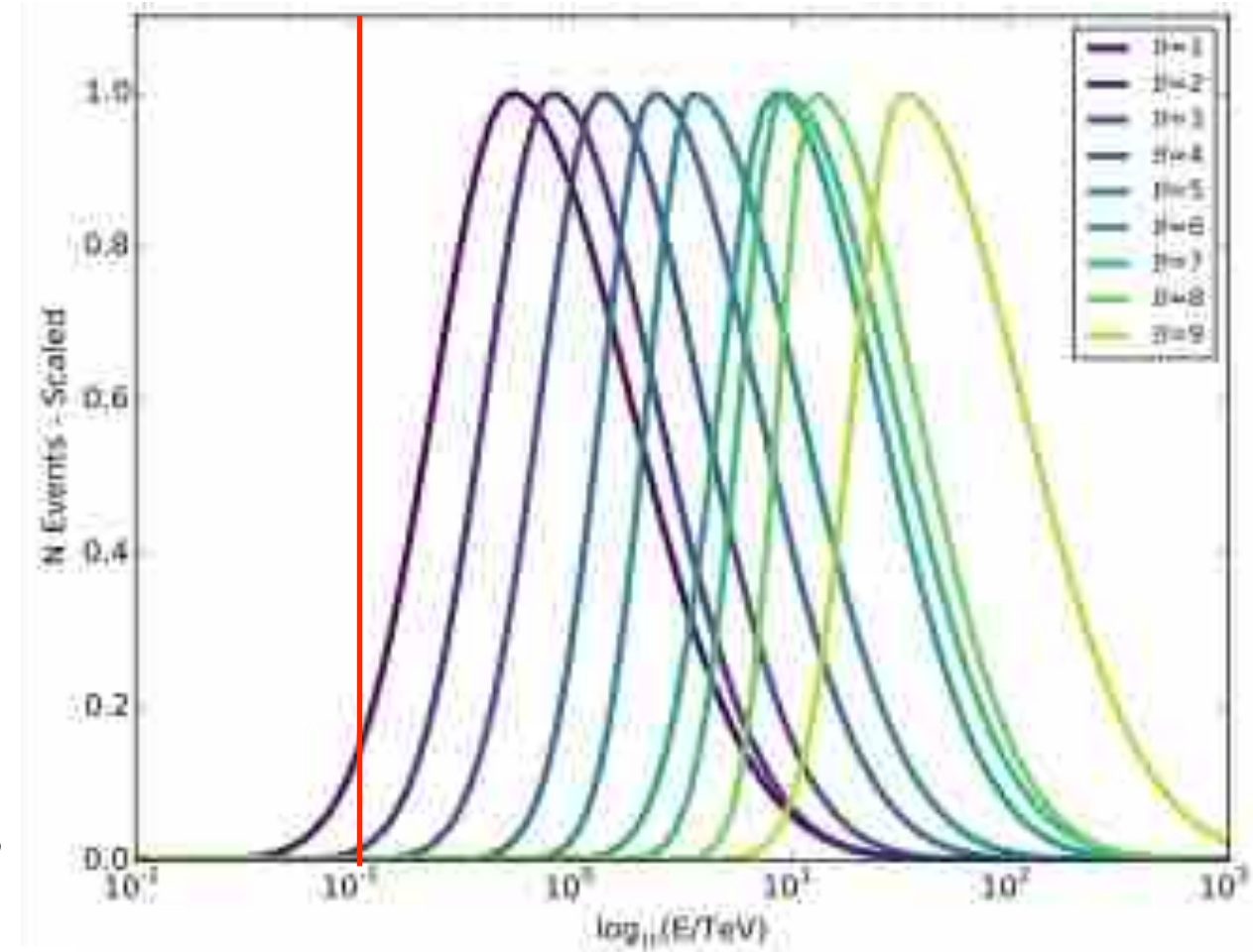
ARGO-YBJ



full coverage RPC carpet operated at 4300 m asl
coverage $\approx 92\%$
high granularity (cm level)
Topological-based Trigger logic;
>20 pads out of 15,000 bkg free !

Median energy first bin = 360 GeV

HAWC (2017)



array of water tanks operated at 4100 m asl
coverage $\approx 60\%$
poor granularity (m level)
free running

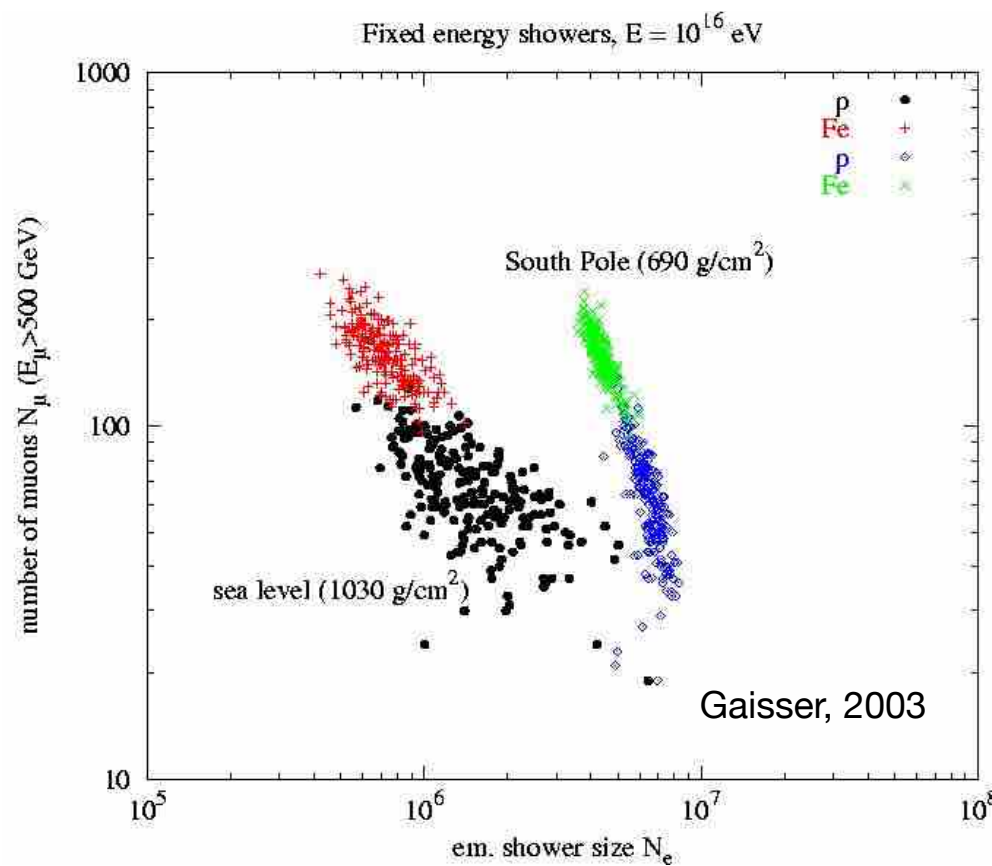
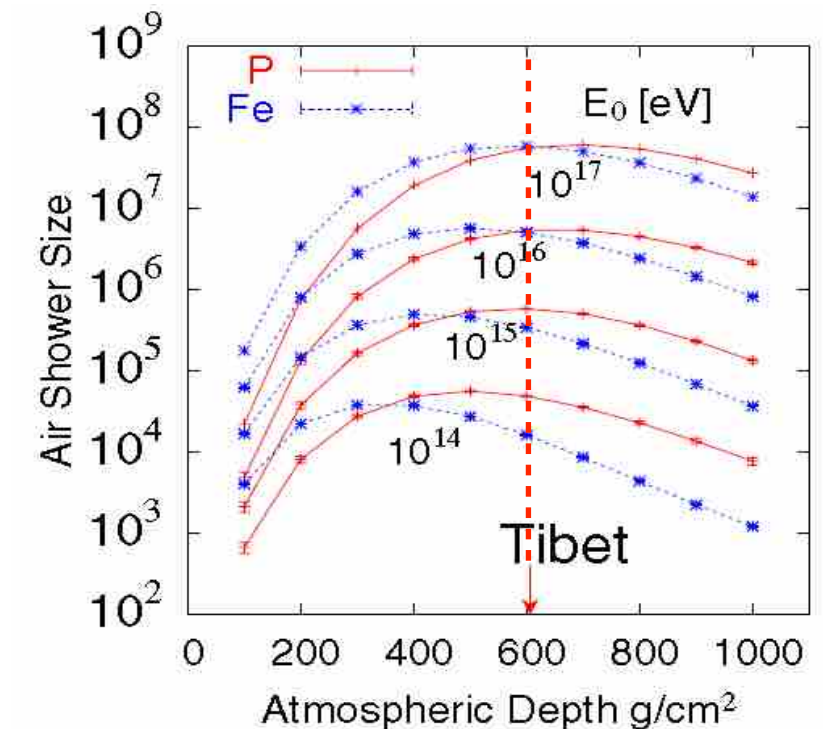
Median energy first bin = 700 GeV

Extreme Altitude

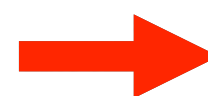
1. All nuclei produce showers with similar size
2. Unbiased trigger threshold for all nuclei
3. Primary energy reconstruction mass-independent
4. Small fluctuations: shower maximum
5. Low energy threshold: absolute energy scale calibration with the Moon
Shadow technique and overposition with direct measurements
6. Trigger probability larger for γ -showers than for p-showers

$$N_{e,\max}^A \approx N_{e,\max}^p$$

$$N_e(E_0, A) = a(A) \cdot E^{\beta(A)}$$



Fluctuations smaller but *reduced sensitivity of the N_e/N_μ technique in selecting primary masses*

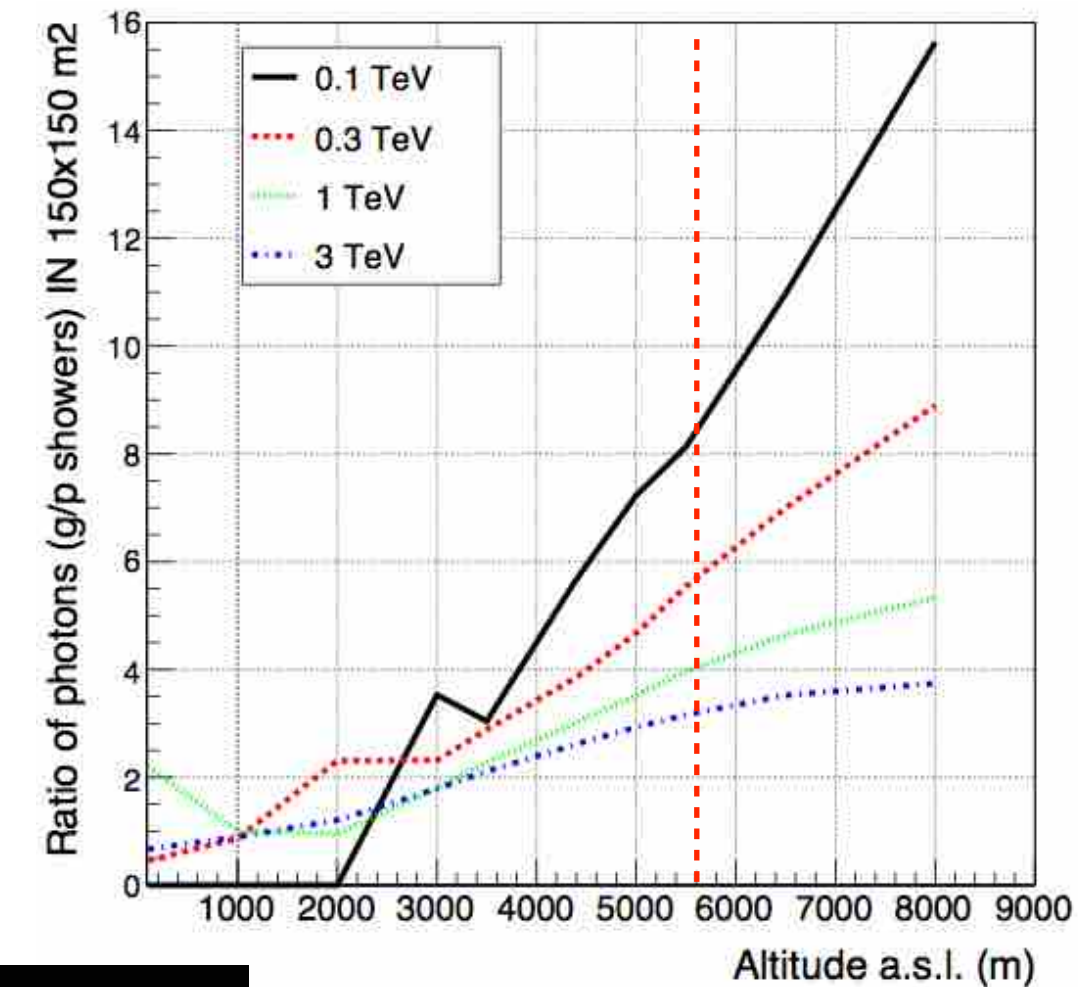
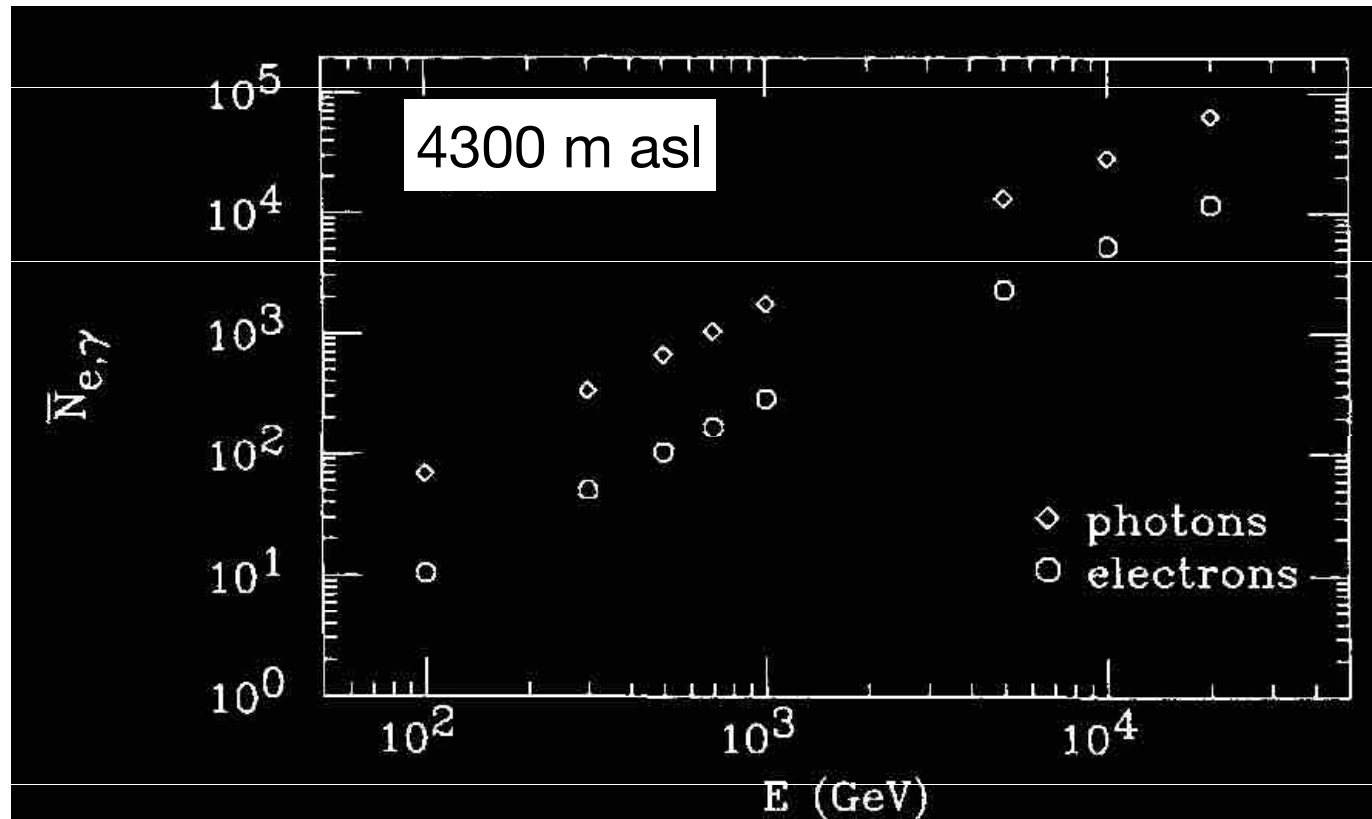


Different technique to select primary masses:
ARGO-YBJ, Tibet AS γ , BASJE-MAS exploited
characteristics of the shower core region.

No muons ? \rightarrow results nearly independent
on hadronic interaction models !

Secondary photons

gamma rays dominate the particles on ground ($\approx 7:1$ for 100 GeV γ -showers at 4300 m asl)



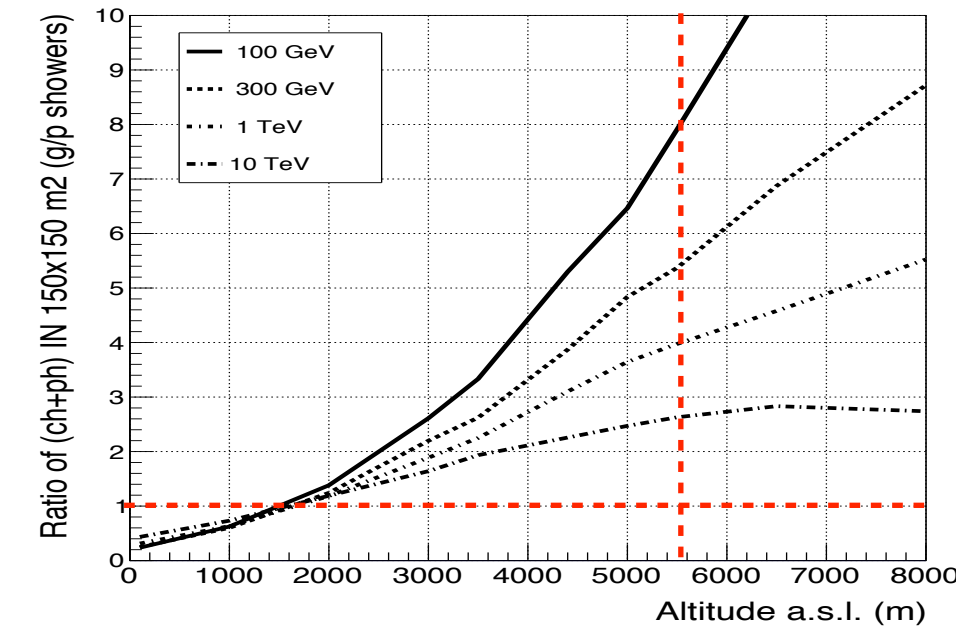
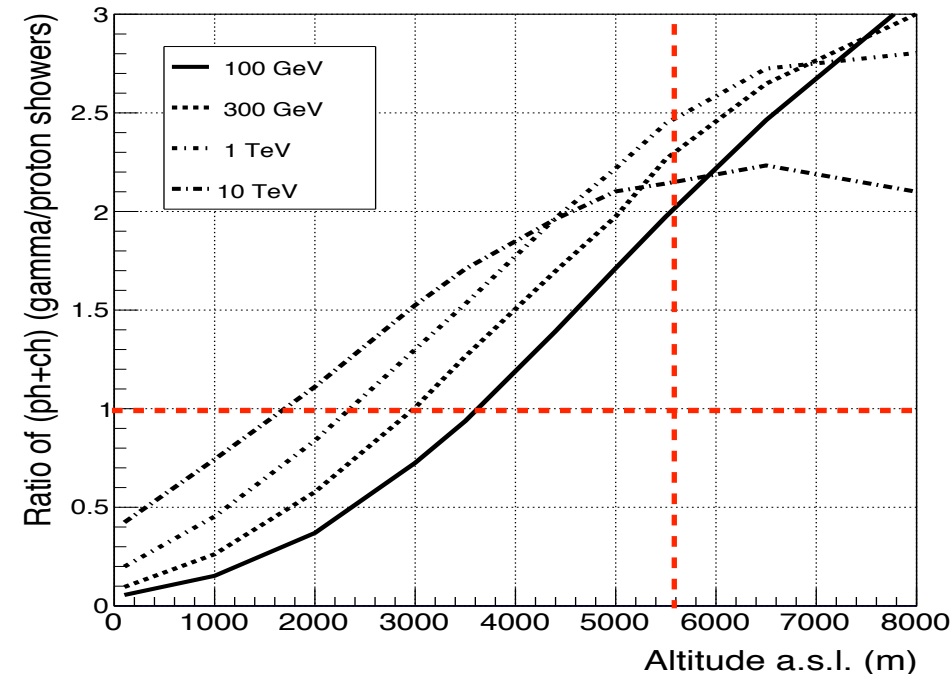
In γ -showers the ratio $N\gamma/N_{\text{ch}}$ decreases if the comparison is restricted to a small area around the shower core. For instance, we get $N\gamma/N_{\text{ch}} \approx 3.5$ at a distance $r < 50$ m from the core for 100 GeV showers.

The number of secondary photons in γ -showers exceeds the number of gammas in p-showers with increasing altitude.

Detection of secondary photons very important to lower the energy threshold
and to improve the angular resolution

γ/p detection efficiency

High altitude → rejection of the background ‘for free’ !



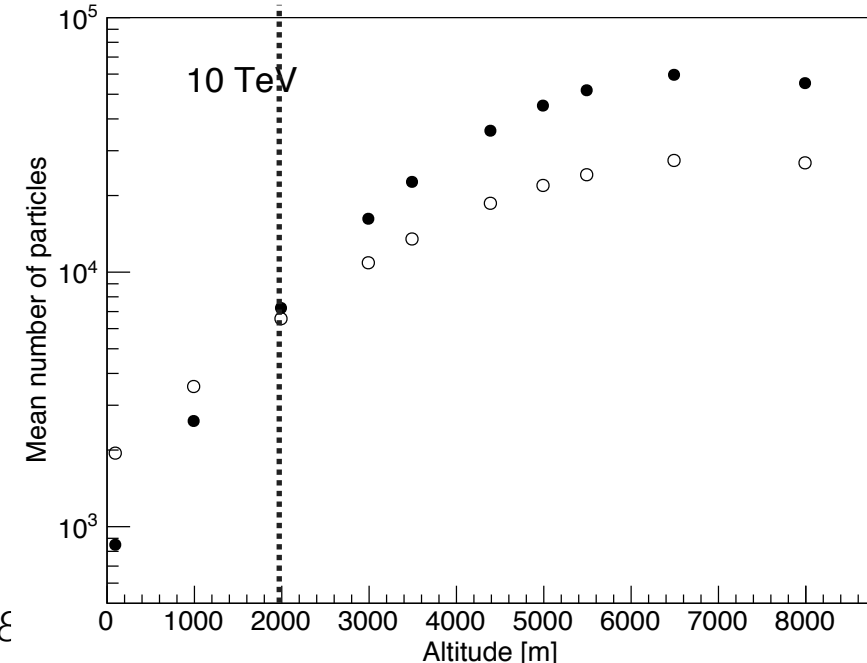
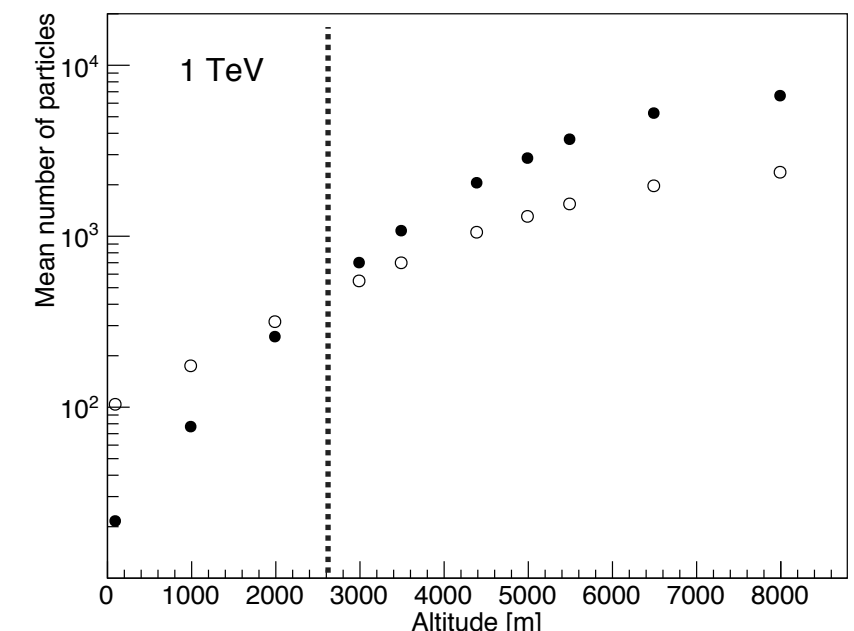
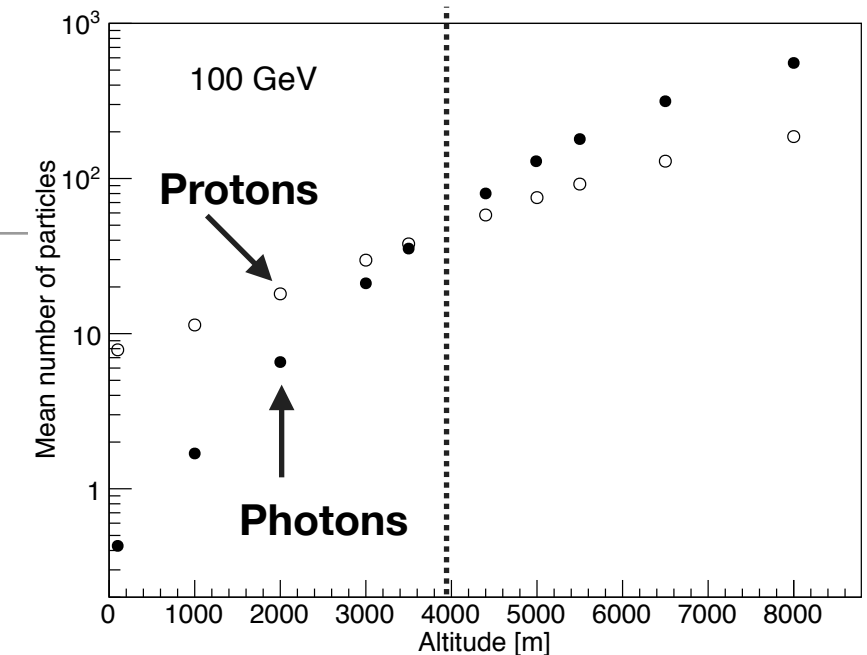
$$R = \sqrt{\frac{A_{eff}^\gamma(E)}{A_{eff}^B(E)}}$$

γ/hadron relative trigger efficiency

The number of particles in γ -showers exceeds the number of particles in p-showers at extreme altitude.

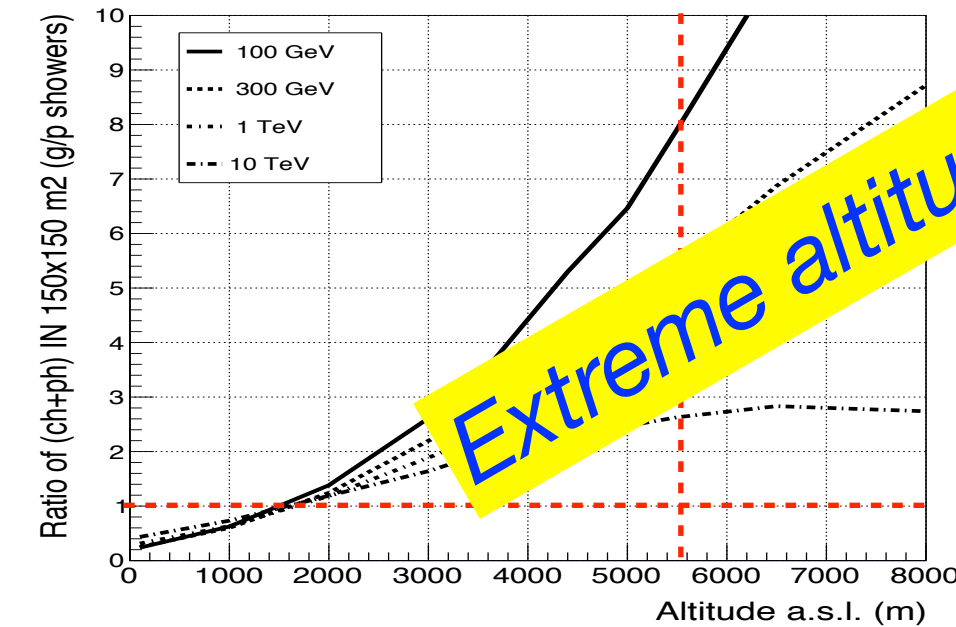
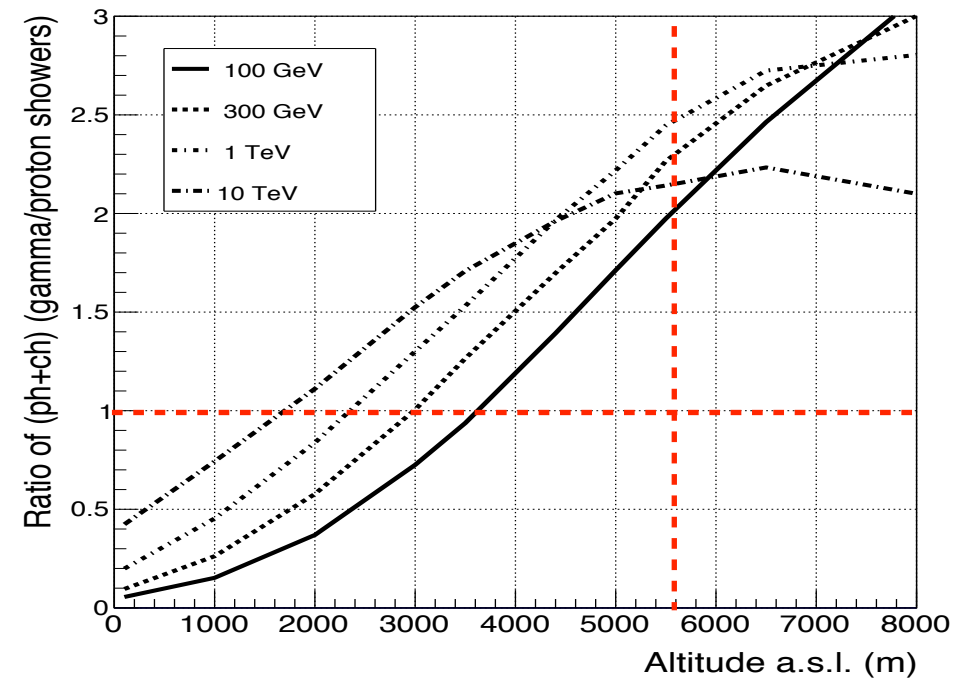


Trigger probability of a detector
larger for γ -showers than for
p-showers at extreme altitude.



γ/p detection efficiency

High altitude → rejection of the background ‘for free’ !



Extreme altitude: not only low energy threshold !!!

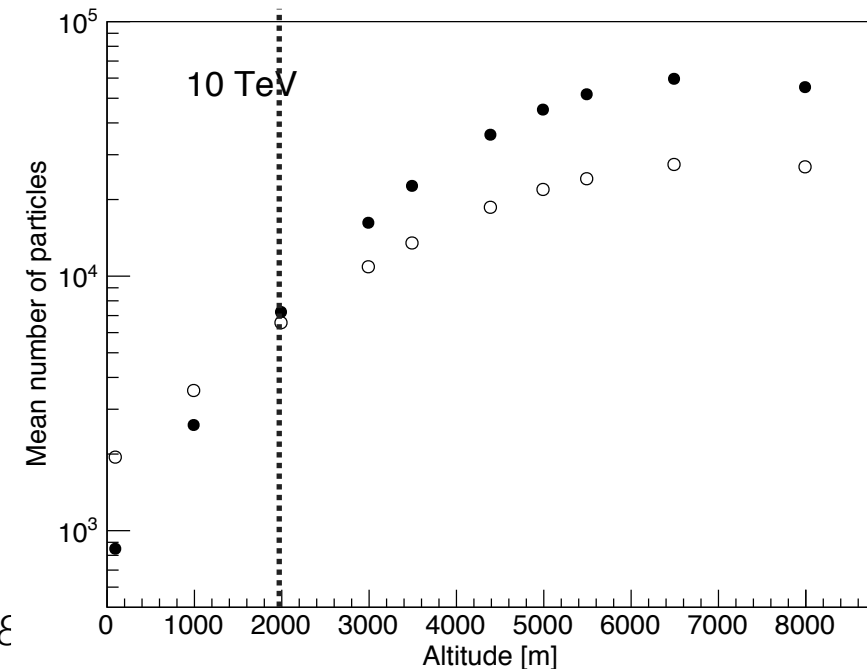
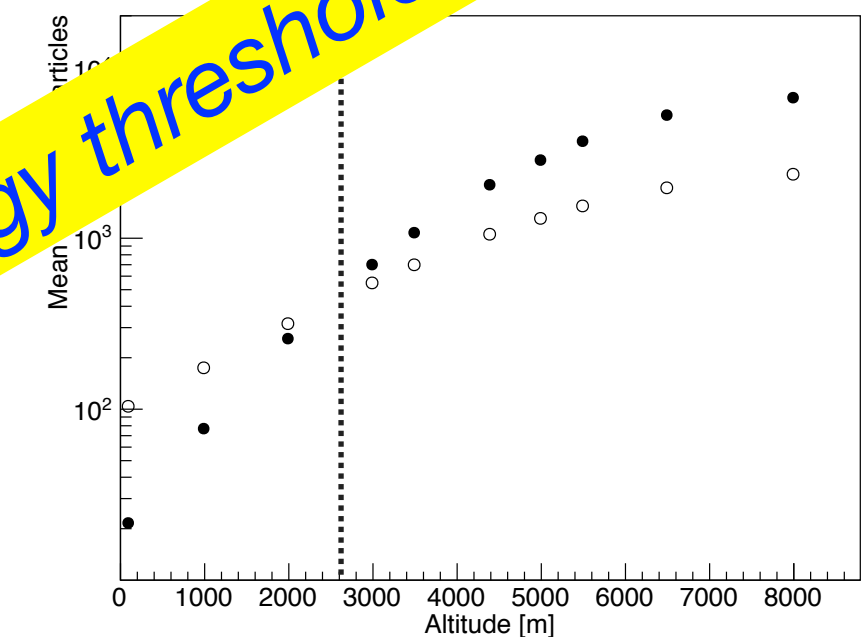
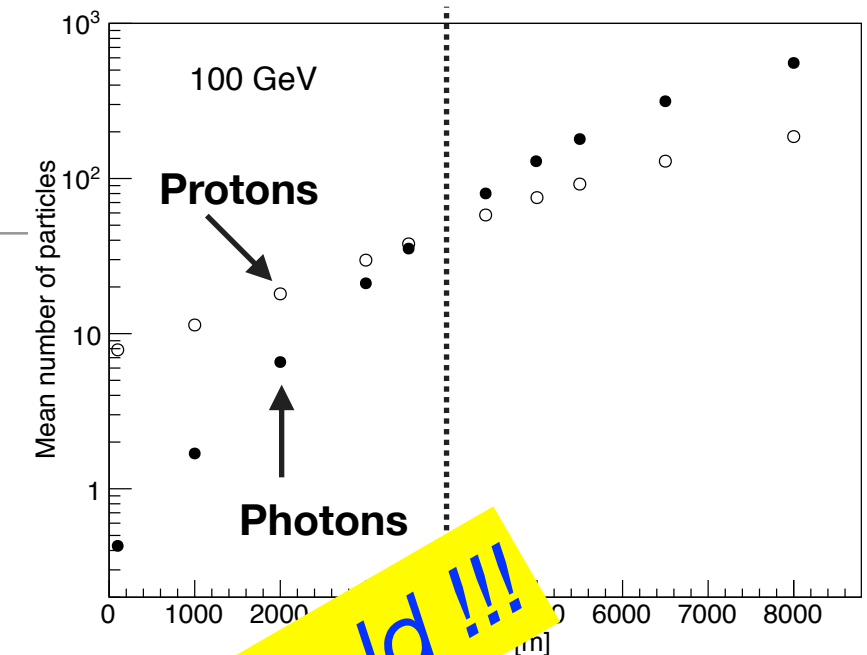
$$R = \sqrt{\frac{A_{eff}^\gamma(E)}{A_{eff}^B(E)}}$$

γ /hadron relative trigger efficiency

The number of particles in γ -showers exceeds the number of particles in p-showers at extreme altitude.



Trigger probability of a detector
larger for γ -showers than for
p-showers at extreme altitude.



Hybrid detector: LATTES

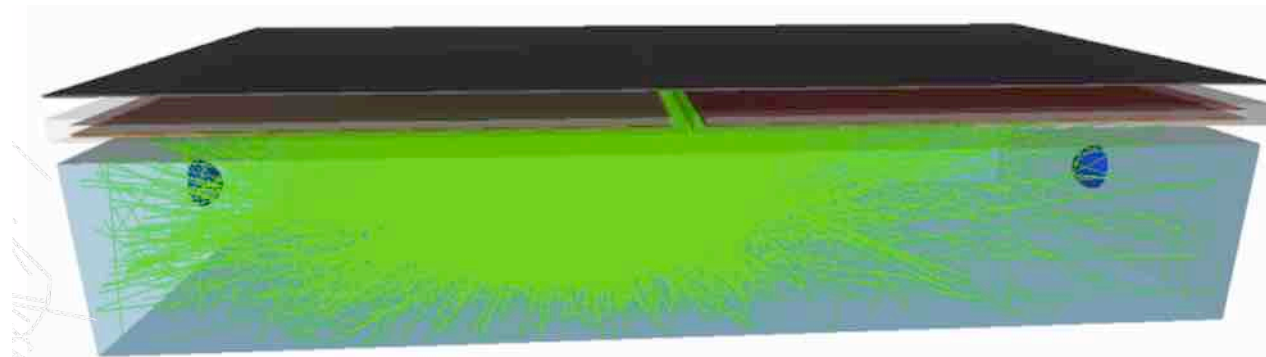
Astroparticle Physics 99 (2018) 34–42

Design and expected performance of a novel hybrid detector for very-high-energy gamma-ray astrophysics

P. Assis^{a,b}, U. Barres de Almeida^c, A. Blanco^d, R. Conceição^{a,b,*}, B. D'Ettorre Piazzoli^e, A. De Angelis^{f,g,b,a}, M. Doro^{h,f}, P. Fonte^d, L. Lopes^d, G. Mattheiaeⁱ, M. Pimenta^{b,a}, R. Shellard^c, B. Tomé^{a,b}

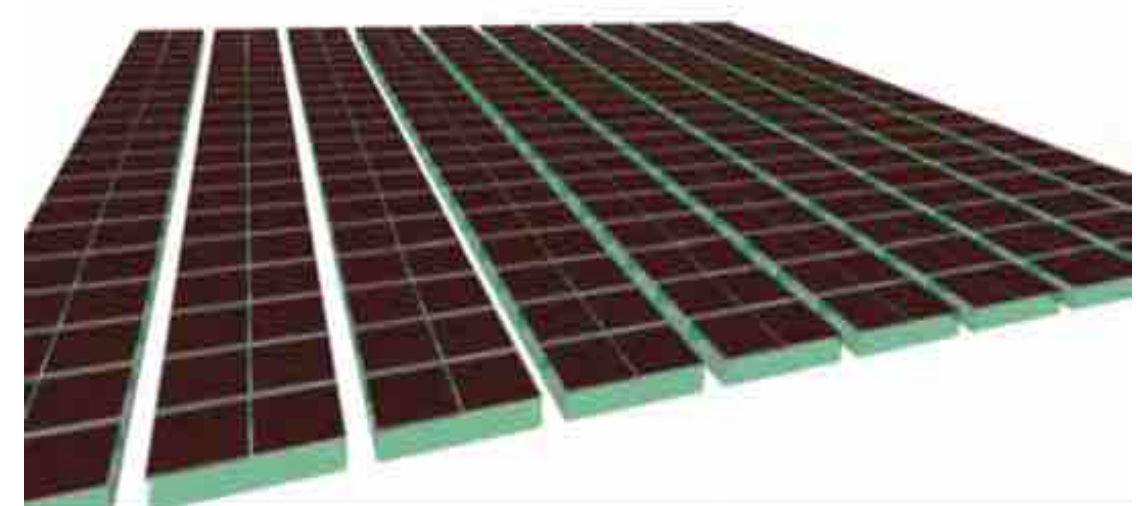
An **array of hybrid detectors** constituted by

1. one Water Cherenkov Detector (WCD) with a rectangular horizontal surface of $3\text{ m} \times 1.5\text{ m}$ and a depth of 0.5 m, with signals read by PMTs at both ends of the smallest vertical face of the block.
2. On top of the WCD there are two MARTA RPCs, each with a surface of $(1.5 \times 1.5)\text{ m}^2$ and with 16 charge collecting pads. Each RPC is covered with a thin (5.6 mm) layer of lead.



- **Thin lead plate (Pb)**
 - 5.6 mm (one radiation length)
- **Resistive Plate Chambers (RPC)**
 - 2 RPCs per station
 - Each RPC with 4x4 readout pads
- **Water Cherenkov Detector (WCD)**
 - 2 PMTs (diameter: 15 cm)
 - Dimensions: $1.5\text{ m} \times 3\text{ m} \times 0.5\text{ m}$

Pb
RPC
WCD

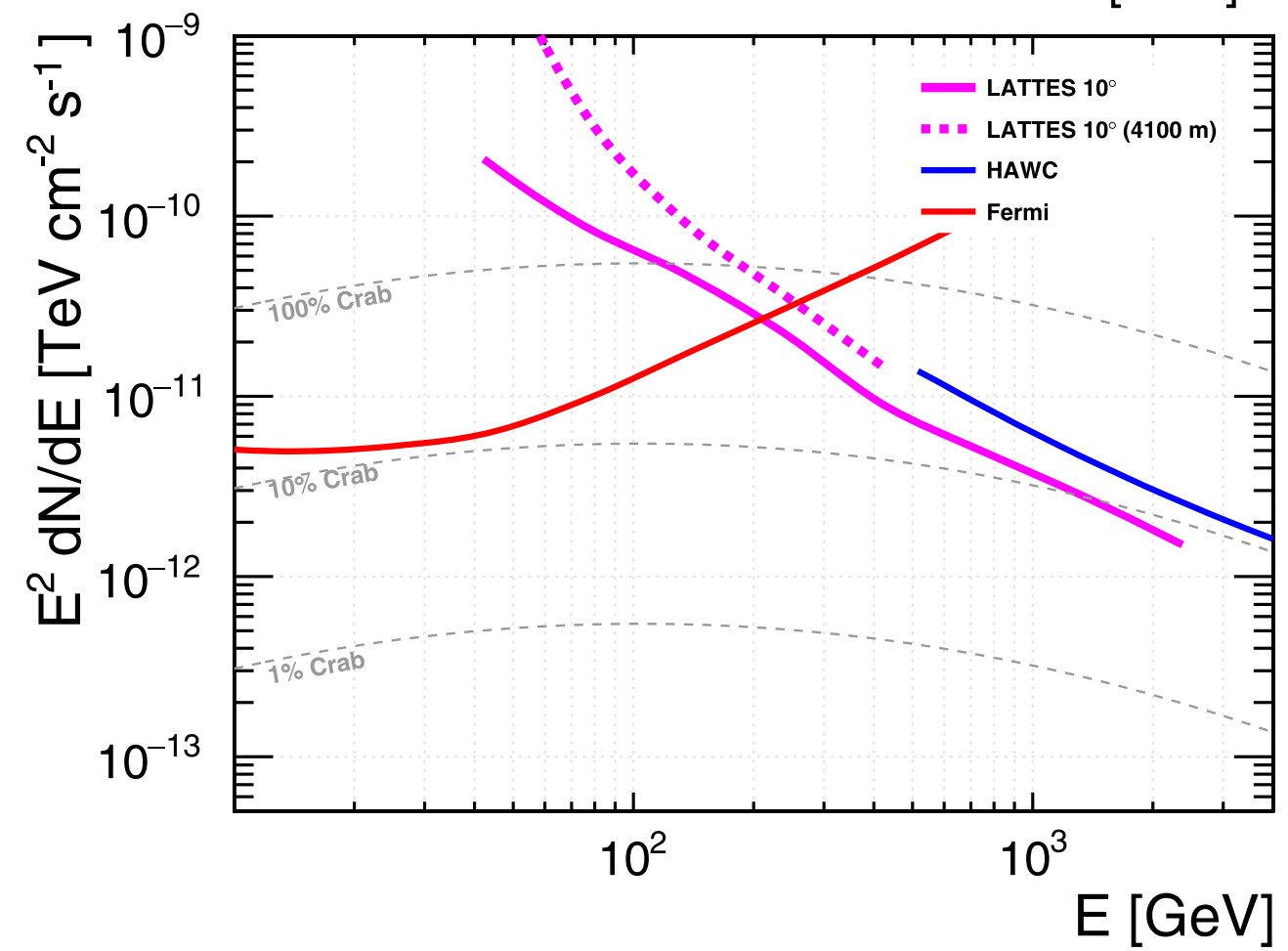
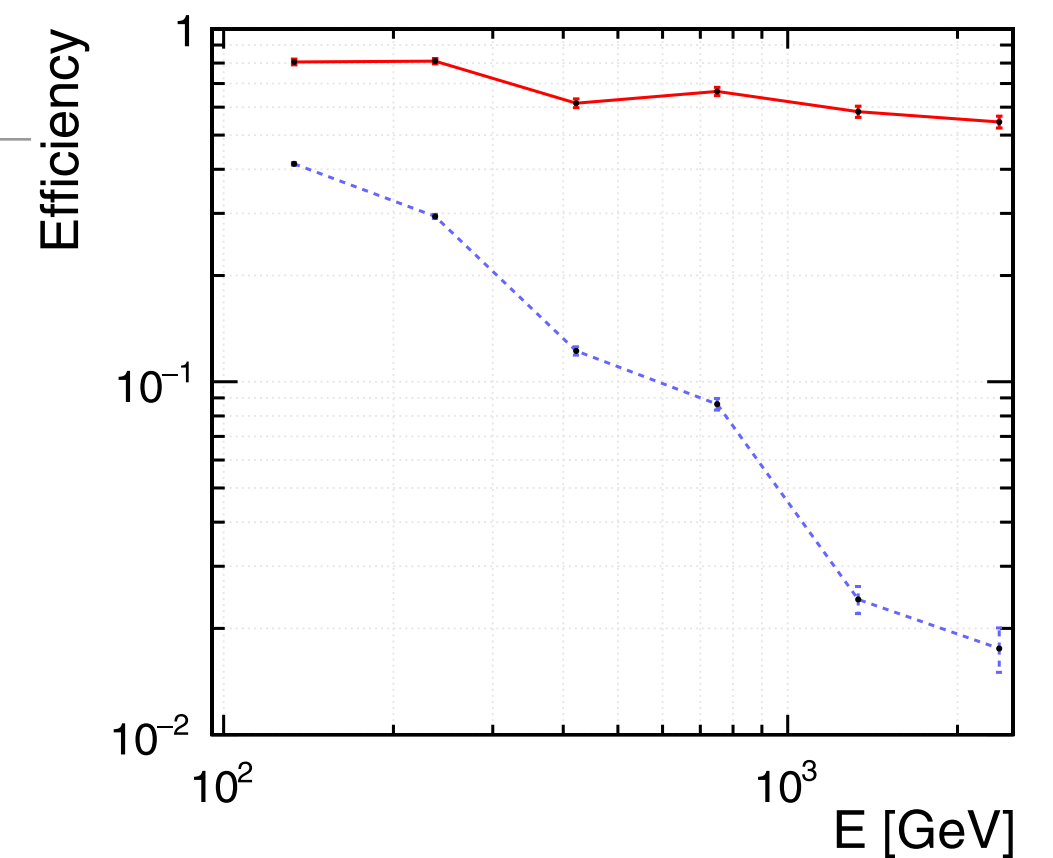
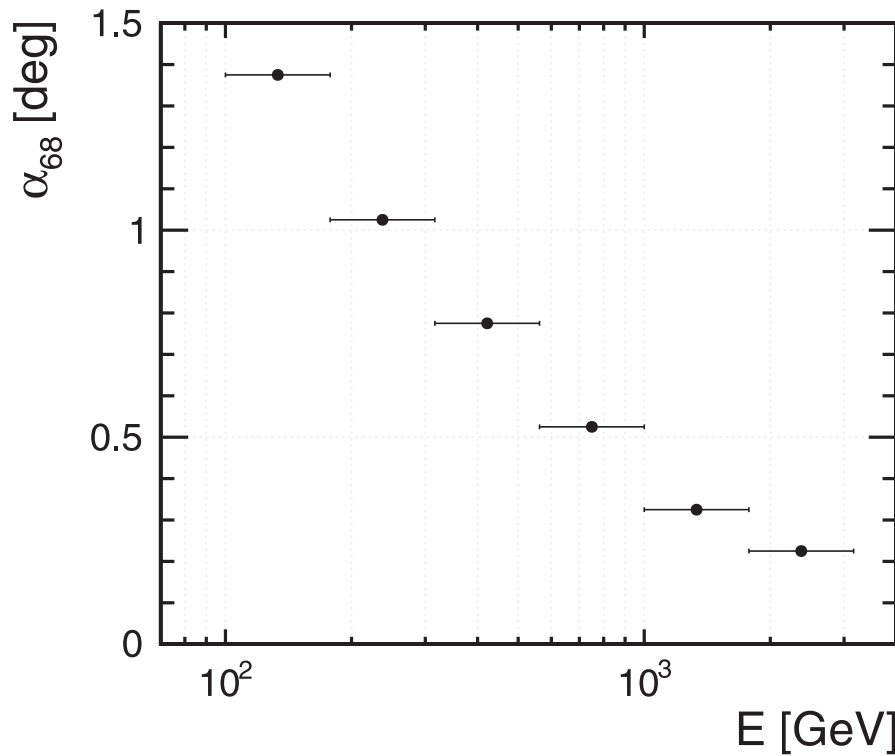
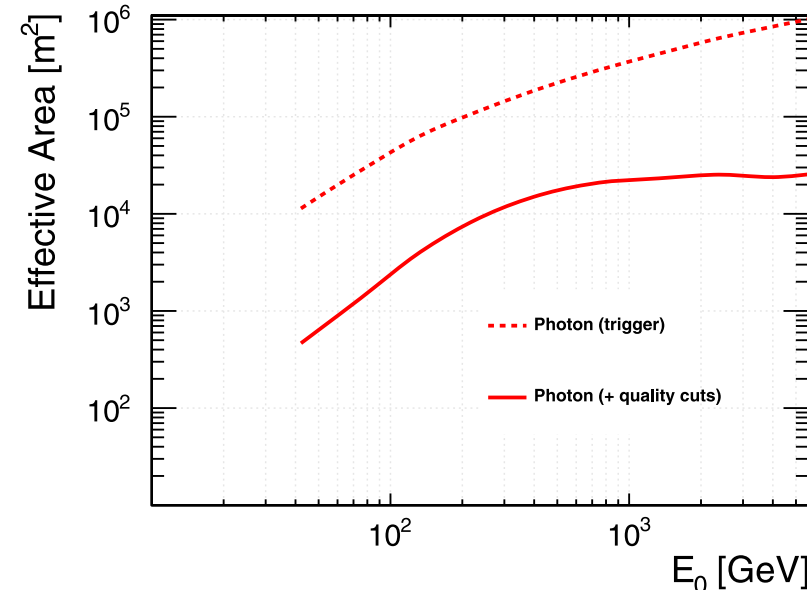


Glass-based RPCs

LATTES performance

Instrumented area $\approx 20,000 \text{ m}^2$

Simulated site at 5200 m asl



Southern Hemisphere: ALPACA



Andes
Large area
Particle detector for **C**osmic ray physics
 and **A**stronomy

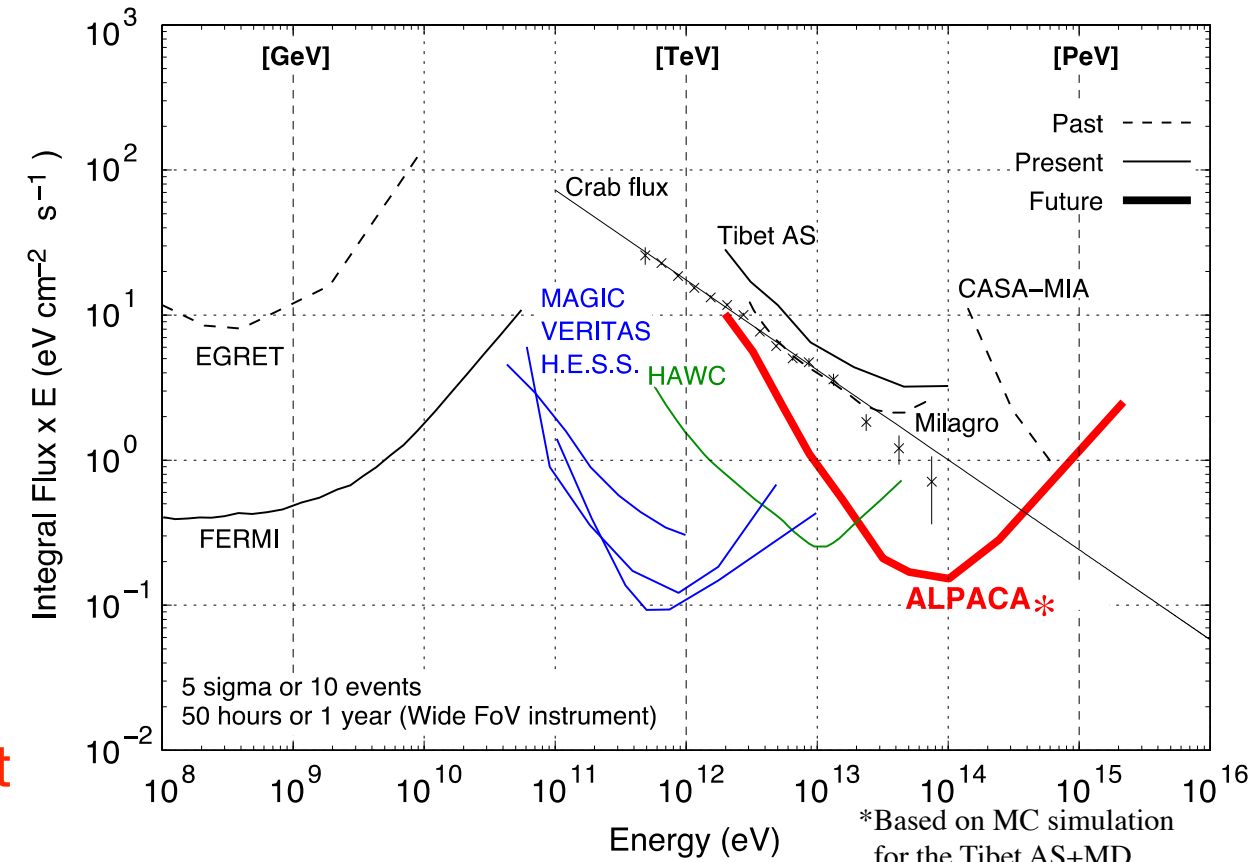
Location: 4,740 m above sea level ($16^{\circ}23' S$, $68^{\circ}08' W$)

# of scintillation detectors	$1 \text{ m}^2 \times 401$ detectors
Effective area of modal energy	$\sim 83,000 \text{ m}^2$
angular resolution	$\sim 5\text{TeV}$
energy resolution	$\sim 0.2 @ 100 \text{ TeV}$
field of view	$\sim 30\% @ 100\text{TeV}$
	$\sim 2 \text{ sr}$
CR rejection power (γ ray efficiency $\sim 90\%$)	$>99.9\% @ 100 \text{ TeV}$

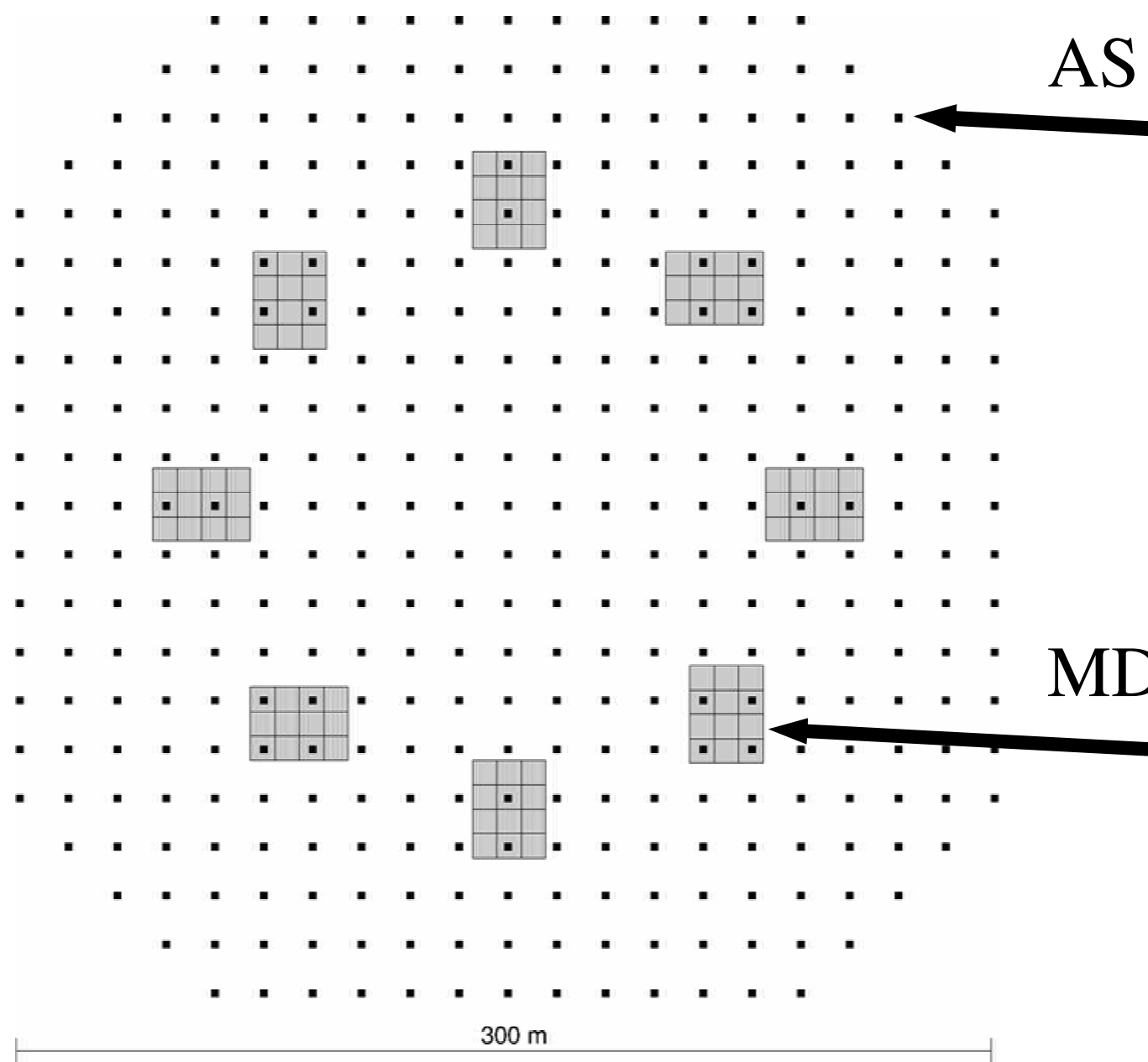
MD Array $56\text{m}^2 \times 96$ detectors

- Effective area for muons $\sim 5400\text{m}^2$
- CR rejection power $>99.9\% @ 100\text{TeV}$
(gamma ray efficiency $\sim 90\%$)

Similar to the Tibet AS γ experiment operated in Tibet



ALPACA layout



AS

MD

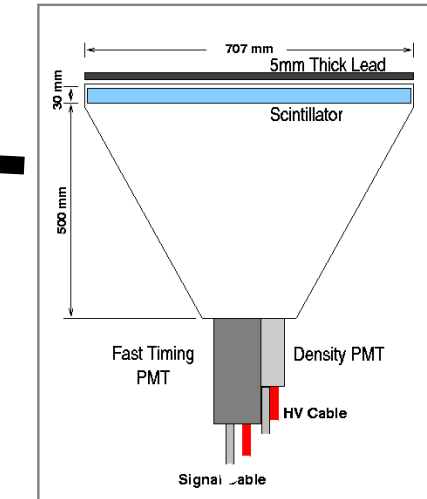


Image of 1m^2 plastic scintillation detector

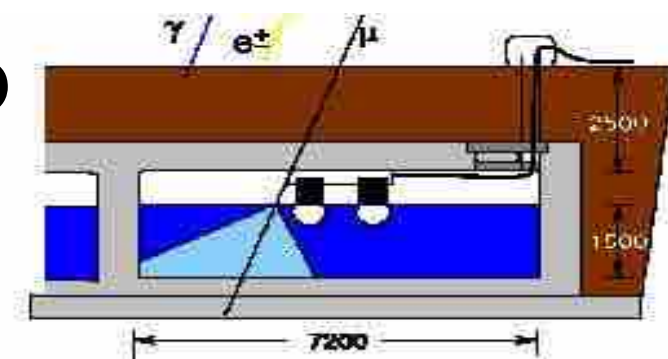


Image of unit (56m^2) underground water Cherenkov muon detector

ALPAQUITA (1/10 scale ALPACA AS , in 2017)

Southern Gamma-Ray Survey Observatory

**SOUTHERN
GAMMA-RAY
SURVEY
OBSERVATORY**

Who are we?...

*H. Schoorlemmer
Recontres du Vietnam 2018*

The alliance

- Advancement of this effort in the Southern-Hemisphere
- **Organizing the writing of a white-paper on the science case**
- Documentation on site-candidates
- No decision on technical design (for now)
- Currently **75 members** from **11 countries**
- Next meeting **8-9 October Heidelberg, Germany**

www.sgso-alliance.org

Science Case White Paper by SGSO

SCIENCE CASE FOR A WIDE FIELD-OF-VIEW VERY-HIGH-ENERGY GAMMA-RAY OBSERVATORY IN THE SOUTHERN HEMISPHERE

ANDREA ALBERT, R. ARCEO, SEGEV BENZVI, THOMAS BRETZ, ALBERTO CARRAMÍANA, SABRINA CASANOVA, PAOLO DESIATI, DANIELA DORNER, JUAN CARLOS DÍAZ-VÉLEZ, GIUSEPPE DI SCIASCIO, NISSIM FRAJJA, JAVIER GONZALEZ, H. MARTÍNEZ-HUERTA, MIGUEL MOSTAFÁ, MAGDALENA GONZALEZ, JIM HINTON, JEAN-PHILIPPE LENAIN, R. LÓPEZ-COTO, FILIPE DE O. SALLES, ANA PICHEL, ELISA PRANDINI, ANDREAS REISENEGGER, JÉRÔME RODRIGUEZ, ADRIAN C. ROVERO, MARCOS SANTANDER, HARM SCHORLEMMER, FABIAN SCHÜSSLER, ANDRES SANDOVAL, MONICA SEGLAR-ARROYO, AION VIANA, THOMAS WEISGARBER, FELIX WERNER, AND YOUR NAME CAN BE HERE...

CONTENTS

1. Introduction and Goal of this document	2
2. Gamma ray astronomy and current instrumentation	3
2.1. Pointing instruments	3
2.2. Wide Field-of-View instruments	3
2.3. Complementarity of ground-based detection techniques	4
3. Unveiling Galactic Particle Accelerators	4
3.1. Pulsars to constrain local positron flux and diffusion coefficients	5
3.2. Fermi bubbles	7
3.3. PeVatrons	8
3.4. Gamma Rays from Molecular Clouds in the Gould Belt	13
4. Monitoring the Transient Sky	13
4.1. Active Galactic Nuclei	13
4.2. Galactic monitor	25
4.3. Gamma-Ray Bursts and Gravitational Waves	28
4.4. Exploratory searches for new transient phenomena	31
4.5. High-energy neutrinos	32
4.6. Multi-messenger correlations	34
5. Probing Physics Beyond the Standard Model	34
5.1. Dark Matter	34
5.2. Axions, Primordial Black Holes, Lorentz Invariance Violation, etc.	37
5.3. Primordial Black Holes	38
5.4. Testing Lorentz invariance with SGSO	39
6. Cosmic-ray observations	40
6.1. Spectrum and composition	40

1

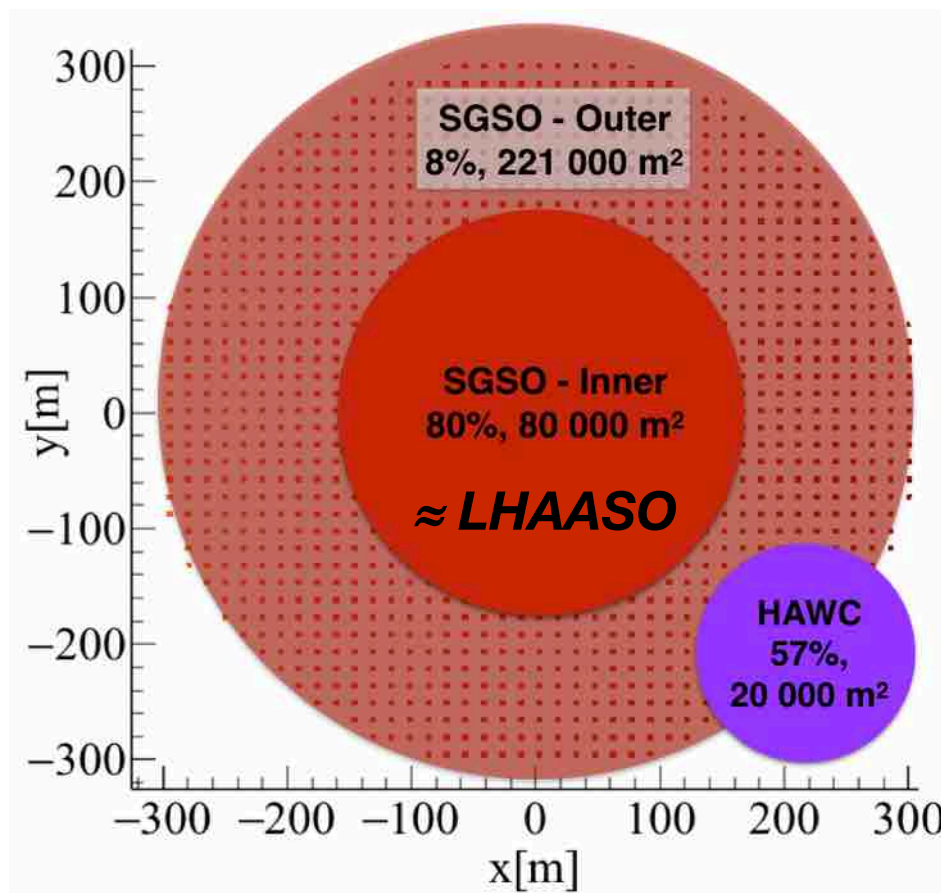
- Community wide contributions
- Focus on how the science will drive detector requirements
- *First version ready this Fall*
- Public tools for writing and calculations
- Regular calls for coordination

H. Schoorlemmer
Recontres du Vietnam 2018

6.2. Anisotropy	43
6.3. Electron spectrum and anisotropy	45
6.4. Space weather	46
7. Design Considerations for a Southern Hemisphere VHE γ -ray Observatory	46
7.1. Detector Unit Design	46
7.2. Straw man Performance	46
7.3. Beyond the straw man performance	48
7.4. Site Considerations: Latitude and Altitude	48
References	49

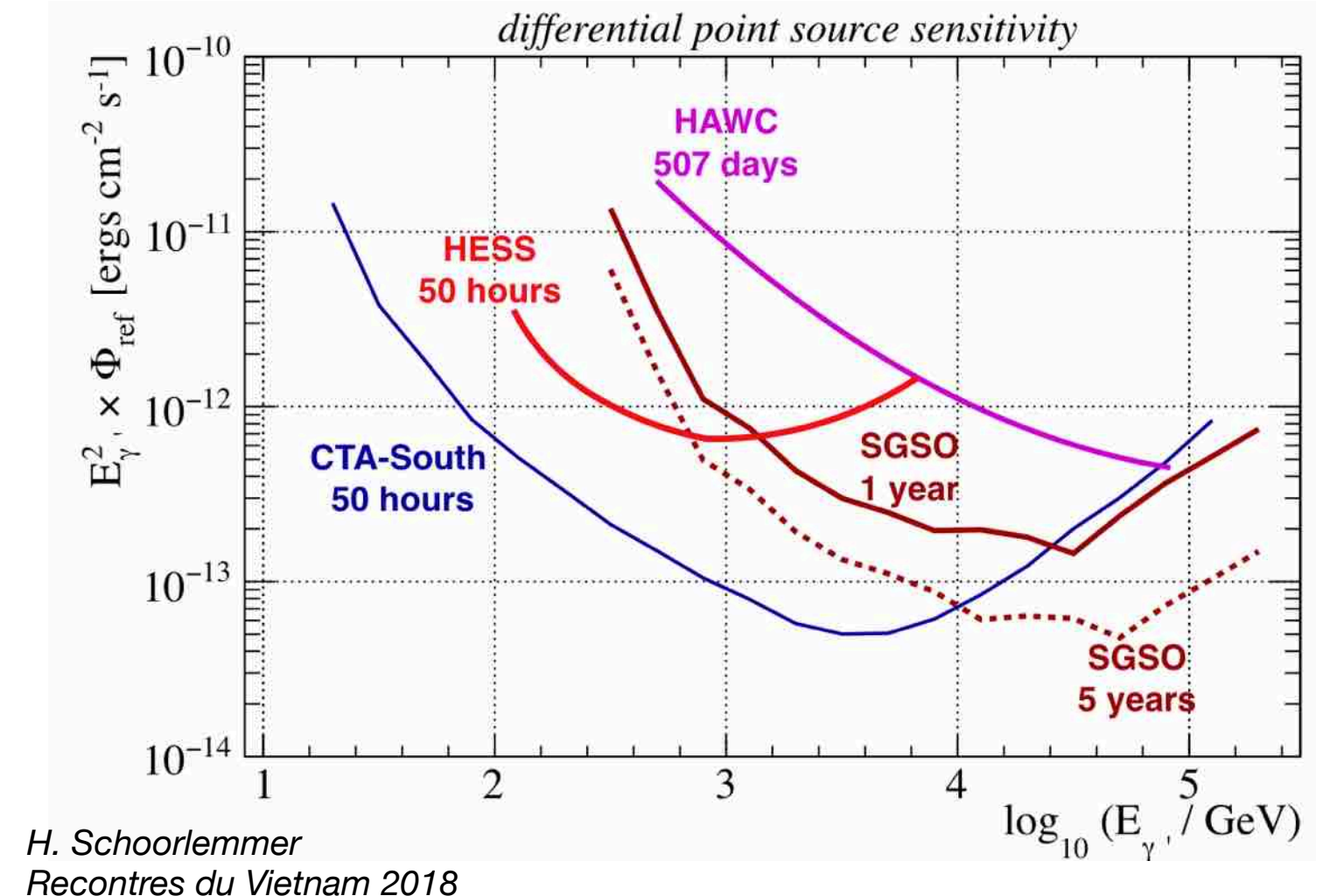
A straw mans design: point source sensitivity

Size & Fill factor



5 km above sea level

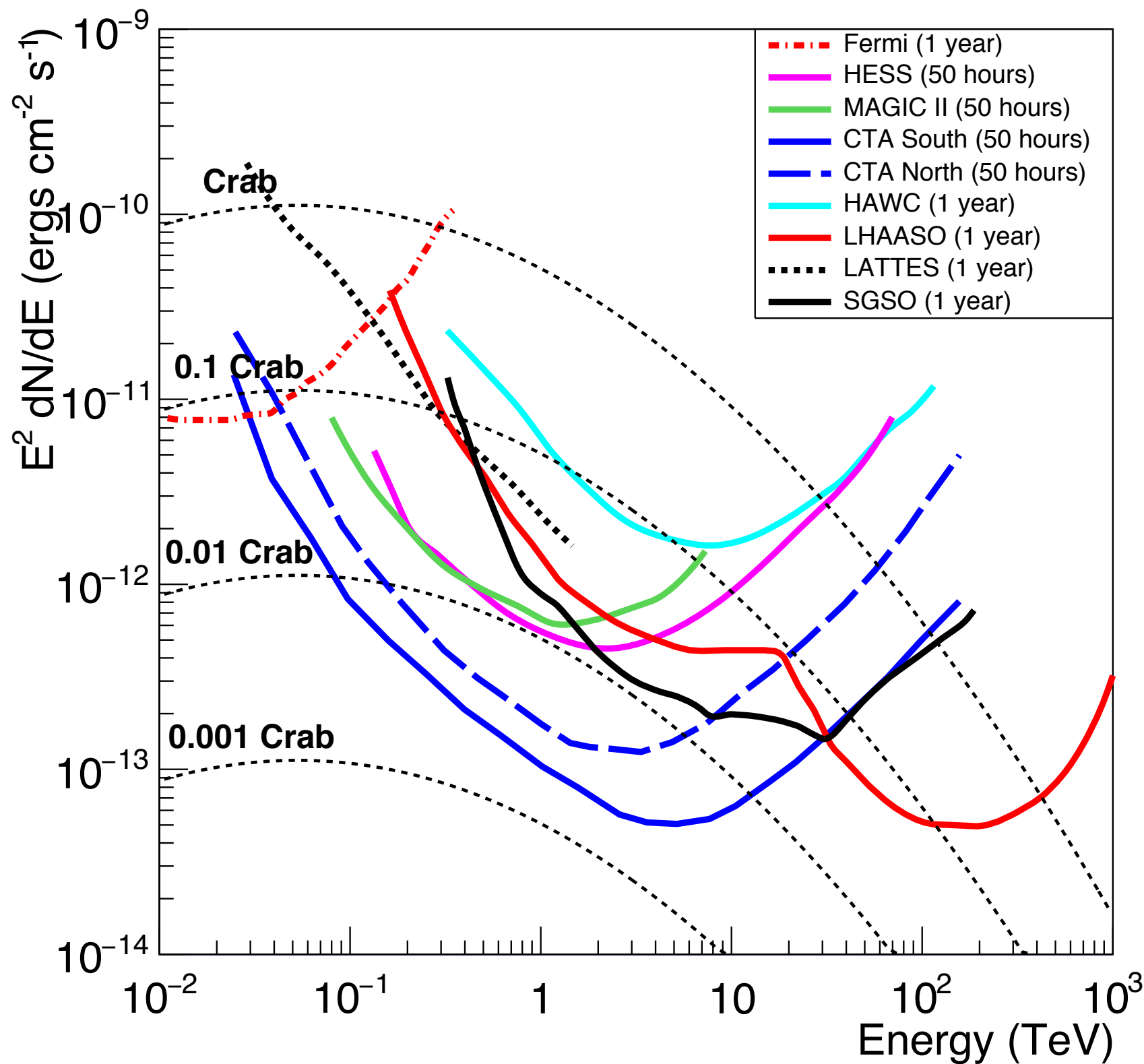
HAWC-based layout



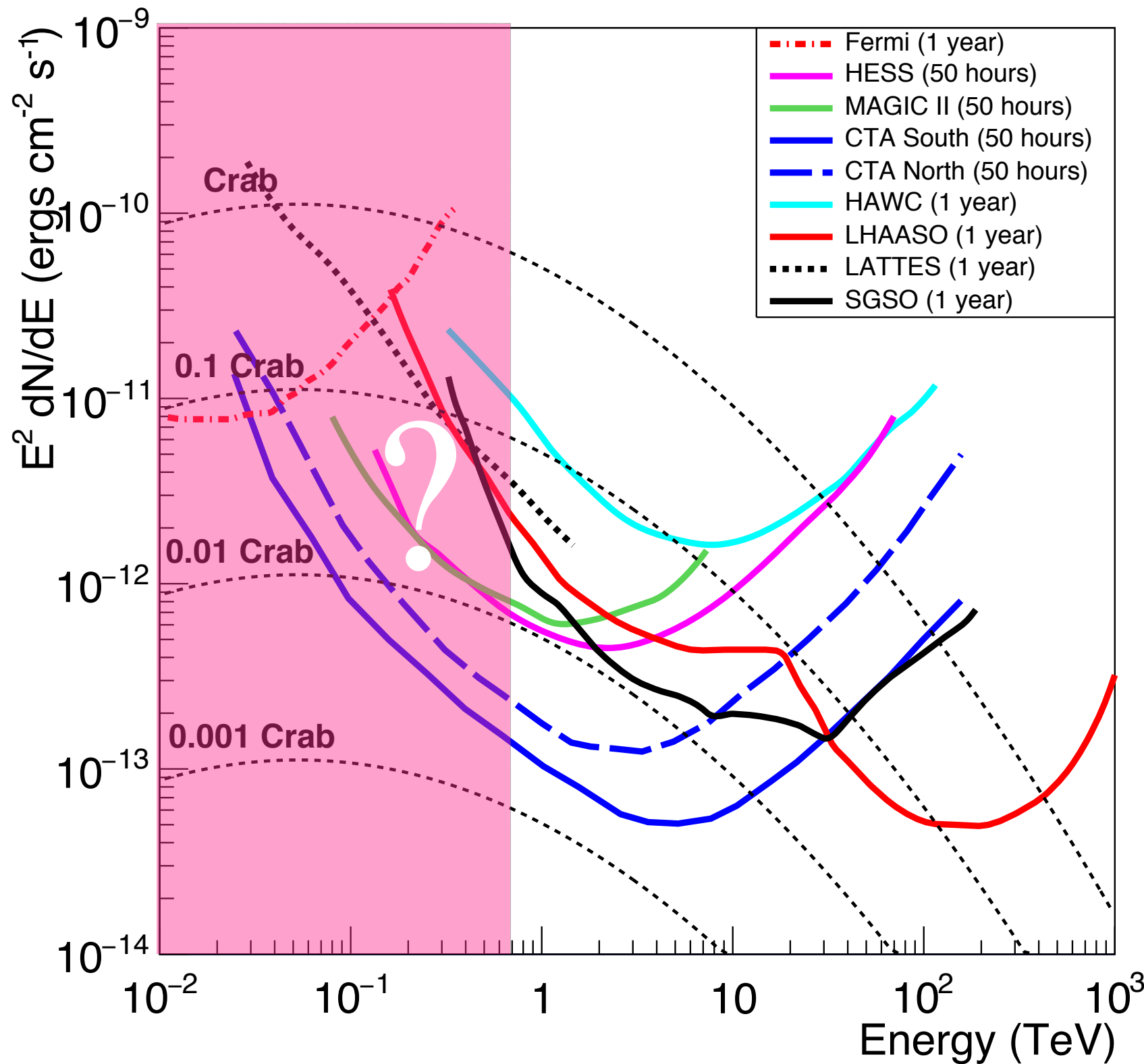
If you are interested join SGSO at

www.sgso-alliance.org

Point source sensitivity



Point source sensitivity



Conclusions

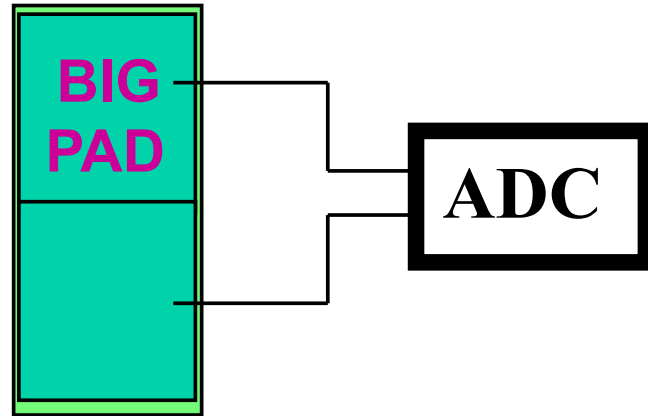
Open problems in cosmic ray physics push the construction of new generation Wide FoV experiments.

In the next decade CTA-North and LHAASO are expected to be the most sensitive instruments to study γ -ray astronomy in the Northern hemisphere from ≈ 20 GeV up to PeV.

- *An all-sky detector in the Southern Hemisphere should be a high priority* to face a broad range of topics.
- Extragalactic transient detection requires *low threshold, ≈ 100 GeV*.
- *Extreme altitude* (≈ 5000 m asl), *high coverage* and *high granularity of the read-out* are key.
- *Background rejection below TeV challenging* → RPCs + Water Cherenkov ?
- *Selection of primary masses* crucial → RPCs + Water Cherenkov ?
- Capability of Water Cherenkov Facilities in selecting primary masses must be investigated.
- Different groups are studying different experimental solutions (ALPACA, ALTO, LATTES, STACEX)
- High energy gamma-ray astronomy (> 10 TeV) and CR physics covered by ALPACA ?

The RPC charge readout

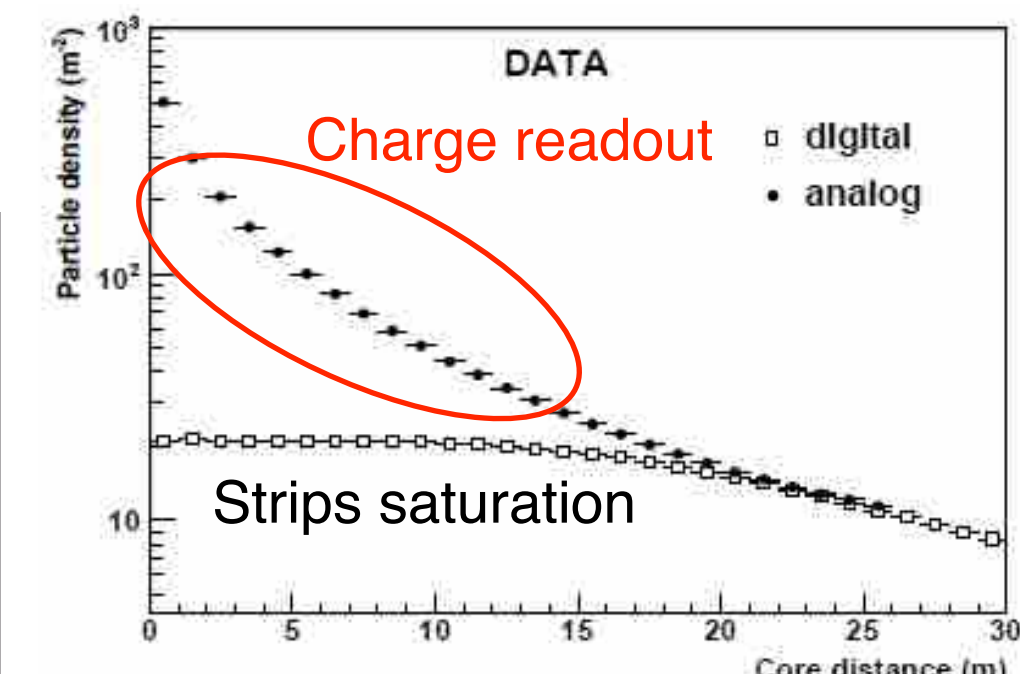
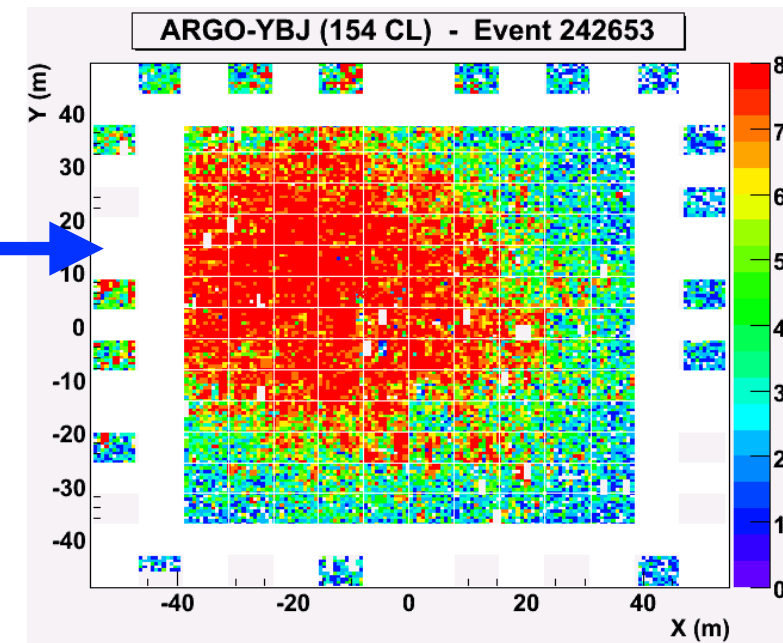
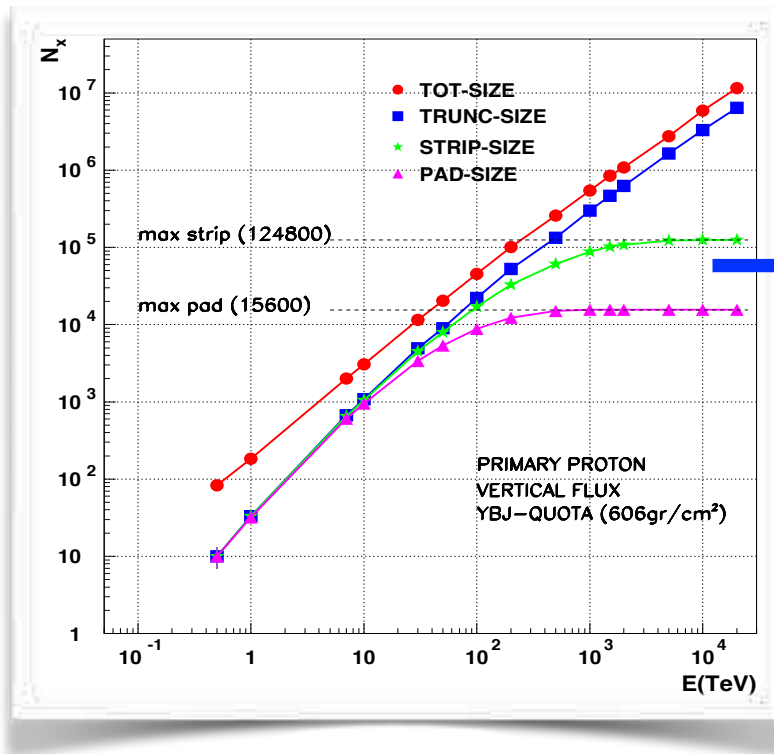
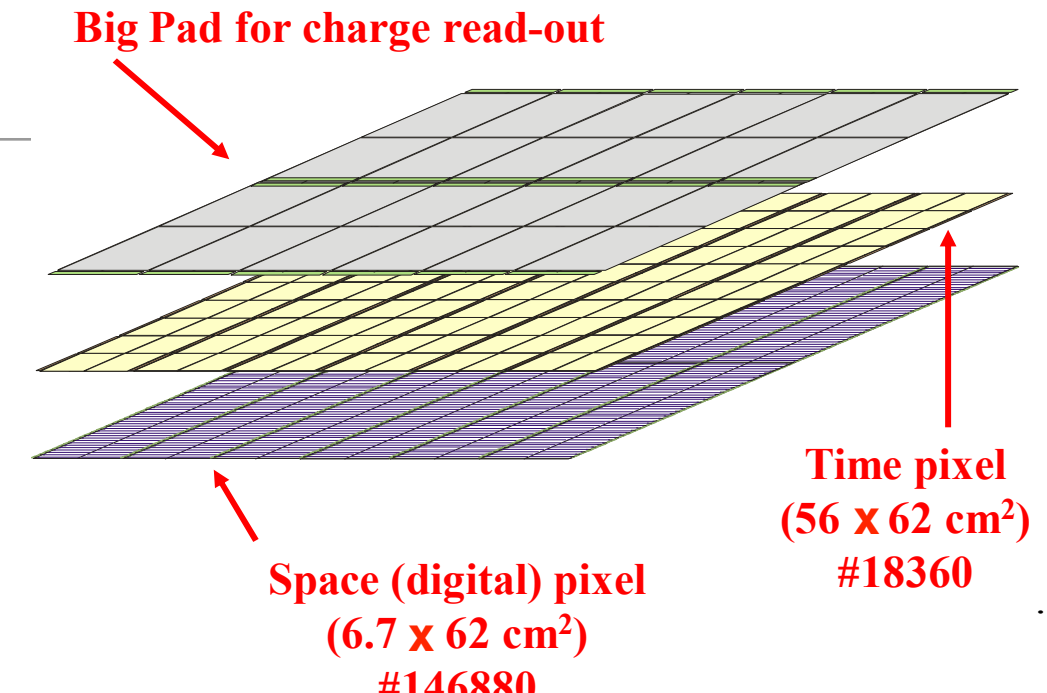
...extending the dynamical range up to 10 PeV



4 different gain scales used to cover a wide range in particle density:

$$\rho_{\text{max-strip}} \approx 20 \text{ particles/m}^2$$

$$\rho_{\text{max-analog}} \approx 10^4 \text{ particles/m}^2$$

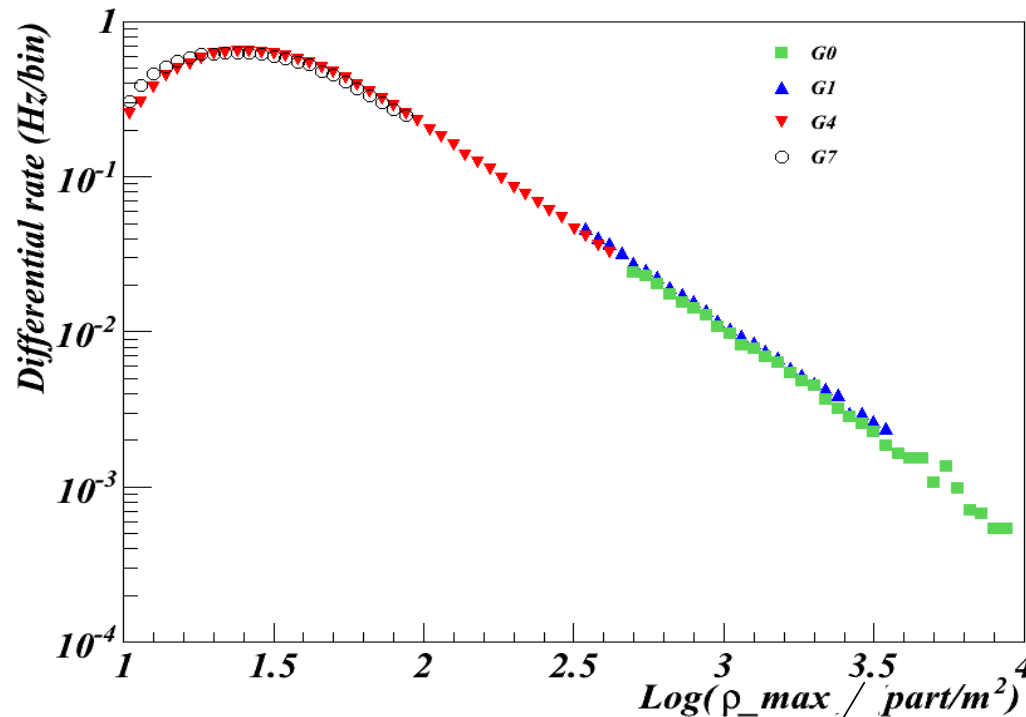


Intrinsic linearity: test at the BTF facility

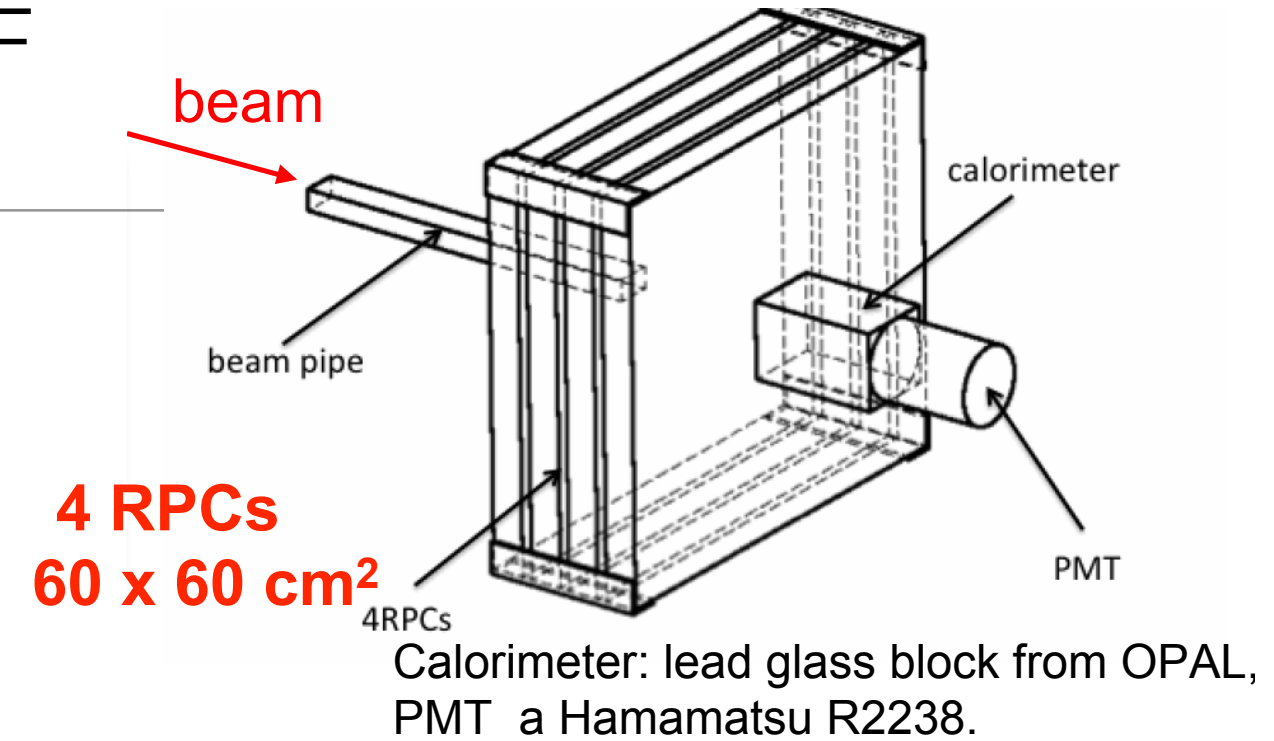
Linearity of the RPC @ BTF in INFN Frascati Lab:

- electrons (or positrons)
- $E = 25\text{-}750 \text{ MeV}$ (0.5% resolution)
- $\langle N \rangle = 1\text{--}10^8 \text{ particles/pulse}$
- 10 ns pulses, 1-49 Hz
- beam spot uniform on $3\text{--}5 \text{ cm}$

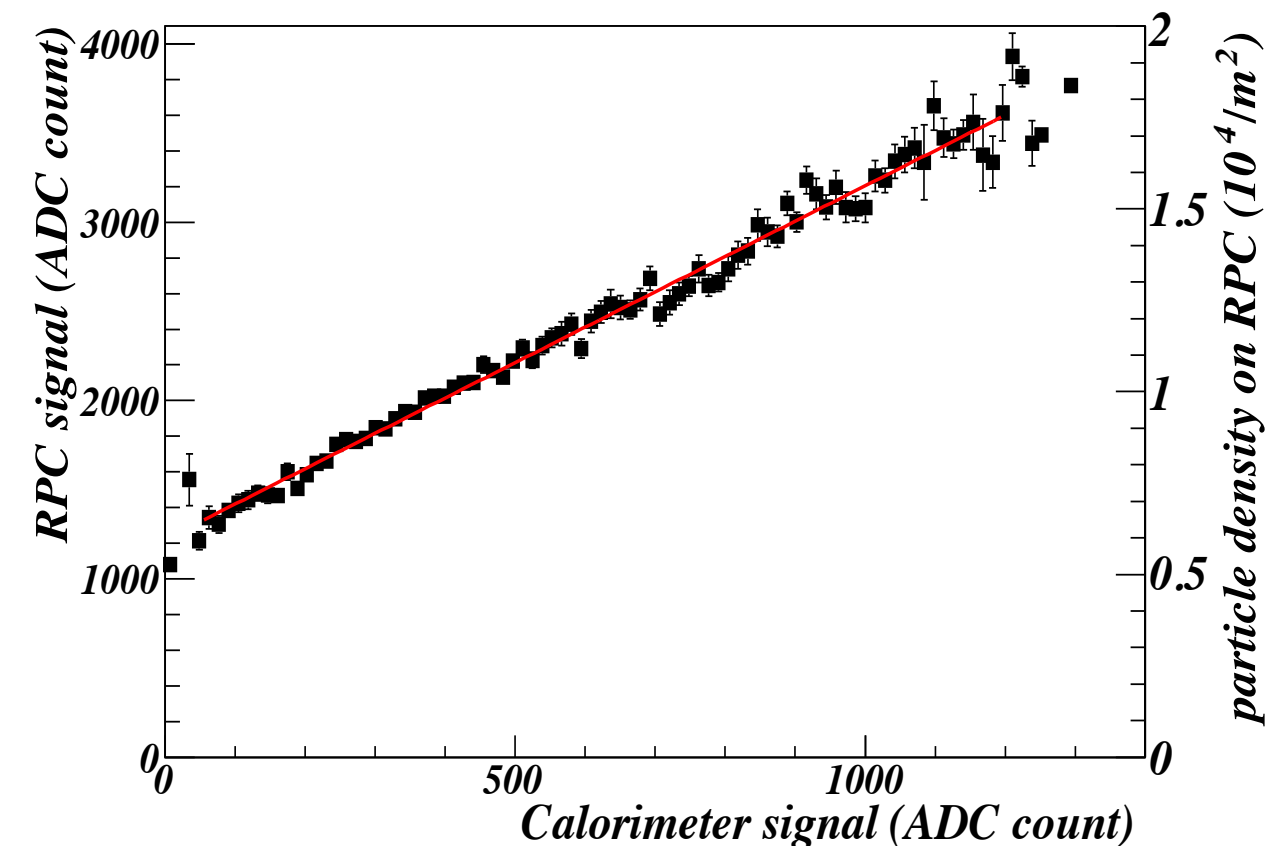
Good overlap between 4 scales with the maximum density of the showers spanning over three decades



Astrop. Phys. 67 (2015) 47



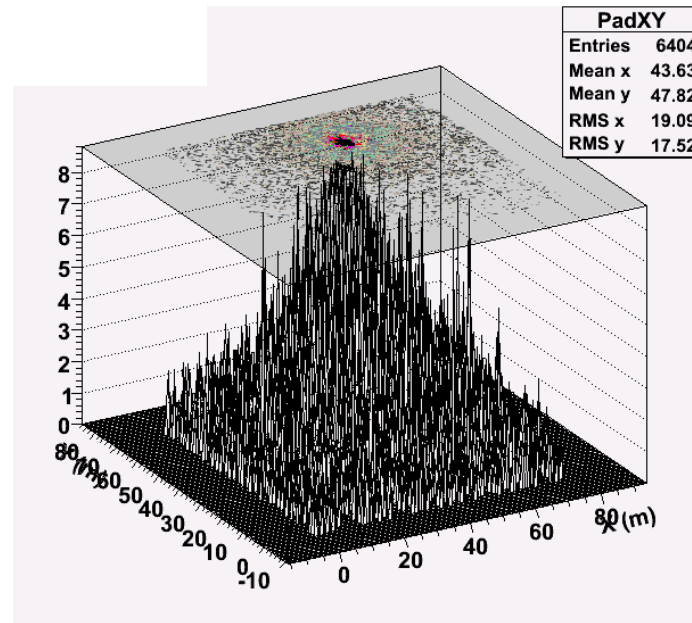
The RPC signal vs the calorimeter signal



→ Linearity up to $\approx 2 \cdot 10^4 \text{ particle/m}^2$

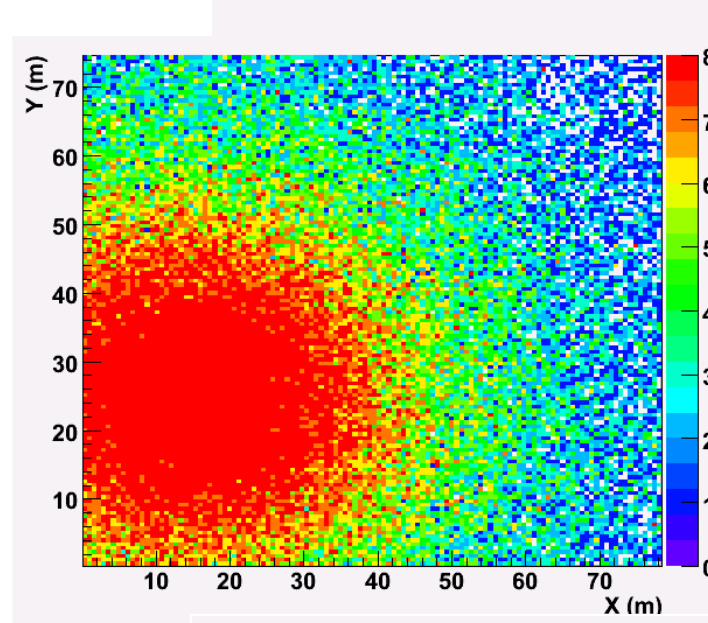
The RPC charge readout: the core region

MC: 100 TeV



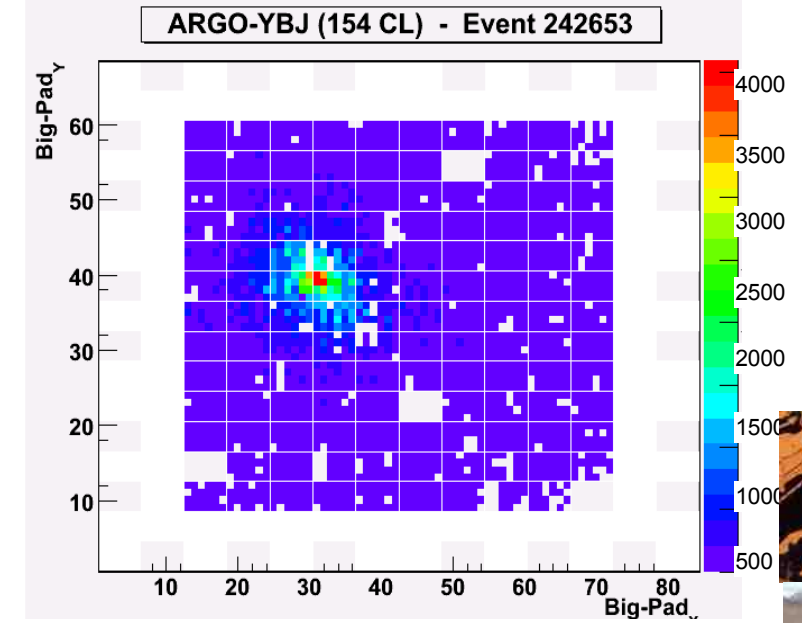
Strip read-out

MC: 1000 TeV

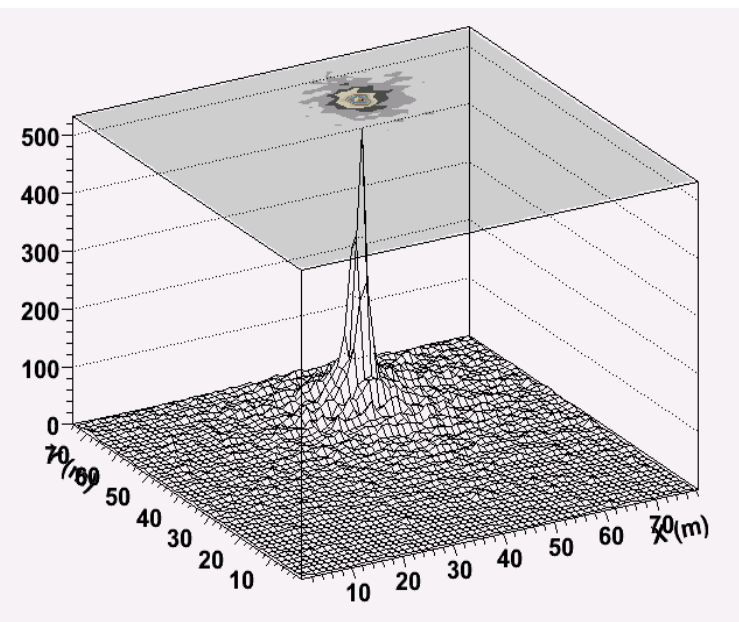


Strip read-out

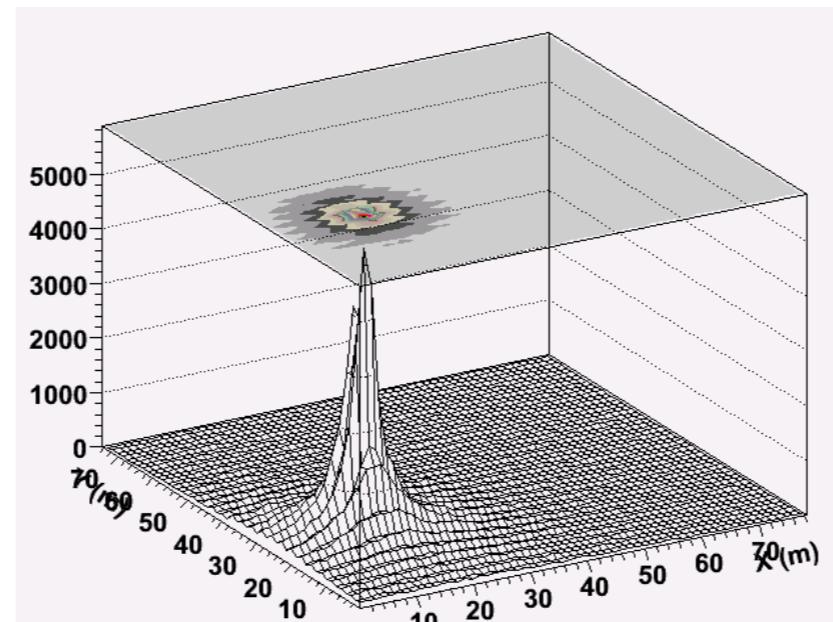
Data



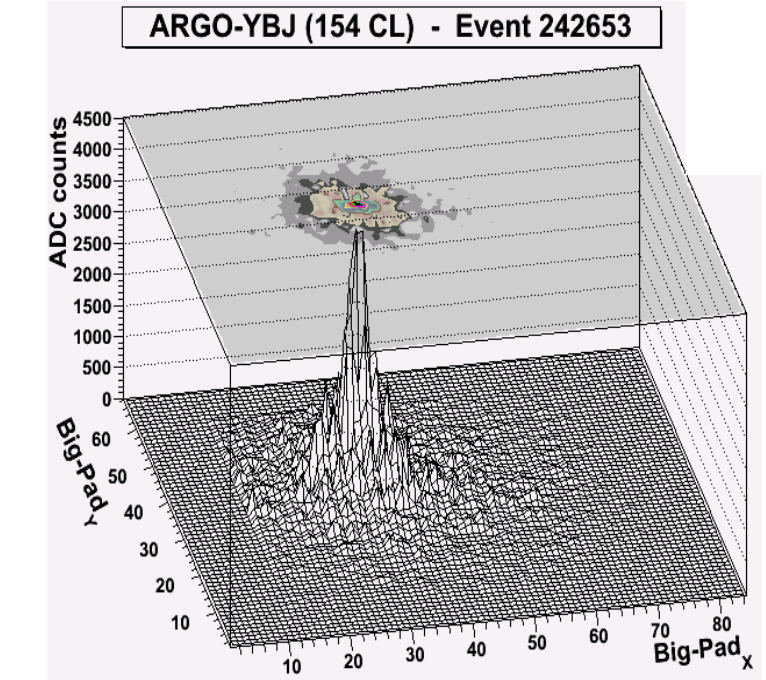
Strip read-out



Charge read-out



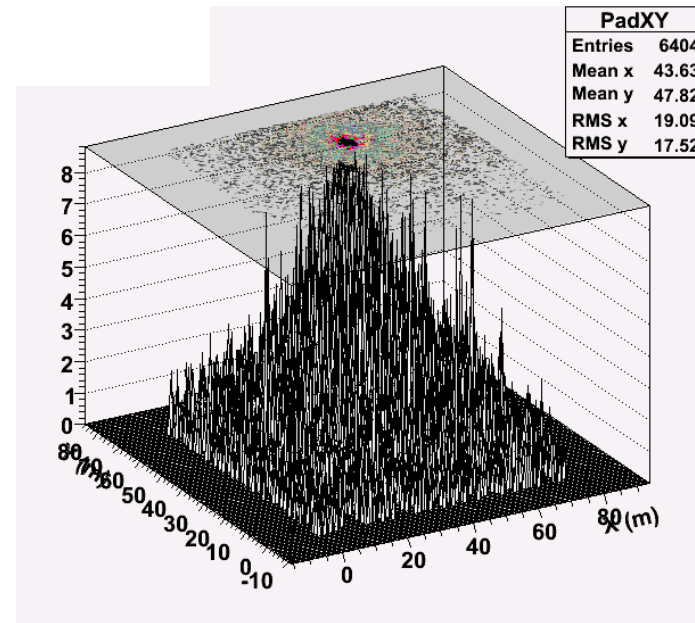
Charge read-out



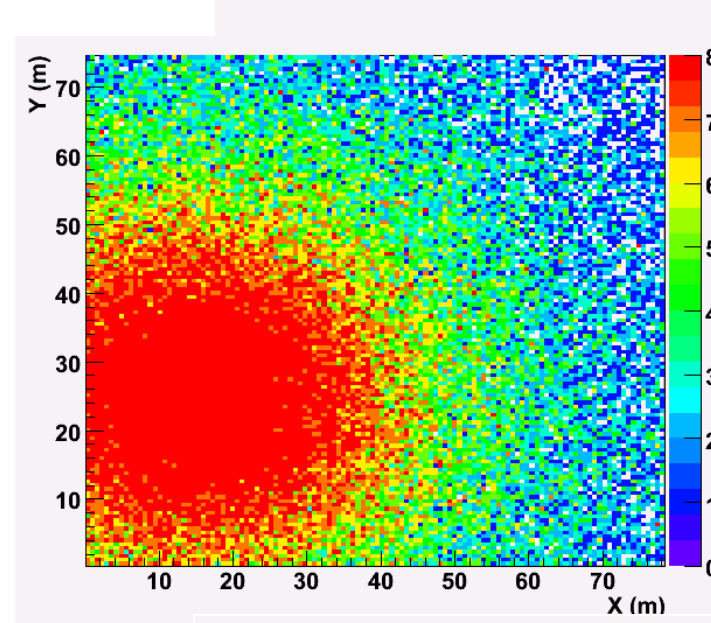
Charge read-out

The RPC charge readout: the core region

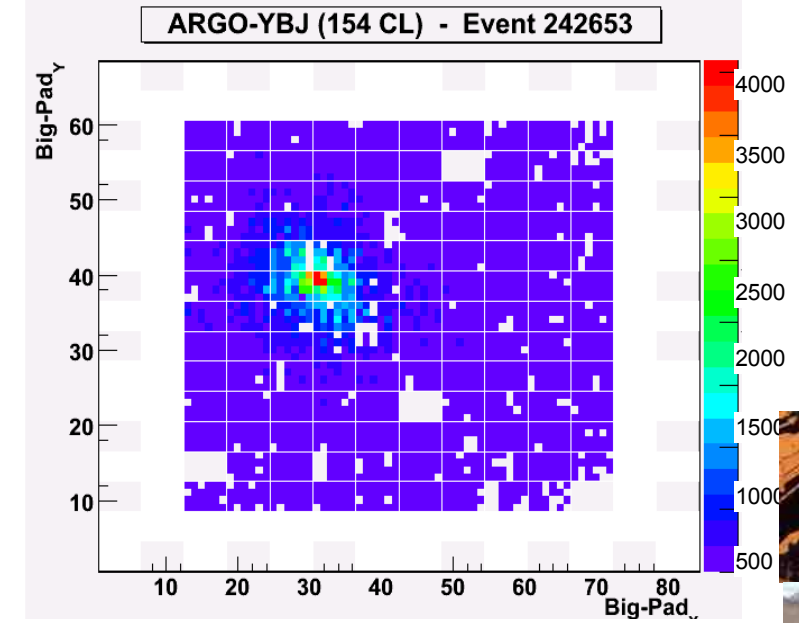
MC: 100 TeV



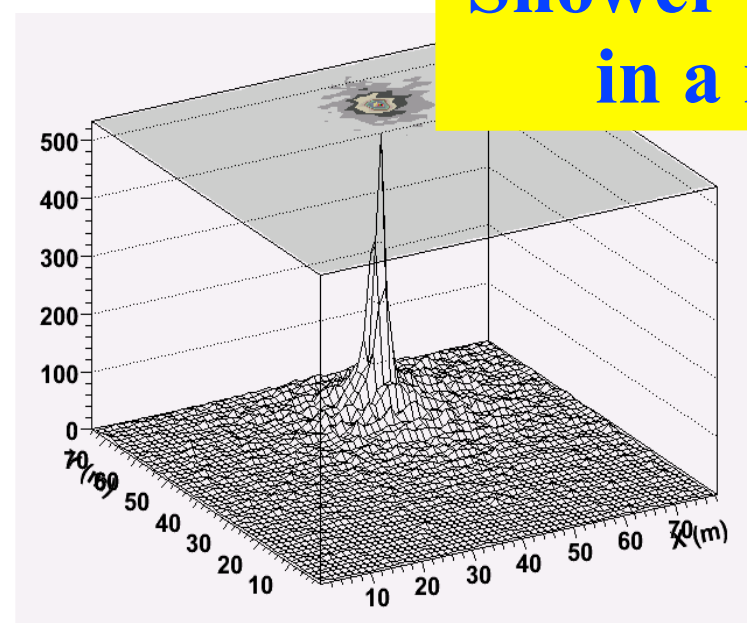
MC: 1000 TeV



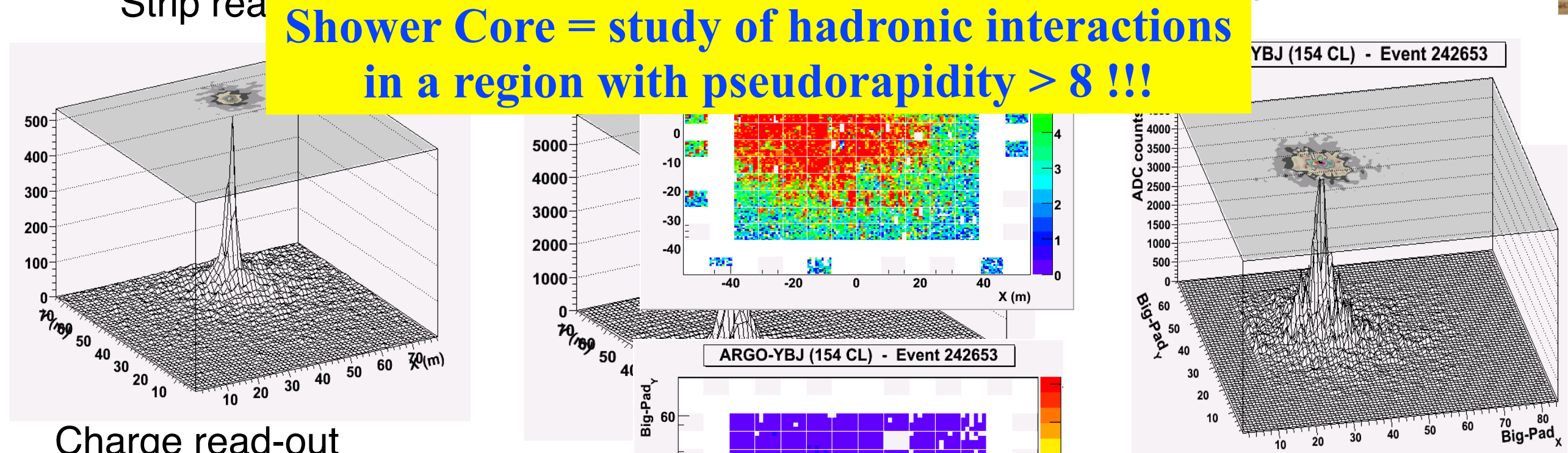
Data



Strip read-out



Charge read-out



Charge read-out

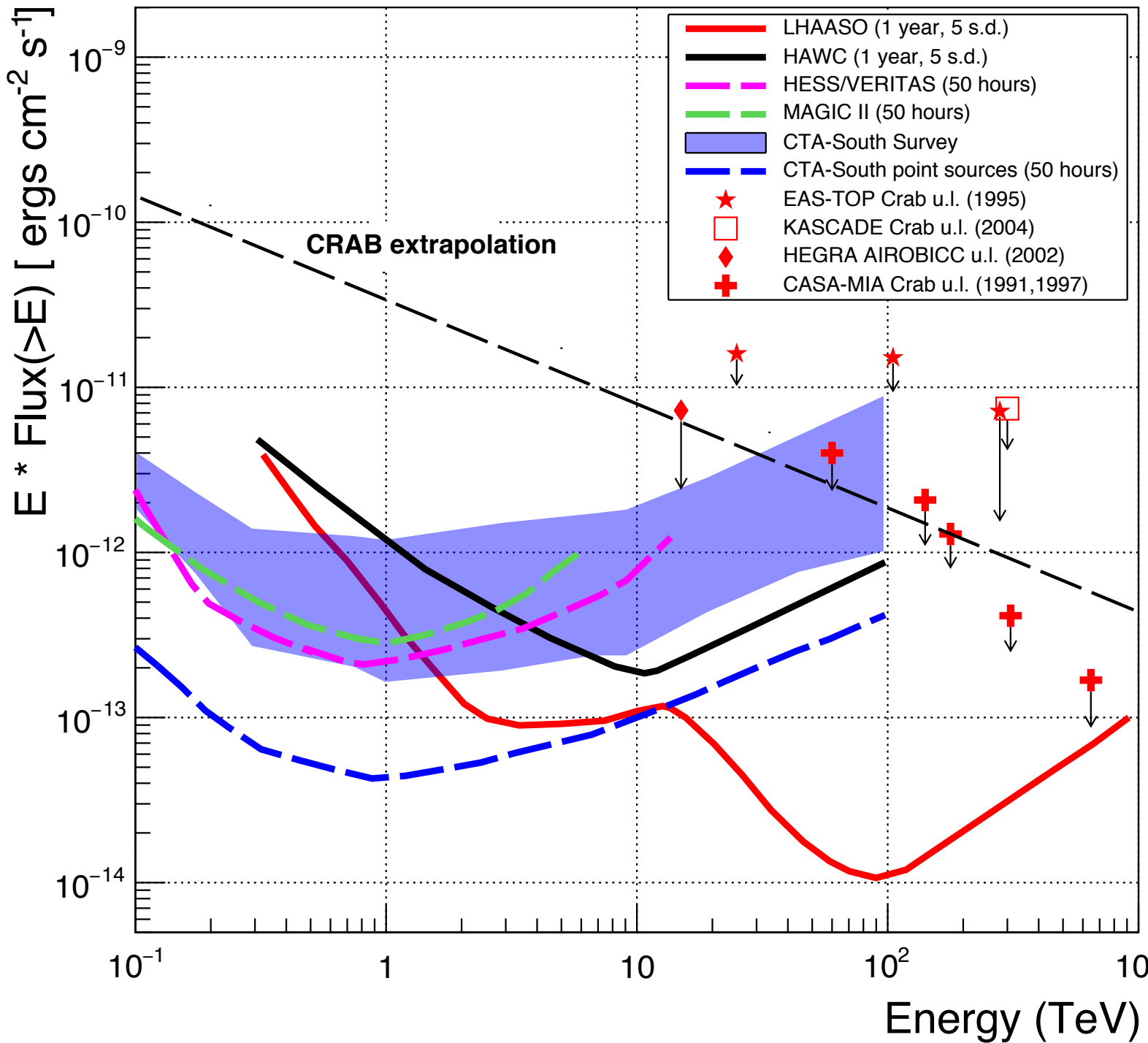
Strip read-out

YBJ (154 CL) - Event 242653

Charge read-out

**Shower Core = study of hadronic interactions
in a region with pseudorapidity $> 8 !!!$**

Sensitivity



EAS-array: 5 s.d. in 1 year

Cherenkov: 5 s.d. in 50 h on source

★ 1 year for EAS arrays means:
 $(5 \text{ h} \times 365 \text{ d}) \sim 1500 - 2200$ of
observation hours for each source
(about 4-6 hours per day).

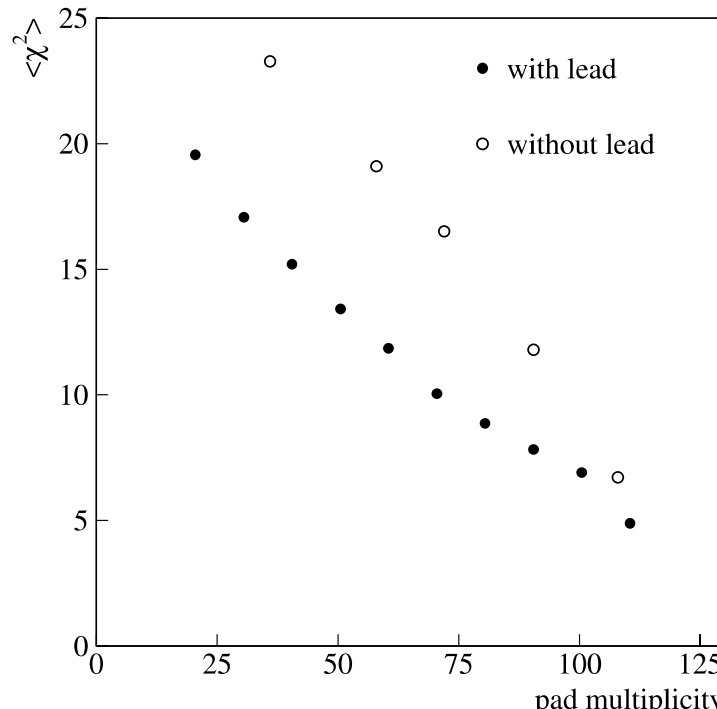
★ For Cherenkov:
 $(5 \text{ h} \times 365 \text{ d}) \times \text{d.c.} (\approx 15\%) \approx 270 \text{ h/y}$
for each source.

Effect of a lead converter above a detector

The consequences of placing a thin sheet of dense, high-Z material, above detectors are, qualitatively:

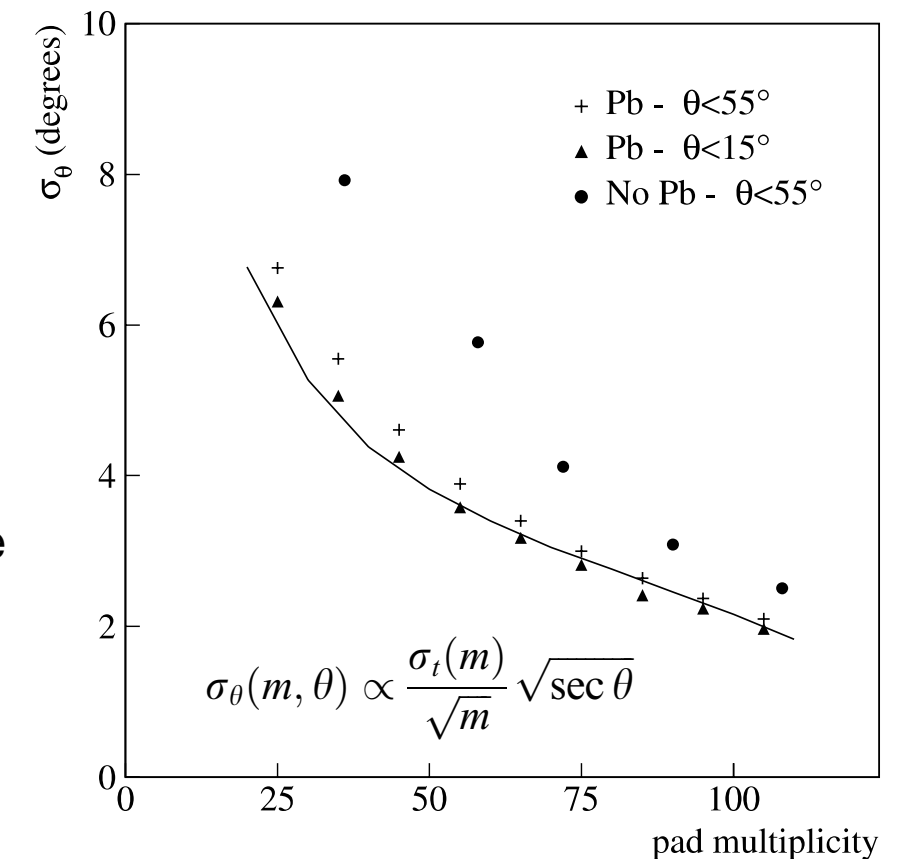
- (1) low-energy electrons are absorbed and no longer contribute to the signal (low-energy photons are also absorbed),
- (2) high-energy electrons produce an enhanced signal size through multiplication,
- (3) high-energy photons materialise, producing additional signal contributions similar in size to those produced by (2).

The number of particles gained from processes (2) and (3) exceeds that lost through (1) and hence the *Rossi transition effect* is observed.



$(\chi^2)^{1/2}$ represents (approximately)
the average time spread

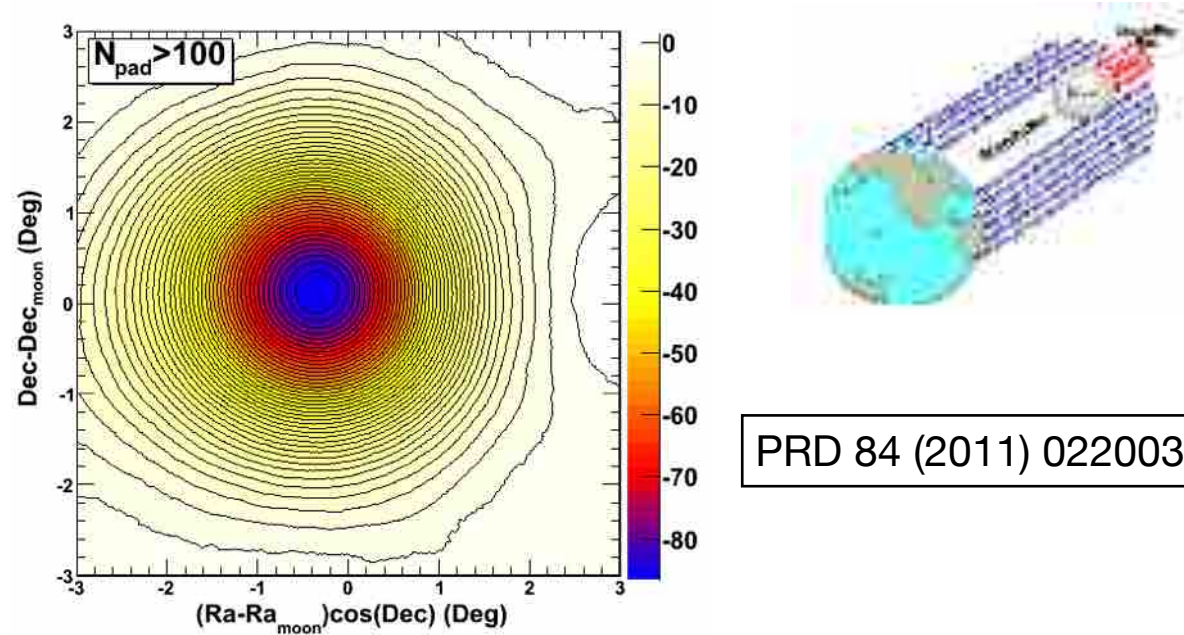
The enhanced signal alone, arising from this, will reduce the timing fluctuations.
In addition, the contributions gained are concentrated near the ideal time because the higher energy electrons and photons travel near the front of the particle swarm (they suffer from smaller time delays) while those lost tend to lag far behind.



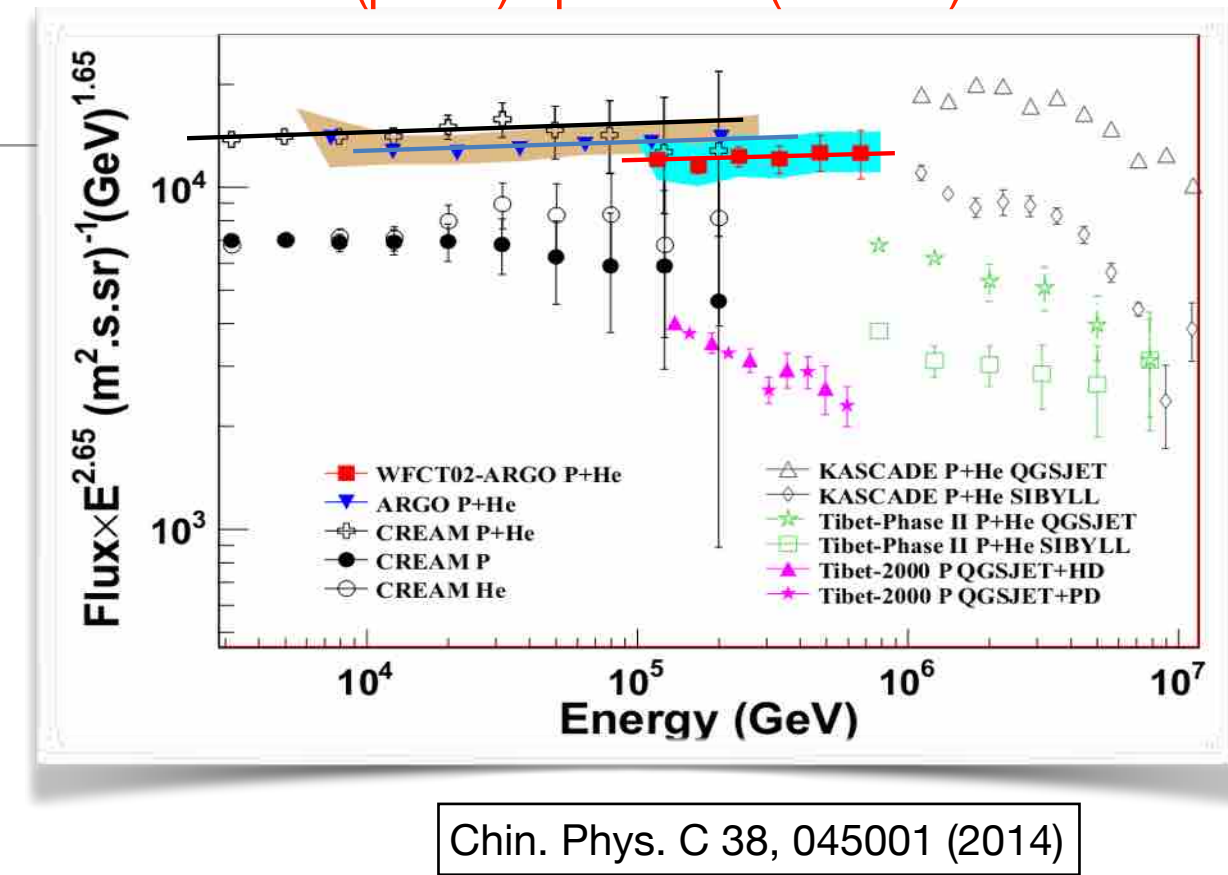
Measurement with ARGO at YBJ

Calibration of the energy scale

ARGO-YBJ: Moon shadow tool



The energy scale uncertainty is estimated at 10% level in the energy range 1 – 30 (TeV/Z).

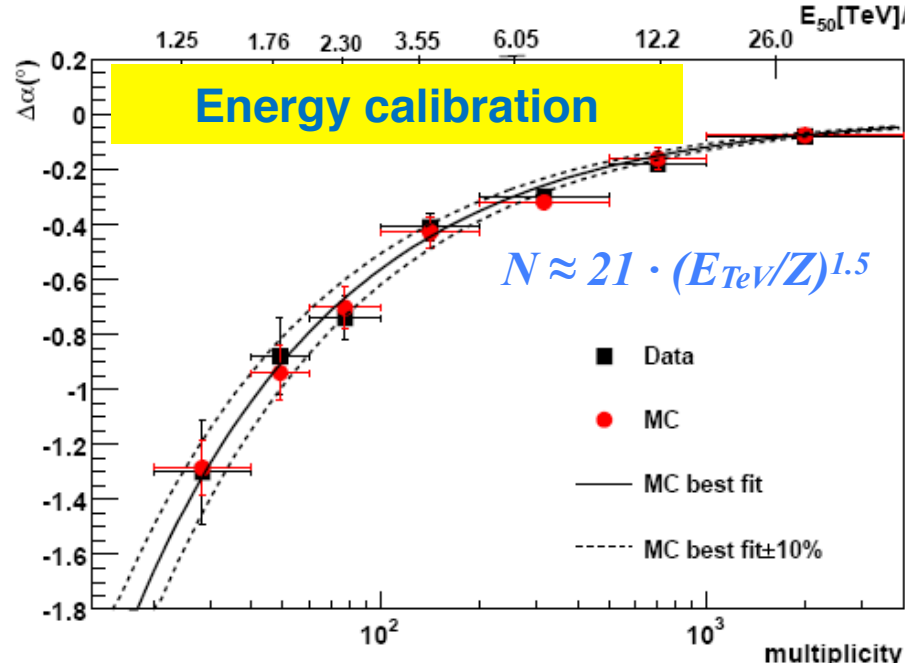


- CREAM: $1.09 \times 1.95 \times 10^{-11} (\text{E}/400 \text{ TeV})^{-2.62}$
- ARGO-YBJ: $1.95 \times 10^{-11} (\text{E}/400 \text{ TeV})^{-2.61}$
- Hybrid: $0.92 \times 1.95 \times 10^{-11} (\text{E}/400 \text{ TeV})^{-2.63}$

Single power-law: 2.62 ± 0.01

Flux at 400 TeV:
 $1.95 \times 10^{-11} \pm 9\% (\text{GeV}^{-1} \text{ m}^{-2} \text{ sr}^{-1} \text{ s}^{-1})$

The 9% difference in flux corresponds to a difference of $\pm 4\%$ in energy scale between different experiments.



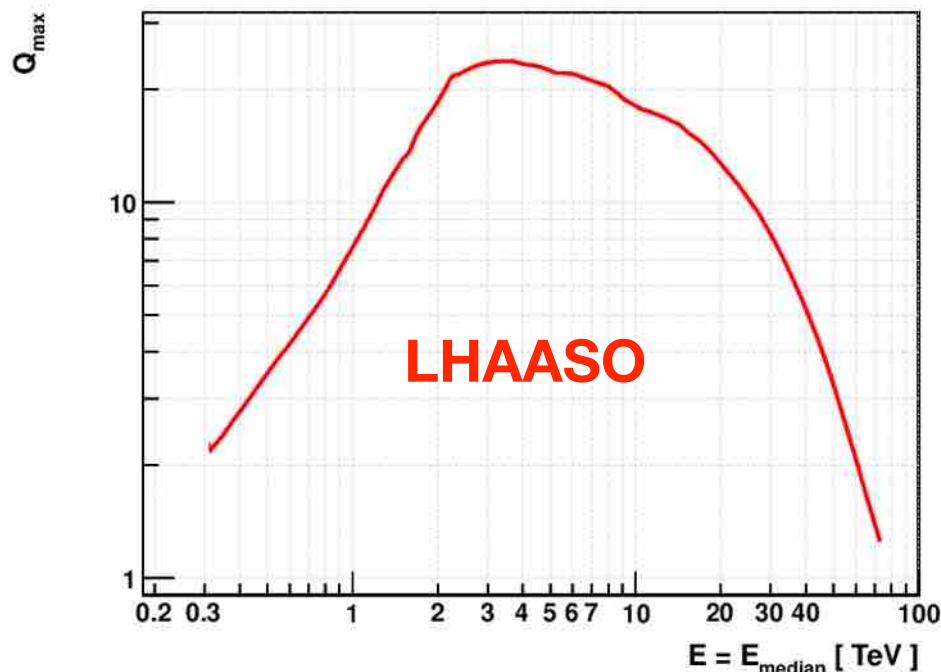
Gamma/Hadron discrimination

Very difficult at low energy (< 1 TeV)

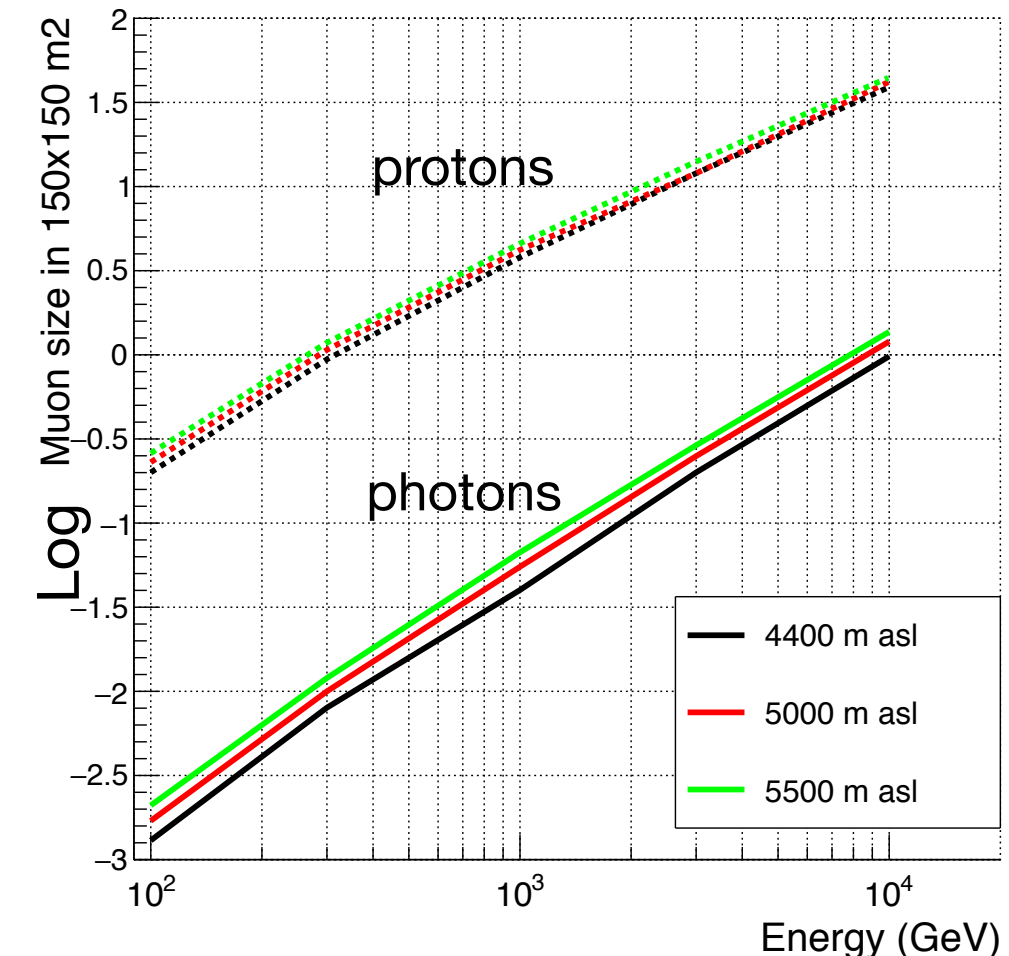
Muon size very small

HAWC/LHAASO approach requires large area:
discrimination based on **topological cut** in the pattern of
energy deposition **far from the core** (>40 m).

Requires sufficient number of triggered channels (>70 - 100)
→ minimum energy required $E > 0.5$ TeV



LHAASO Q-factor: 3 at 500 GeV, 7 at 1 TeV, 22 at 5 TeV.



Discrimination capability depends on detector area

→ according to HAWC/LHAASO calculations
sensitivity $\approx A_{\text{eff}}^{0.8}$ and not $A_{\text{eff}}^{0.5}$ up to $\approx 300 \times 300$ m²
at TeV energies

New ideas ?

Extended sources

$$S_{ext} \sim \frac{\Phi_\gamma(>E)}{\sqrt{\Phi_{bkg}(>E)}} \cdot R \cdot \sqrt{A_{eff}^\gamma} \cdot \sqrt{T} \cdot Q \times \frac{1}{\theta_{ext}} \cdot \frac{\theta_{PSF}}{\theta_{PSF}}$$

S point-source

$$S_{ext} = S_{point} \cdot \frac{\theta_{PSF}}{\theta_{ext}}$$

dimension of the extended source

Detectors with a ‘poor’ angular resolution are favoured in the extended source studies.

The minimum integral flux (in Crab units) detectable by LHAASO and CTA-South as a function of the source angular diameter, for two different photon energies.

